Risk-based Optimization Models for Maritime Safety and Security

A Dissertation

Presented to

the Faculty of the Department of Industrial Engineering,

University of Houston

In Partial Fulfillment

of the Requirements for the Degree

Doctor of Philosophy

in Industrial Engineering

By

Taofeek Olumuyiwa Biobaku

August 2016

Risk-based Optimization Models for Maritime Safety and Security

Taofeek Olumuyiwa Biobaku

Approved:

Chair of the Committee
Gino J. Lim, Professor,
Industrial Engineering

Committee Members:

Qianmei Feng, Associate Professor,
Industrial Engineering

Jiming Peng, Associate Professor,
Industrial Engineering

Elebeoba May, Associate Professor,
Biomedical Engineering

Zhu Han, Professor,
Electrical Engineering

Suresh K. Khator, Associate Dean,
Cullen College of Engineering

Gino J. Lim, Professor and Chair,
Industrial Engineering

Acknowledgments

Foremost, I express my heartfelt gratitude to my advisor, Dr. Gino Lim. His financial supports throughout the course of my education, technical insights, motivations and criticisms have, in no small measure, contributed to the successful completion of this dissertation. I have benefitted immensely from his wealth of knowledge, technical experience, and administrative acumen. He availed me the opportunity of pursuing independent research and was always available to re-direct my research in the right direction. I also appreciate his consistent interest in the welfare of my family.

Many thanks to the dissertation committee members, Dr. Qianmei Feng, Dr. Jiming Peng, Dr. May Elebeoba and Dr. Zhu Han for providing valuable comments that improved contents of the dissertation. My appreciation also goes to the quartet of Ms. Sharon Hall, Ms. Cyrena Edward, Ms. Kiki Mimms and Ms. Andreeka Lewis for all their kind support during my stay in the department. To my colleagues in the Industrial Engineering department and my research group (both past and present), I am indeed grateful for your friendship and the camaraderie we all share.

During this journey and throughout my entire academic career, I have enjoyed the unalloyed support of my parents, Mr. and Mrs. A.O. Biobaku, and siblings, Abdul-Lateef, Fatimah, Qudroh and Ibrahim. Their parental, financial and moral supports have been of immense benefits. Finally, I acknowledge the patience and perseverance of my darling wife, Dr. (Mrs.) Fatimah Biobaku. She had to make a difficult choice of suspending her medical residency career in Africa to join me on this voyage. Thanks for finding me worthy of your love and unquestioning affection.

Dedicated to my loving spouse, Dr. (Mrs.) Fatimah Biobaku and our lovely kids: Khalid (leader of the pack), Aisha (my adorable and mischief-laden princess) and baby Abdul-Musawwir (the ever cheerful little man). I love you all!

Risk-based Optimization Models for Maritime Safety and Security

An Abstract

Of a

A Dissertation

Presented to

the Faculty of the Department of Industrial Engineering,

University of Houston

In Partial Fulfillment

of the Requirements for the Degree

Doctor of Philosophy

in Industrial Engineering

By

Taofeek Olumuyiwa Biobaku

August 2016

Abstract

Considering that unprotected assets and infrastructures in the Maritime industry are vulnerable to attacks, we present models and methodologies for protecting these maritime resources from malicious or terrorist attacks. Using risk-based analysis, we use conditional probabilities to establish relationships between consequences, vulnerabilities and threat incidences of maritime events.

In the first part of this dissertation, we address safety/security of maritime assets. We consider vessel routing and scheduling in LNG vessels as a hazardous cargo, and present a risk-based methodology in the choice of alternate vessel routes between a liquefaction terminal and receiving depot(s). While derivations are presented for the quantification of each constituent of the risk-based model, actual historical data of terrorist/piracy attacks made available by a national consortium on the study of terrorism are used in the analysis approach. With a multivehicle routing model, we test our methodology and present results using a practical test case involving delivery of LNG.

In the second part of this dissertation, we address safety/security of maritime infrastructures and use underwater sonars for threat detection. Models and algorithms are developed for providing surveillance to maritime infrastructures such as ports, harbors, jetties, etc. The methodologies in these models include a quantitative risk analysis approach, a network fortification approach, a greedy-based heuristic approach, and a robust optimization approach. The network fortification approach considers the ability of an intending *'attacker'* to possess information related to resource limitations and protection procedure of a *'defender'*. Consequently, the *'attacker'* attempts to use this

information to evade detection, thus compromising safety and security of maritime infrastructures. In developing greedy-based algorithms to solve large scale problems in our placement methodology, we exploit the principle of submodularity to propose efficient solution algorithms with some theoretical guarantees. Lastly, we developed a robust formulation for our placement methodology to address uncertainties related to some modeling parameters. To illustrate that the new sonar placement methodologies developed help to improve protection coverage plans for maritime infrastructures, we use practical case studies to provide safety and security to ports. In addition, we provide analytical and experimental results on each of these studies.

Table of Contents

List of Figures

List of Tables

Chapter 1

Introduction

1.1 Background

Global economic success is heavily dependent on the maritime industry since over 90% of the world's international trade takes place by sea (IMO, 2014). Specifically, the US economy is largely dependent on the maritime sector as 95% of its foreign trade is moved by ships (United States Department of Transportation Maritime Administration, 2007). Consequently, the integrity of maritime assets and sustained surveillance of maritime infrastructures is a critical requirement of ensuring safety and security, thus assuring the industry's continued success.

Regrettably, the scourge of terrorism and incidences of arson attacks have threatened the continued success of the maritime industry. To address these threats, an increase in the protection of maritime assets (vessels and their cargoes) and sustained surveillance of marine infrastructures (ports, harbors, waterways, high-risk sea routes, etc.) is an important requirement of ensuring safety and security.

Maritime infrastructures have been extensively used in the transportation of hazardous consignments such as chemicals, petroleum and liquefied natural gas LNG cargoes. Unfortunately, the hazardous nature of these cargoes means they are attractive targets to attacks. In addition, the construction and use of high-volume transportation vessels due to their economies of scale benefits not only makes them targets of attacks,

but their dependence on non-conventional energy source such as nuclear-powered plants for propulsion also makes them more vulnerable to these attacks.

Due to the nature of the maritime environment, terrorist and arsonist attacks may be aerial-borne, water-borne, or even land-borne because maritime assets and infrastructures, at one point or another are always in contact with at least two of these media. However, in order to avoid detection, such threats have increasingly become waterborne. Both acoustic and non-acoustic methods have been employed in the surveillance of maritime resources against underwater threats. A few of the established non-acoustic methods include the use of magnetic signatures, optical signatures, electric field signatures, thermal detection, and hydrodynamic changes. However, none of these methods are known to be as effective as the acoustic methods (Waite 2002). As a viable alternative, acoustic sensors possess several advantages in the detection of these water-borne threats; For example, sound waves attenuate less in water and the devices can also be placed deeper underwater. Hence, their use in underwater threat detection for surveillance is desirable.

1.2 Problem Descriptions

For the purpose of this dissertation, Maritime assets refer to shipping vessels and their cargoes; and Maritime infrastructures refers to structures that provide service to the maritime industry such as ports, harbors, waterways, voyage routes, straits, jetties, receiving terminals, etc.

Figure 1.1: Maritime Assets and Infrastructures- LNG Port, Jetty, and Tug boats during loading operations of an LNG vessel (BAM Clough Joint Venture, 2000)

1.2.1 Protection of Maritime Assets

The appropriate choice of a voyage route can be argued to influence the safety and security of ocean-going vessels and their contents. While the choice of an alternative voyage route is mainly dependent on travel distance, consideration should also be accorded to historical safety records of these alternate routes. With specific reference to LNG vessels as a hazardous cargo, the first problem area addressed in this dissertation deals with the incorporation of a risk-based methodology in planning the timely delivery of LNG cargoes. Given a fleet of LNG vessels with different capacities and different restrictions, it is required to transport LNG to and from several ports (customers with facilities at receiving ports), satisfying the known supply/demand of each port at minimal shipment cost and minimal expected risk cost (due to likelihood of piracy, terrorist or

arson attacks). In addition, policy related and operational constraints need to be taken into consideration. Different policies and operational constraints are expected to depend on type of demand (Contract/Spot demands), vessel types, destination ports (countries), etc.

Figure 1.2: Maritime Assets- Two types (Membrane and Moss) of LNG Vessels on voyage routes (Oil and Gas people, 2014)

1.2.2 Protection of Maritime Infrastructures

One of the ways of protecting critical infrastructures is the use of sensors for surveillance purposes. Within the context of risk analysis and under budget limitations, the second problem in this dissertation proposes optimization models, algorithms and methodologies to efficiently determine the number and regional locations to allocate different sonar types of different sonar coverage orientations and ranges such that detection probabilities is optimized based on the criticality (regional importance) attached to these regions in a multi-period deployment scheme.

Figure 1.3: LNG Infrastructures: Loading platforms (Gate terminal B.V, 2014)

1.3 Contributions

This dissertation contributes to the literature by proposal of new optimization models, methodologies and algorithms for risk-based optimal vessel routing and optimal placement of underwater sonars in a maritime environment to detect underwater threats. Within the context of protecting assets and infrastructures, the risk-based methodology essentially attempts to highlight how potential threats and vulnerabilities influence expected consequences. Mitigation of these consequences is a major purpose of the methodology. Our modeling approach in this dissertation makes use of the quantitative approach in risk analysis.

1.3.1 Protection of Maritime Assets: Risk-based LNG vessel scheduling and routing

To incorporate the concept of quantitative risk analysis in the alternate choice of LNG vessel routes, we present a risk-based vessel routing scheme in the LNG

transportation network. While acknowledging that the lofty safety records of the LNG business emphasized by its successful transportation of over 66,000 loaded voyages and six billion m^3 of LNG without any major loss of LNG cargo (Hightower and Albuquerque, 2012) cannot be overlooked, the possibility of a large displacement vessel or missile (either accidental or intentional) at high speeds that may result in penetration of the cargo containment system should also not be totally ignored. To the best of our knowledge, no similar work currently exists in literature that provides an optimization model on LNG transportation using a risk-based approach.

1.3.2 Protection of Maritime Infrastructures- Sonar Placement Problems (SPP)

For protecting maritime infrastructures, we address the optimal placement of sonars for providing surveillance to maritime infrastructures against impending underwater threats. While literature on the use of terrestrial sensors for surveillance is rich and extensive, its underwater counterparts have not been well addressed (Heidemann et al., 2012).

Based on the specific placement problem being considered, SPP is usually addressed under the following distinct problem areas: Point Coverage, Barrier Coverage and Area Coverage. Point Coverage essentially deals with providing sensor coverage to specific infrastructures; Barrier coverage is involved with ensuring sensor coverage is provided to routes leading to an infrastructure, and Area Coverage deals with providing sensor coverage to an entire region. Although earlier works broadly consider the SPP in general terms, latter works are often dedicated to these distinct problems. In this study,

two approaches are used for the SPP. Both approaches are mixed integer linear optimization formulations. In addition to risk analysis, our approaches include a fortification approach, a procedure for solving large problems and a methodology for incorporating uncertainty considerations in the sonar placement problem.

The study in the first approach contributes to the literature by proposing a new mathematical model for placing underwater sonars in a maritime environment to monitor potential underwater threats. The model integrates both static and mobile sensors in a deployment methodology within a multi-period deployment scheme using a hexagonal-grid based placement methodology. Unlike terrestrial sensors, sonars are quite expensive. Thus, this placement methodology is to be achieved under strict budgetary limitations. To the best of our knowledge, no work exists in literature that proposes the use of hexagonal-grid based methodology in the placement of sensors within a maritime environment. In addition, we extended the work by proposing greedy-based algorithms and also studied uncertainty considerations under a robust optimization approach in the sonar placement problem.

Another approach we studied in this dissertation is a trilevel 'Defender-Attacker-Defender' model, referred to as a 'Fortification model'. The model is suitable for the defense planning of critical infrastructures and involves three levels of interactions between a *'Defender(s)'* and an *'Attacker'*. The *'Defender'* initially deploys resources to mitigate potential damage or disruption and the '*Attacker'* in turn responds to the initial deployment within the limits of his resources. Thereafter, a '*Defender'* (which could be the original agent responsible for the initial deployment or another agent with similar goal) counteracts the attacker's response in order to mitigate overall system damage or

disruption. The Fortification approach considers the expected actions of an intelligent 'attacker' with access to existing protection capabilities and who attempts to use this information to evade detection. Due to the relative easy access (legal or otherwise; publicly available or otherwise) to information in modern times, it is imperative to consider the perceived reaction of a resolute attacker familiar with a protector's resource capabilities. Currently, literature indicates the fortification concept is yet to be applied in sonar placement problems.

Figure 1.4: Sentinel Intruder Detection Sonar system (SIDSS), a compact underwater surveillance sonar used by the US Navy (Maritime Journal, 2009)

1.4 List of Publications

Journal Publications

- T. Biobaku and G. Lim (2016), "A greedy-based approach for detecting underwater threats under a limited budget," working paper.
- T. Biobaku and G. Lim (2016), "Underwater sonar placement problem under uncertainty considerations," working paper.
- T. Biobaku and G. Lim (2016), "A fortification approach for detecting underwater threats under limited budget," (submitted to Reliability Engineering and System Safety).
- T. Biobaku, G. Lim, S. Bora, J. Cho, and H. Parsaei (2016). An optimal sonar placement approach for detecting underwater threats under budget limitations. *Journal of Transportation Security*, 9(1-2), 17-34.
- T. Biobaku, G. Lim, S. Bora, J. Cho, and H. Parsaei (2015), "Literature survey on underwater threat detection," *Transactions on Maritime Science*, 4(01), 14-22.
- J. Cho, G. Lim, T. Biobaku, S. Bora, and H. Parsaei (2015), "Planning for LNG Inventory Routing under Dust Storm," (submitted to European Journal of Operational Research).
- J. Cho, G. Lim, T. Biobaku, S. Bora, and H. Parsaei (2014), "Liquefied Natural Gas Ship Route Planning Model Considering Market Trend Change," *Transactions on Maritime Science*, 3(02), 119-130. DOI: 10.7225/toms.v03.n02.003.

- S. Bora, G. Lim, T. Biobaku and S. J. Cho, H. Parsaei. Models and Computational Algorithms for Maritime Risk Analysis: A review," (submitted to Annals of Operations Research).

Conference Proceedings and Presentations

- J. Cho, G. Lim, T. Biobaku, and S. Kim, "Safety and Security Management with Unmanned Aerial Vehicle (UAV) in Oil and Gas Industry," *Procedia Manufacturing* 3, 1343-1349., DOI: 10.1016/j.promfg.2015.07.290
- T. Biobaku, G. Lim, J. Cho, S. Bora, H. Parsaei, and S. Kim. "Liquefied Natural Gas Ship Route Planning: A Risk Analysis Approach." *Procedia Manufacturing* 3 (2015): 1319-1326. DOI: 10.1016/j.promfg.2015.07.282
- J. Cho, G. Lim, T. Biobaku, and H. Parsaei, "Use of Unmanned Aerial Vehicle (UAV) for risk monitoring in oil and gas industry," in IIE Annual Conference, Nashville, 2015.
- T. Biobaku, G. Lim, J. Cho, H. Parsaei, and S. Kim, "Optimal Sonar Deployment in a Maritime Environment: A Fortification Approach," in INFORMS Annual Conference, Philadelphia, 2015.
- S. Bora, G. Lim, T. Biobaku, J. Cho and H. Parsaei, "Case Studies on Maritime Incidents: A Review," in IIE Annual Conference, Nashville, 2015.
- T. Biobaku, G. Lim, J. Cho, H. Parsaei, and S. Kim, "Optimal Sonar Deployment in a Maritime Environment: A Fortification Approach," in INFORMS Annual Conference, Philadelphia, 2015.

- T. Biobaku, G. Lim, J. Cho, H. Parsaei, and S. Kim, “Optimal Voyage Planning of Liquefied Natural Gas Vessels: A Risk-Analysis Perspective,” in UH Industrial Engineering Conference & Exhibition, 2015.

Poster Presentations

- T. Biobaku, G. Lim, J. Cho, S. Bora, and H. Parsaei, “Sonar Placement for Maritime Surveillance - A Fortification Approach,” in University of Houston - Graduate Research and Scholarship Projects (GRaSP) Day, Houston, TX, 2015.
- J. Cho, G. Lim, T. Biobaku, S. Bora, and H. Parsaei, “Global LNG supply chain under Shamal disruptions,” in University of Houston - Graduate Research and Scholarship Projects (GRaSP) Day, Houston, 2014.
- T. Biobaku, G. Lim, J. Cho, S. Bora, and H. Parsaei, “Underwater Sonar Placement for Maritime Surveillance,” in University of Houston - Graduate Research and Scholarship Projects (GRaSP) Day, Houston, TX, 2014.
- S. Bora, G. Lim, T. Biobaku, J. Cho, H. Parsaei, “Assessing Supply Chain Resiliency,” in 3rd TAMUQ Annual Research and Industry Forum, Doha, Qatar, 2014.
- T. Biobaku, G. Lim, S. Bora, J. Cho, H. Parsaei, “Underwater Sonar Placement with Static and Mobile Sensors, “in 3rd TAMUQ Annual Research and Industry Forum, April 7, Doha, Qatar, 2014.
- J. Cho, G. Lim, T. Biobaku, S. Bora, H. Parsaei , “Liquefied Natural Gas (LNG) inventory routing problem under weather disruptions: a case study of dust storm in Persian Gulf,” in Proceedings of THC-IT-2014 Conference and Exhibition, August 1 2014, Houston, TX, USA.

- T. Biobaku, G. Lim, S. Bora, S. Ahmadi, H. Parsaei, “Sonar Placement and Deployment in a Maritime Environment,” in Qatar Foundation Annual Research, Doha, Qatar, 2013.

1.5 Dissertation Overview

This dissertation is organized as follows. In Chapter 2, we present a comprehensive review of underwater threat detection. Risk-based analysis, Sensor placement and Interdiction/Fortification methodologies are reviewed as techniques for evaluating vulnerabilities and consequently providing protection to critical maritime assets and infrastructures. In Chapter 3, a new risk-based framework is presented for optimally planning the voyage of LNG vessels (maritime assets) between liquefaction plants and regasification terminals. While Chapter 4 presents an optimal risk-based placement methodology to protect LNG ports, harbors, etc. (maritime infrastructures) from underwater-borne attacks, Chapter 5 presents a fortification modeling approach in the placement methodology presented in Chapter 4 and discusses an algorithm implemented to solve the placement problem using the approach. In Chapter 6, we present greedy-based algorithms for solving the SPP problem and Chapter 7 addresses the issue of data uncertainty in the SPP by studying a robust optimization approach. Finally, Chapter 8 concludes the dissertation with an overview of the studies in Chapters 3-7 and discusses future work related to the extension of the models, algorithms and methodologies studied.

Chapter 2

Literature Review

2.1 Underwater Threat Detection

World trade is heavily dependent on maritime transportation (Organisation for Economic Co-operation and Development, OECD, 2003). This dependence indicates why global distribution of economic goods is done mostly via oceans, seas, estuaries and other maritime waterways. The unique position the maritime industry holds in the world economy (without even addressing its importance in military warfare) accentuates the need to protect its infrastructural resources from threats and disasters. Apart from the scourge of terrorism in the current global economy, the age-old threats of piracy, arson attacks and unfortunate accidents are incidences the maritime industry must also contend with. Similar to the use of terrestrial sensors in the identification and classification of land-based threats and targets, underwater sensors are used in the maritime domain for the same purpose.

In a review presented by Biobaku et al. (2015), Sensor placement and deployment within underwater/maritime framework was identified as an area requiring more contributions. There is an indication of the preponderance of acoustic sensors as a dominating sensing technology; however, discussions in Biobaku et al. (2015) also emphasized that in practical implementations of maritime surveillance systems, the combination of various technologies contributing their individual and unique benefits,

rather than the use of a specific sensing technology, is the reality in most practical surveillance systems.

2.2 Susceptibility of Critical Assets and Infrastructures - A Risk Analysis Approach

In the US, the department of Homeland Security (DHS) has primary responsibility for maintaining and preserving homeland security through its agencies/directorates (such as United States Customs and Border Protection – CBP, Transportation Security Administration – TSA, National Protection and Programs Directorate – NPPD, etc.). As a prominent component of the Homeland Security Act of 2002 (as amended) that established the cabinet department, DHS is vested with the responsibility of developing a comprehensive plan for securing the nation's critical infrastructures (composed of Physical, Cyber, and Human elements). In discharging this responsibility, DHS, amongst other endeavors, developed a critical infrastructure risk management framework whose overall objective is to provide recommendations that maximize the protection of assets and infrastructures. The risk methodology helps to focus on the threats/hazards with the highest impacts, and adopt procedures that are designed to prevent or mitigate the effects of these incidents.

The critical infrastructure risk management framework supports a decision-making process that critical infrastructure partners collaboratively undertake to inform the selection of risk management actions (NIPP, 2013). It also compliments efforts in conducting industry-specific and/or geography-specific Threat and Hazard Identification and Risk Assessment (THIRA) process.

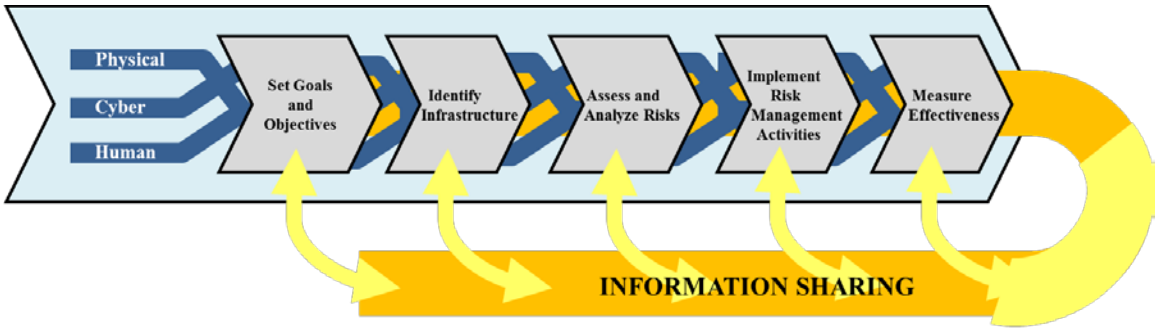

Figure 2.1: DHS Risk Management Framework (NIPP, 2013).

The risk management framework is flexible and a major feature inherent in the methodology is in the constant sharing of information across its components to identify voids in security and resilience efforts. Our work in this dissertation addresses the ***"Assess and Analyze Risks"*** component of the framework, where critical infrastructural risks are assessed in terms of three components defined (NIPP, 2013) thus: **Threat** – *Natural or man-made occurrence, individual, entity, or action that has or indicates the potential to harm life, information, operations, the environment, and/or property*; **Vulnerability** – *Physical feature or operational attribute that renders an entity open to exploitation or susceptible to a given hazard*; **Consequence** – *Effect of an event, incident, or occurrence*.

In the terminology of formal Risk analysis, Risk is taken as the expected consequence of incidents. Calculation of expected consequence is conditioned on the types of possible incidents (Ghafoori and Altiok, 2012) in equation (2.1).

$$E(C) \quad = \quad \sum_{j} E(C|I_j)p\,(I_j), \tag{2.1}$$

where $E(C|I_j)$ is the expected consequence given the occurrence of an incident j and $p(I_j)$ is the probability that an incident of type j occurs. However, a successful intrusion

(attack) may or may not lead to an incident. Hence, equation (2.1) can be written as equation (2.2) (Willis, 2007; Ghafoori and Altiok, 2012).

$$E(C) \quad = \quad \sum_{j}\left(E\left(C\middle|I_j\right)\times\left(\sum_{k}p\left(I_j\middle|A_k\right)p\left(A_k\right)\right)\right), \tag{2.2}$$

where $p\left(I_j\middle|A_k\right)$ is the conditional probability of a successful attack/intrusion given that the attack has already occured and $p(A_k)$ is the occurrence probability of attack *k.*

It is pertinent to note that the risk formula (Willis 2007; McGill et al. 2007; Ezell et al. 2010, Ghafoori and Altiok, 2012, etc.), in consonance with the DHS Risk Management Framework (NIPP, 2013), quantifies risk as,

$$Risk \quad = \quad C\times V\times T, \tag{2.3}$$

where $E\left(C\middle|I_j\right)$, $p\left(I_j\middle|A_k\right)$, and $p(A_k)$ in equation (2.2) are respectively referred to as: expected consequence of an incident *C,* vulnerability of targeted assets/infrastructure *V,* and probability that an attack (activity) occurs *T*. While some existing works in literature are able to individually include all these components of E(C) in their risk-based formulations, others simply concentrate on either one or two of them (Ghafoori and Altiok 2012).

2.3 Protection of Maritime Assets: Risk-based LNG Vessel Scheduling and Routing

Similar to the maritime transportation of crude oil and other petroleum products, LNG transportation models often take into account the whole supply chain of the

commercial product. In this dissertation, we present only a brief review of recent works on LNG transportation models.

2.3.1 LNG Transportation Models

Grønhaug and Christiansen (2009) formulated the LNG inventory routing problem as a mixed integer program to satisfy monthly demand with sales activities and inventory level at the customer's regasification terminal as major considerations. Andersson et al. (2010) proposed LNG supply chain optimization models to determine sailing schedules and vessel assignments to serve a single buyer on each voyage. Also, Grønhaug et al. (2010) proposed a branch-and-price method that involves the use of a dynamic programming algorithm to solve a sub-problem in the LNG inventory routing problem formulated. Afterwards, Rakke et al. (2011) developed an annual LNG delivery schedule with a diverse fleet of LNG carriers, taking into consideration only the traditional long-term LNG contracts but failed to consider the emerging trend of spot demands and short-term delivery contracts. Similarly, Stålhane et al. (2012) presented a heuristic to solve a large scale annual LNG inventory routing problem that considers amongst others, inventory, berth capacity at the loading port and a heterogeneous fleet of ships. Simultaneously fulfilling the producer's long-term contracts at minimum cost and maximizing the revenue from selling LNG in the spot market are major goals of the developed model.

Bopp et al. (1996), Halvorsen-Weare and Fagerholt (2013), and Halvorsen-Weare et al. (2013) considered some uncertainties related to general vessel movements in their modeling approaches. However, none of these studies considered internal system

dynamics of LNG carriers as principal sources of the uncertainties but instead, focused only on external environmental impacts (Cho et al., 2014). To address this issue, Chatterjee and Dobrota et al. (2013), and recently, in Cho et al. (2014), we considered these internal dynamics. The effect of boil off gas (BOG) is a major uncertainty factor considered in these works. Particularly, Cho et al. (2014) proposed a deterministic LNG vehicle routing problem model. Thereafter, a stochastic extension of the model using Monte Carlo optimization techniques was presented. Notably, Chatterjee and Geist (1972) had earlier attempted to study the effect of this uncertainty; however, their work was specific to LNG storage tanks as opposed to LNG vessels.

2.3.2 Risk-based Transportation of LNG Vessels

Due to the nature of LNG cargo, LNG transportation should be treated as a hazardous material. To the best of our knowledge, studies considering hazmat transportation risk assessment and routing with specific reference to LNG vessels is non-existent in literature. However, a brief review on a closely related cargo vessel (crude oil tankers) is provided in this section.

Li et al. (1996) developed a model for transportation of oil that considered operational risk in a multimodal and multiproduct network with specific application to the Gulf of Mexico. A few years later, Iakovou et al. (1999) proposed a model to solve the strategic level routing problem of hazardous materials in marine waters over a multi-commodity network with multiple origins; minimization of expected risk cost was considered in the developed model. Thereafter, an efficient two-phase solution approach was proposed and the methodology was illustrated through a single hazmat problem

followed by a large scale case study of the marine transportation system of oil products in the Gulf of Mexico. Likewise, Iakovou (2001) presented a strategic interactive multi-objective network flow model that considered risk analysis and routing. This was also developed with specific reference to the Gulf of Mexico and permitted decision makers to customize model parameters to suit their needs.

In addition, van Dorp and Merrick (2011) reviewed a methodology which integrated simulation of Maritime Transportation Systems (MTS) with incident data collection, expert judgment elicitation and a consequence model. The risk analysis and assessment presented were within the context of oil spillage concerns. To illustrate the effectiveness of this methodology, three risk intervention case studies were evaluated. Of recent, Siddiqui and Verma (2013) proposed an expected consequence approach for assessing oil-spill risk from intercontinental transportation of crude oil and made use of oil spill global data to estimate accident probabilities.

2.4 Protection of Maritime Infrastructures - Sonar Placement Problems (SPP)

2.4.1 Sonar Placement Problem: Offshoot of the Set-Covering Problem

The problem of underwater sonar placement could be considered a variant of the classical Set-covering problem (SCP). The SCP is a NP-Hard problem in the strong sense (Garey and Johnson, 1979; Yelbay et al., 2012) and has found extensive use in a diverse range of applications. Scheduling, routing and telecommunications are some of the research areas in which various variants of the famous problem have been used. Introductory insights into SCP can be found in Yelbay et al. (2012) and Wang (2010).

2.4.2 Optimal Sensor Placement Problems

Chakrabarty et al. (2002), Wang and Zhong (2006), Altinel et al. (2008) and others have addressed the problem of placing the least number of sensors to cover all targets as a model objective. Likewise, other constraints can be included to depict actual problem requirements. For example, in wireless network deployment, it is often required to limit the proximity between any two adjacent sensors within the network (Sen et al., 2007). In essence, different modifications of the problem exist with modification of the objective function(s), the constraint(s), or both.

There also exist sensor placement models (such as Lin and Chiu, 2005) that stipulate coverage of a target by at least *k* sensors. In a sensor network, if all targets are covered by at least one sensor, then the network is said to provide complete coverage for all targets (Wang, 2010). Using the grid approach (introduced in Section 2.5) to approximate area coverage allows modeling of various variants of the sensor placement problem. Optimization of sensor orientation angles to maximize sensor coverage, minimization of sensor deployment costs, and maximization of the number of covered targets with respect to a given number of sensors are some of these variants found in literature.

2.4.3 Review of Selected Literature Related to Sensor Coverage and Grid Networks

Without solely restricting the literature on sensor placement to the maritime sector, there exist vast amounts of literature directly or indirectly related to the problem. Irrespective of the problem domain or problem statement, these studies involve attaining

an efficient placement methodology to satisfy a given requirement (or requirements) in the presence of some inhibiting factors (ranging from connectivity, physical structures, economic considerations, etc.).

Chakrabarty et al. (2002) presented an Integer Linear programming model to minimize the cost of sensors for complete coverage of a sensor field using a 3-D network grid to allocate sensors. Given a surveillance region and sensors of different types, the objective was to determine the placement and the types of sensors needed to be placed in the sensor field such that the desired coverage is achieved at minimum cost. Hence, the problem entailed placing sensors at grid points such that every grid is covered by a unique subset of these sensors. Although consideration was given to only two different types of sensors, the model could be easily extended to include more sensors. In addition, the study also proposed an alternate heuristic for solving large scale problems. Apart from its assumption of limitless budget (which may be applicable to generic sensors but not acoustic sonars due to prohibitively high costs), other identified model weaknesses in the work includes the assumptions that a sensor will always detect a target lying within its range and full coverage of all sensors.

Lin and Chiu (2005) developed a model for the deployment of a set of sensors on a grid point to monitor the sensor field under the constraints of cost limitations to achieve complete coverage. Coverage is considered to be *'full'* if distance between the particular grid point and a sensor is less than the sensor's detection radius. Otherwise, coverage is assumed to be ineffective (a binary decision). For practical purposes, this may not be applicable. Even if a cell is covered by the smallest of margin, it could still be considered as covered by the sensor (though with a loss of detection probability). Modeled as a

combinatorial optimization problem, the formulation minimizes the maximum distance between grid points and sensor locations. An algorithm based on simulated annealing is also presented for large scale problems. Like Chakrabarty et al. (2002), an identified model weakness is that sensor detection is considered to be binary: either a sensor covers a grid/cell or not. To address issues in computational times, Ngatchou et al. (2006) present efficient greedy algorithms for the optimal placement of multi-static sensors with cost and coverage as principal objectives using particle swarm optimization. Also, to stimulate interest in the use of underwater sensors, Heidemann et al. (2006) summarized their ongoing research in underwater sensor networks, highlighting potential applications and research challenges.

Using a Game Theory-based approach, Golen et al. (2007) proposed an underwater sensor field design placement. Given four different quadrants of water bodies with distinct underwater acoustics, the study derives the probability of visitation by a threat submarine based on a quadrant's acoustics. Based on the derived probabilities, a number of sensors are placed in each area to maximize detection capabilities of the intruder. The paper approximates sensor detection probabilities using Koopman (1980)'s search equation (an exponential function depicting loss in sensor capabilities as distances increase) in its formulation. Introducing other constraints, the Linear Programing LP technique used is based on the Mini-max Theorem. To prove model validity, a series of Monte Carlo simulations are also presented. Assumptions of non-overlap of detection coverage and non-consideration of false alarm probability rates (probability of signal detection in the absence of no threat) are some of the identified model weaknesses.

Extending the problem described in Golen et al. (2007), Golen et al. (2010) takes into consideration the acoustics of the area of interest to account for transmission loss due to geometric spreading, absorption by sea, ambient noise influence, etc. Substantial reference is made to the model described in Golen et al. (2007), adopting the Game Theory approach used in the prior paper. Each player must choose an optimal strategy by solving two LPs. For practicality, the defender's optimal strategy is ignored while the attacker's is analyzed; for comparison purpose, two distinct models were proposed: SAFD (size aware field design) which considers only geographic size of each sensor when allocating sensors and RAFD (radius aware field design) which allocates sensors to each sector by only considering radius that a sensor can attain in each sector.

For our study, the most relevant portion of Yates et al. (2011) is its first segment where consideration is given to the optimal placement of sensors whose goal is to detect vehicles on transportation networks posing potential threats to regional infrastructures. With a restriction to a single sensor type, the formulation adopts the zero-sum game approach and attempts to decrease the attack probability of an aggressor by monitoring and protecting the possible assault routes. The paper divides the network into a set of possible attacker entry points (origins), possible attacker targets (destinations) and intermediate nodes, and separates the defender sensor location problem from the network-based attacker shortest path problems.

Recently, Ghafoori and Altiok (2012) proposed an optimization model to keep ports and waterways under surveillance against threats from divers, torpedoes or explosives mounted on the hull of vessels. The proposed mixed linear integer programming model incorporates the feature of multiple sonar coverage and range-

dependent detection probability and strictly aims to mitigate the effects of a terrorist attack without considering other threat factors (e.g., natural conditions like inclement weather or visibility). As a realistic scenario for the model, the New York Harbor is presented as a test case. Also, a greedy heuristic approach which attains near-optimal solutions for large scale scenarios is presented; and numerical results are provided to show the accuracy and speed of the heuristic algorithm.

Other relevant works related to sensor placement for surveillance include: Meguerdichian et al. (2001), Dhillon et al. (2002), Clouqueur et al. (2003), Shakkottai et al. (2003), Dhillon and Chakrabarty (2003), etc., and others related to general sensor placements include: Esseghir et al. (2005), Mhatre et al. (2005), Krause et al. (2006), Armaou et al. (2006), Schoellhammer et al. (2006) Ibrahim et al. (2007), Altinel et al. (2008), Pashko et al. (2008), Lee and Kulesz (2008), Li et al. (2010), Wilhelm and Gokce (2010), Castelo et al. (2010), Yates et al. (2011), etc.

2.4.4 Heuristics: Case for the use of Approximation Algorithms

With small case problems (those with limited number of decision variables), a full enumerative search of all placement combinations is easily carried out and can be executed in a relative short period of time using widely available optimization tools such as CPLEX, Gurobi, etc., ensuring that a global optimum is always obtained. However, total enumerations to be considered increases considerably as the complexity of the problem increases. The computational complexity for exhaustive search increases exponentially with the number of available sites (Wang, 2010). This exponential increase in the solution space indicates large scale problems cannot be solved with exact

formulations (the execution time increases with an increase in the solution space). Like most integer programming (IP) problems, compromise is made between obtaining exact optimal solutions and arriving at a solution within a reasonable time frame. Hence, approximation algorithms (heuristics) are used in large scale and practical problems.

Some of the heuristics known to have been implemented in sensor placement literature are listed as follows.

Greedy Algorithm: Perhaps the greedy set algorithm is the most widely used heuristic in classical set cover problems. However, their myopic nature may easily yield solutions far from optimality (Yelbay et al., 2012). Greedy algorithms build up a solution sequentially, choosing the next solution space that offers the most obvious and immediate benefit. A greedy algorithm makes a locally optimal choice in the hope that this choice will lead to a global optimal solution (Cormen et al., 2009). While the algorithm is not guaranteed to always produce optimal solutions, it is a powerful, works quite adequately for a wide range of problems, and is also known to be computationally efficient for large scale problems.

A greedy algorithm terminates if a predefined optimal threshold has been achieved or the maximal allowable stages have been performed (Wang, 2010). Modifications of the greedy set cover algorithms exist in literature for solving different sensor problem formulations. Dhillon et al. (2002), and Zou and Chakrabarty (2004) are some of these. More recently, Ghafoori and Altiok (2012) used the greedy algorithm to solve an underwater sonar placement problem.

Simulated Annealing: As a generic probabilistic metaheuristic, Simulated Annealing provides an acceptable estimation of the global optimal solution for problems with a large search space. It is often used when the search space is discrete like sensor placement within well-defined discrete regions. The algorithm traces its root to metallurgy where a technique (Annealing) is used to describe controlled heating and cooling of a material to increase the size of its crystals, thus reducing its defects.

Simulated annealing has been applied in solving different sensor placements in Lin and Chiu (2005). Lin and Chiu (2005) formulated the sensor placement problem as a min-max mathematical optimization model where the accuracy of discrimination is the required objective. Thereafter, the simulated annealing-based algorithm is developed to solve the optimization problem. The cooling schedule of their algorithm initially assumes the deployment of sensors at all grid points. Afterwards, individual attempts are made to remove sensors if the cost constraint is not met. If a cost constraint is met, the procedure will be to attempt moving a sensor to another randomly chosen position. With the latter, the stopping criterion is also introduced and modified to improve efficiency. The experimental results presented indicate the proposed algorithm can efficiently obtain a high-quality and scalable solution.

Genetic Algorithm: Initially proposed by Holland (1975), Genetic Algorithm (GA) mimics the process of natural selection. As an evolutionary algorithm, it generates solutions to optimization problems using techniques inspired by natural evolution principles such as inheritance, mutation, selection, and crossover, etc. Seo et al. (2008), Wu et al. (2007), and Zhao et al. (2007) used genetic algorithm heuristics in the sensor network problems they addressed. Seo et al. (2008) proposed a hybrid steady state GA to

find high-quality solutions of the wireless surveillance sensor deployment and applied it to a practical surveillance case study. The proposed genetic algorithm introduces two-dimensional geographic crossovers and mutations as unique features of its proposal. In contributing to the node optimal design of heterogeneous Sensor Networks, Zhao et al. (2007) proposed a GA solution of integer planning based on the grid network model. Their method addresses the issue of maximizing energy saving efficiencies of a sensor network under multiple deployments.

ABC Algorithm: Initially developed by Karaboga (2005), the Artificial Bee Colony (ABC) is a relatively recent meta-heuristic technique based on the intelligent food search of honey bees. Based on Karaboga (2005) and later related works, for the purpose of food location, bees are classified as: 'employed' (Bees currently exploiting food sources and responsible for bringing food back to the hive and sharing food locations with other bees), 'on-lookers' (those awaiting arrival of the former to get information about food location) and 'scouts' (Bees exploring new food sources). The following, amongst others hold according to bee behaviors:

1. Probability of food-location choice made by 'onlookers' is dependent on the intensity/quality of the 'dance' performed by an 'employed' bee.
2. Continued role changes among the bees, e.g., when an 'employed' bee has fully exploited a food choice, it could transform into either an 'on-looker' or a 'scout'.

The natural behaviors of these bees as summarized above (with some modifications) constitute the basic algorithmic steps of ABC. The iterative algorithm initiates by associating each 'employed' bee with a randomly generated food source

(solution). Each ‘employed’ bee determines a new food source in the neighborhood of its currently associated food source and computes the food quantity of this new source. If this metric is higher than that of its currently associated food source, then this ‘employed’ bee moves to the new food source abandoning the old one, otherwise, it continues with the old one. After the completion of this process by all employed bees, information about their food sources is shared with the ‘onlookers’.

Sundar and Singh (2012) developed a hybrid heuristic, combining ABC with a local greedy search technique proposed by Ren et al. (2010) to solve a variant of the SCP. In comparison with other population methods considered in their work, the hybrid heuristic outperforms all (with the only exception being a single population method). However, their results indicate the hybrid heuristic is slower than some other population-based methods considered.

2.5 Sensor Deployment: Grid-based Placement

Random and grid-based methods are placement methodologies identified in literature. In deployment operations where the environment is unknown, random placement is often the only choice and sensors may be randomly distributed with the aid of say, aircrafts or vessels. The alternative is to deploy sensors on a predetermined sensor field with well-defined boundaries. The field is generally divided into grids and sensors are carefully deployed at the grid points. This approach is called grid-based placement (Lin and Chiu, 2005). Dividing a region of interest into cells on a grid basis enables depiction of the significance/importance of each cell by parameter values. Thus, sensor coverage for a cell is prioritized based on the individual cell parameter values.

Unlike most sensor network problems, especially in the wireless network domain which often deals with 'full' coverage (i.e., all grids are required to be covered by at least *n* number of sensors), underwater sonar deployment usually deals with 'partial' coverage with preference given to sub regions within the network grid considered to be more important compared to other sub regions.

The most common grid used in sensor deployment is the conventional square (rectilinear) grid system. However, it is known from literature that a triangular coordinates system (triangular grid or its derivatives such as the hexagonal grids) in sensor placement will offer a more efficient way of area coverage (Nagy 2003a, Nagy 2003b, Nagy 2004, and Nagy and Strand 2008). The optimal tessellation using regular triangles with side length equal to $\sqrt{3}Rs$ (where *Rs* is the radius of the sensor sensing disk) achieves the minimum sensor density for complete area coverage (Wang, 2010). Indeed, other regular polygons can also be used in sensor grid deployment.

Nagy (2003a) described a family of n-plane triangular grids (*Hexagonal, Triangular and 3-planes triangular grids*), showed geometric interpretation of both the hexagonal and triangular grids and proved both could be considered as sets of points in 3D digital space. Hexagonal and triangular grids are described as first and second members of a family of triangular grids (n-plane triangular grids). In addition, the neighborhood structures of the duals of the n-plane graphs are described. Nagy (2003b) presented a suitable method for the formulation of neighborhood sequences in a triangular grid. Algorithms were presented to find the shortest distance between two arbitrary points. The study further analyzed certain properties of the triangular and

hexagonal grids in 2D digital space, defining distances based on neighborhood relations that could be introduced in these grids.

Also, Nagy (2004) analyzed the 3-plane triangular grid and its dual from the basis of their neighboring conditions; and thereafter, extends this analysis to *n*-plane grids. Other grid systems such as 'circular' three-plane grids and the higher dimensional triangular grids are also analyzed. Nagy et al. (2008) dealt mainly with 3D graphs. Amongst others, it showed how non-standard 3D models could be embedded in 4D digital space and how a triangular grid could be described using 3D digital space. Unlike wireless network problems, where placement problems indicates either coverage of a unique grid point (considered the trivial case where every grid point should be occupied by a sensor) or placement of a sensor in a grid such that it is able to cover itself and some of its neighboring grid points with the use of the least number of sensors (considered as non-trivial), the placement problem in sonar deployment entails the latter but without the requirement of the coverage of all regions. This is due to the very high cost of sonars as specialized classes of sensors. In addition to the complexities involved in the non-trivial case of wireless network deployment, sonar placement entails selective deployment of the sonars (sensors) to cover sub-regions within the region of interest based on the level of importance attached to these sub-regions.

2.6 Interdiction and Fortification Models - Protection of vital Infrastructures

Ghafoori and Altiok (2012) provided a compendium of works related to the defense of critical infrastructures and argued that the studies were in response to security challenges as a result of terrorist attacks, especially after the 9/11 incident. Some of these

studies include Leung et al. (2004), Berry et al. (2005), Brown et al. (2005), Brown et al. (2006), Golen et al. (2007), Simonoff et al. (2007), Golen et al. (2010) Yates et al. (2011), etc. A component of a critical infrastructure is said to be vulnerable to attack unless it is specifically hardened or defended (Brown et al., 2006). Hence, Vulnerability analysis should consider the 'intelligence' of an adversary, its ability to discern information about a protected infrastructure and consequent use of this knowledge to compromise existing security measures. Making informed plans based on this reponse will assist in reducing vulnerability. Of course, hardening infrastructure from attack can be inherently expensive; however, understanding the nature of the most catastrophic attacks can improve a system's robustness for a given budget (Brown et al., 2006).

2.6.1 Attacker-Defender (A-D) and Defender Attacker-Defender (D-A-D) Models

According to Alguacil et al. (2014), A-D (Interdiction) models characterize a decision-making problem that involves two different agents –*'**A**ttacker'* and a *'**D**efender'*. The Attacker determines the set of out-of-service system components with the goal of maximizing the system damage subject to limited disruptive resources. The Defender (or system operator) reacts against the actions of the attacker to minimize harm done to the system.

However, defending those components that are identified as critical by an A-D model does not necessarily provide the best protection against a system disruption (Brown et al., 2006). D-A-D (Fortification) models help to assuage limitations inherent in A-D models. In essence, the D-A-D model produces a superior protection plan because it

considers an additional level of interaction between the defender and the attacker, and thereafter selects the optimal strategy to thwart the attacker's efforts (Brown et al., 2006). Essentially, it involves three agents acting sequentially: (i) a system planner who identifies the system components to be defended in order to minimize the damage, (ii) a disruptive agent who determines the most-damaging set of out-of-service components, and (iii) the system operator who responds to any disruptive action by means of some counteractive measures to minimize the overall damage (Brown et al. , 2006, Bier et al., 2007, Delgadillo et al., 2011,Yao et al., 2007, Yuan et al., 2014, and Alguacil et al., 2014).

2.6.2 Selected Literature Overview

To provide an optimal solution to a protection plan, Brown et al. (2005) proposed to extend a bi-level A-D model to a tri-level D-A-D model. Later, Brown et al. (2006) described and presented three different general models (A-D, D-A, and D-A-D models). Detailed description of the application of each model was presented under a case study application. In addition, applications to supply chain networks, military and diplomatic exercise were also discussed.

Literature indicates interdiction and fortification models have found more extensive applications in optimal allocation of resources in power grid networks. Prior to Brown et al. (2005), Salmeron et al. (2004) formulated a power grid interdiction problem as a max–min bi-level program (A-D model), and used Benders decomposition to solve it. Motto et al. (2005) transformed the model described in Salmeron et al. (2004) into an equivalent single level MIP by dualization of the lower level program and subsequently

solved the problem using a commercial solver. Yao et al. (2007) described a decomposition approach by iteratively solving smaller bi-level sub-problems of a proposed D-A-D model. Taking inspiration from Brown et al. (2006), the D-A-D model was formulated for defense planning of a power grid system. A drawback of Yao et al. (2007) is that it is computationally time consuming (Alguacil et al., 2014). In addition, Bier et al. (2007) proposed yet another heuristic iterative approach to determine the optimal defense of power system components using D-A-D techniques. To address the computational inefficiency observed in Yao et al. (2007), Delgadillo et al. (2011) developed another algorithm to solve this tri-level programming problem.

Most recently, Yuan et al. (2014) proposed a new approach using Column-and-Constraint Generation algorithm to find the optimal protection plan for a power grid system within an acceptable computational time. In addition, a case study of interdiction strategy based on the algorithm was carried out on a power grid network against terrorist attacks. Similarly, Alguacil et al. (2014) presented a new optimization-based two-stage approach for a D-A-D model aimed at attaining optimal allocation of defensive resources in an electric power grid so that its vulnerability against multiple contingencies is mitigated.

Chapter 3

Optimal Voyage Planning of Liquefied Natural Gas (LNG) Vessels: A Risk-Analysis Approach

3.1 Introduction

The global Liquefied Natural Gas (LNG) trade is expected to grow due to readily available supplies of gas worldwide and the renewed enforcement of a global climate regime (Kumar et al., 2011). Recent advances in technologies such as hydraulic fracking have made it easier to access oil and gas deposits that were hitherto difficult to explore. Interestingly, the success of a recent nuclear negotiation involving Iran, a country known to have very large oil and gas reserves, is expected to lead to political rapprochement and a consequent increase in global oil and gas supplies. It may interest readers to know that while a framework deal of the nuclear agreement was announced in April 2015, a comprehensive long term nuclear agreement was declared in July 2015.

The LNG industry's existing safety performance, especially in handling and transportation between regional markets is a factor contributing to the growth of LNG trade that needs to be sustained. Since LNG is usually transported over long distances across maritime infrastructures to their final destinations, safety along these sea routes is of paramount importance. As most of the confirmed gas reserves are located far away from their demand markets, usually between continents, it is apparent that maritime transportation will continue to play a pivotal role in the LNG trade.

Although historical records strongly indicate the involvement of LNG carriers in accidents to be negligible in comparison to other types of vessels (Vanem et al., 2008), the consequent economic and catastrophic losses that may occur when a single vessel is involved in an accident needs to be accorded great attention. Despite the industry-wide practice of equipping LNG vessels with special double hulls as well as different protective layers in their cargo containment systems, the worst case scenario of a successful breach in any of the vessel's tanks is enough motivation for a risk analysis-based approach for the vessel's voyage. In this chapter, we apply a risk-based methodology to the LNG routing problem we presented in Cho et al. (2014).

3.2 Methodology- Risk-based LNG routing

The details of the LNG Vehicle Routing Problem we proposed in Cho et al. (2014) are provided in appendix I and highlights of the risk-based model re-formulation are presented in Section 3.2.1.

Based on our adopted methodology, LNG spillage is identified as a consequence due to the following compelling reasons:

1. Compared to other indices such as ship damage and fatality (related to human lives), spillage can be easily quantified and its economic effects can be readily computed with widely available data.
2. Liquefied Natural Gas (LNG) spillage, through the compromise of vessel cargo containment can be attributed to other vessel accident scenarios such as Collisions, Groundings and Contacts. In fact, Vanem et al. (2008) identifies the

culpability of these three generic scenarios in about 90% of total risk related to LNG carriers.

Since risk information for rare events inherently suffers from sparseness of accident data, expert judgment is often used in developing frequency data for risk analysis (Mosleh et al., 1988, Li et al., 2014, etc.). However, experts' biases and individual experiences may affect the integrity of information recommended. Moreover, the information at their disposal will usually be solely based on their past experiences and may be inadequate in predicting the occurrence of future incidents. In the alternative, we propose the use and integration of data available from the transport of a closely related cargo vessel (Oil Tanker vessels) in our methodology.

In recognition of the past reliance on LNG imports by the US economy as well the future expansion of US LNG exports, the US Department of Energy (DOE) has funded several studies related to the large scale spillage of LNG. As a part of these studies, Spillage as a result of accidental or intentional breach of LNG cargo tanks has been studied in Hightower et al. (2013). Some parameters required as inputs in our methodology can be readily obtained from this study.

3.2.1 LNG Spillage -Risk Estimation Mathematical Model and Assessment

In addition to the indices included in Cho et al. (2014), we add the index $rt \in RT$ as defined in this section.

Sets, Indices, Variables, and Parameters:

RT Set of alternative routes from i to j

$rt \in RT$ Index of alternative routes

Hence, $x^1_{i,j,k}$ as defined in Cho et al. (2014) and provided in appendix I is re-defined as:

$x^1_{i,j,k,rt}$ Binary variable to represent whether the arc from $i, i \in V$ to $j, j \in V\backslash\{i\}$ by vessel type k using route rt;

All other variables remain as defined in Cho et al. (2014). In addition to parameters defined in Cho et al. (2014), the following parameters are included:

$nDAY_{i,j,rt}$ (Normalized) Estimated travel time from i to j: $= distance(nautical\ miles)$ using route rt;

$nRisk_{rt}$ (Normalized) Aggregated Risk consequence on alternative route rt

λ Risk tolerance (between 0 and 1)

Objective Functions and Constraints:

The objective function (aggregated cost) is redefined in equation (3.1),

$$\min \left(\begin{array}{c} (1-\lambda) \sum_{rt \in RT} \sum_{(i,j) \in A} \sum_{k \in K} (nDAY_{i,j,rt} \times DSC_k \times x^1_{i,j,k,rt}) \\ +\lambda \sum_{rt \in RT} \sum_{(i,j) \in A} \sum_{k \in K} (nRisk_{rt} \times DSC_k \times x^1_{i,j,k,rt}) \end{array} \right). \quad (3.1)$$

All constraints presented in Cho et al. (2014) still remain applicable, albeit with the new indexing and variable declarations taken into consideration. For example, equation (2) in Cho et al. (2014) becomes equation (3.2),

$$\sum_{rt\in RT}\sum_{k\in K} x^1_{s,s+|S|(t-1),k,rt} = 0, \qquad \forall s \in S, t \in T\backslash\{1\}. \tag{3.2}$$

Likewise, equation (16) in the same study becomes equation (3.3),

$$y_{i,j} \geq \alpha V C_r x^1_{i,j,r,rt}, \qquad \forall (i,j) \in A, r \subseteq K, rt \in RT. \tag{3.3}$$

In addition, we include equations (3.4) as new constraints in our re-formulation,

$$\sum_{rt\in RT} x^1_{i,j,k,rt} = 1, \qquad (i,j) \in A, k \in K. \tag{3.4}$$

Equations (3.4) ensure only a single route is chosen for any voyage.

Risk Assessment: In accordance with the terminologies adopted in the Risk literature and our specific problem, the first two conditional probabilities in equation (2.2) of Chapter 2 are *'The expected consequence given the occurrence of a spill incident j'* and *'Conditional probability of a spill occurrence given that the breach (in the LNG cargo containment system) has already occurred*' respectively, and the last term is the *'Probability of a breach occurrence'*.

Risk on a route rt can be computed as equation (3.5),

$$R_{rt} = \sum_{w\in W} C^w_{rt} \times V^w_{rt} \times T^w_{rt}\,, \tag{3.5}$$

It should be noted that since neither of the risk component in equation (2.2) is strictly a function of the same index (j and k in equation 2.2), an index w of set W is introduced to indicate this. In reality, the risk components on a route segments are non-

homogenous. Therefore, we use segments to represent route subdivisions where a route is made of segments or zones $l, l+1, \ldots\ldots, q$. Hence, risk on a segment l is given in equation (3.6),

$$R_{rt,l} = \sum_{w \in W} C_{rt,l}^{w} \times V_{rt,l}^{w} \times T_{rt,l}^{w} \,. \tag{3.6}$$

For ease of notation, we drop subscript rt and the expected consequence for segment $l+1$ is given in equation (3.7),

$$R_{rt,l+1} = \sum_{w2 \in W2} \left((1 - T_{l}^{w2}) \sum_{w \in W} C_{l+1}^{w} \times V_{l+1}^{w} \times T_{l+1}^{w} \right), \tag{3.7}$$

where $W2$ represents the set of activities (breaches) that do not result into LNG spillage.

Likewise, the expected consequence on segment $l+2$ is given in equation (3.8),

$$R_{rt,l+2} = \sum_{w2 \in W2} \left((1 - T_{l+1}^{w2}) \sum_{w \in W} C_{l+2}^{w} \times V_{l+2}^{w} \times T_{l+2}^{w} \right). \tag{3.8}$$

Thus, total expected consequence on route rt with a total number of q segments is then shown in equation (3.9a and 3.9b),

$$Risk_{segment\ 1} + \sum_{k \in K \setminus \{k \neq 1\}} \left(\sum_{w2 \in W2} \left(Risk_{segment\ k} \prod_{l \in K \setminus \{l > 1, l \leq k\}} (1 - T_{l-1}^{w2}) \right) \right) \text{and} \tag{3.9a}$$

=

$$Risk_{segment\ 1} + \sum\nolimits_{k=2}^{q} \left(\sum_{w2 \in W2} \left(Risk_{segment\ k} \prod_{l=2}^{k} (1 - T_{l-1}^{w2}) \right) \right). \tag{3.9b}$$

Based on studies in Hightower et al. (2013), spill events considered are: '*Small/No spill m', 'Medium spills M', and 'Large spills L'*. Since the consequence of low breach size typically falls within current spill detection and safety systems on

existing LNG ships in active service (Hightower et al., 2013), we reasonably assume an LNG vessel continues to travel except when a medium or large breach occurs (implying the occurrence of a small breach doesn't terminate the voyage).

Therefore, spill risk on route rt is,

$$Risk_{route\ rt} = C^M V^M T^M + C^L V^L T^L, \tag{3.10}$$

and spill risk on a segment l is

$$Risk_{route\ rt,segment\ l} = C^M_{rt,l} V^M_{rt,l} T^M_{rt,l} + C^L_{rt,l} V^L_{rt,l} T^L_{rt,l}\ . \tag{3.11}$$

Hence, Expected consequence for segment $l+1$ (we drop subscript rt for ease of writing) is on route rt is,

$$\begin{aligned} Risk_{segment\ l+1} &= (1 - T^L_l)(C^M_{l+1} V^M_{l+1} T^M_{l+1} + C^L_{l+1} V^L_{l+1} T^L_{l+1}) \\ &+ (1 - T^M_l)(C^M_{l+1} V^M_{l+1} T^M_{l+1} + C^L_{l+1} V^L_{l+1} T^L_{l+1}) \text{ and} \qquad (3.12a) \\ &= (2 - T^L_l - T^M_l)(C^M_{l+1} V^M_{l+1} T^M_{l+1} + C^L_{l+1} V^L_{l+1} T^L_{l+1})\ . \qquad (3.12b) \end{aligned}$$

Likewise, expected consequence for segment $l+2$ is given in equation (3.13),

$$Risk_{segment\ l+2} = (2 - T^L_{l+1} - T^M_{l+1})(C^M_{l+2} V^M_{l+2} T^M_{l+2} + C^L_{l+2} V^L_{l+2} T^L_{l+2})\ , \tag{3.13}$$

and total Expected consequence on route rt with a total number of q segments is

$$Risk_{route\ rt} = Risk_{segment\ 1} + \sum_{k=2}^{q} \left(Risk_{segment\ k} * \prod_{l=2}^{k} (2 - T^L_{l-1} - T^M_{l-1}) \right). \tag{3.14}$$

3.2.2 LNG Spillage - Expected Consequence of a spill event

Apart from loss of cargo, the incident of LNG spillage can lead to pool fires, damage to vessel steel structures partly caused by cryogenic LNG flow, large fires, human casualty, etc. (Hightower et al., 2013). While all these are identified as possible consequences of LNG spillage, only the loss of cargo consequence can be readily ascertained without extensive use of complex estimation models or large scale expensive experimental procedures. LNG Spill size volume as a function of breach volume extracted from experimental results presented in Hightower et al. (2013) is shown in Table 3.1.

Table 3.1: Spill size volume as a function of breach volume (Hightower et al., 2013)

Spill Size	**LNG Flow Rate**	**Volume Rate Loss per time t**
Small	0.001X >	< 0.001Xt
Medium	~ 0.167X	~ 0.167Xt
Large Spill	X	Xt

where X is the volume of LNG cargo

Using the loss of cargo criterion, all that is needed is the volume of cargo as well as its current market price (or price previously agreed to in the contractual agreements). Hence, for our purpose, we consider the expected consequence of LNG spillage as the

cost per billion cubic meters (bcm) cost of cargo spill (to include cargo loss, contract penalty –if any, regulatory environmental fee–if any, etc.). It should be noted that different quantitative models have been developed for the cost involved in cleaning crude oil spills (e.g., Etkin, 2000, Psarros et al., 2011, etc.). However, unlike Oil spills, there is no need for environmental clean-up of LNG spills because the liquid will quickly evaporate, thus making the environmental cleaning of LNG spills unnecessary.

3.2.3 LNG Spillage - Vulnerability of LNG Vessels

The probability of a successful breach on a vessel (and by extension, its tanks) cannot be easily ascertained. The double-hull feature and other features on the vessel suggest minimal intrusion in the case of small collisions. However, deliberate attacks on vessels, severe unexpected inclement weather, Groundings or Collisions with very large vessels, etc. are scenarios expected to result into high probabilities of successful breaches.

We propose estimation of this probability thus:

1. Identify an acceptable division of alternate sea routes between origin ports and regasification terminals using division of world oceans (navigated by the LNG vessels) into 31 zones as done in Li et al. (2014). In the alternative, the approach adopted in Siddiqui and Verma (2013) where route divisions are determined by lines of longitude and latitudes will also suffice.
2. Depending on the events under consideration, a database of events is obtained and its contents analyzed. The database (related to piracy attacks) we use in our study

is that made available by the National Consortium for the Study of Terrorism and Responses to Terrorism, START (2013).

3. For each segment in the route, a corresponding probability is computed based on a utility function. Events having the highest frequency are assigned a vulnerability of 1 or a probability close to 1.

3.2.4 LNG Spillage- Probability of breach occurrence

Ideally and in accordance with accepted risk methodologies, this probability should be obtained from historic safety data in LNG shipping and is usually computed as incident frequency per ship year (e.g., in Papanikolaou, 2006). Without access to such recent data, we use data presented in Vanem et al. (2008) and identify the *'failure of cargo containment system'* as a specific accident category related to LNG spillage. Amongst other reasons, the category is chosen from intuition. Moreover, the referenced study clearly identified it as an incident that could have resulted from other categories such as Groundings, Collisions and Contacts.

Hence, T_l^i from equation (3.14) can then be estimated in equation (3.15),

$$T_l^i = \alpha_i \times frequency\ per\ ship\ year \quad \text{and} \tag{3.15}$$

$$= \alpha_i \times 0.0095\,, \tag{3.16}$$

where $i \in (M, L)$. Again, due to lack of historic data on LNG vessel spills, we make use of oil tanker spill statistics compiled by the International Tanker Owners Pollution Federation, ITOPF (2013) to approximate α_i. While we acknowledge that the two spillages are quite different, we rationalize that spill category based on volume of oil

spillage as reported by ITOPF is similar to the LNG spill types we have adopted and that the proportions of these categories in both spill situations are analogous because liquid natural gas handling is more like handling oil (Shukri et el., 2004).

Table 3.2: Comparison- LNG Spill Types (Hightower et al., 2013) versus ITOPF oil spill sizes (ITOPF, 2013).

LNG Spill types	Oil Spill Size equivalents
Small Spill	<7 tonnes (<50 bbls)
Medium Spill	7–700 tonnes (50–5,000 bbls)
Large Spill	700 tonnes (>5,000 bbls)

The ITOPF data includes the type of oil spilled, the spill amount, the cause, location of the incident, and the vessel involved. Although the actual amount spilled is also recorded, the spill size categorized is as shown in Table 3.2.

With about 10,000 incidents, the vast majority of all incidents (81%) fall under the smallest category i.e. <7 tonnes (ITOPF, 2013). In the absence of specific LNG spill data for the failure of cargo containment system, we use available data on oil spills related to historical spillage from 1970-2013 and approximate α_i based on data in Table 3.3.

We approximate α_i for both the medium and large spills by aggregating the spill incidences. We implicitly assume that the reported incidents as categorized are indicative of their contribution to the total reported number of incidents.

Table 3.3: Available oil Tanker Spill Statistics (ITOPF, 2013)

Spill Year	OIL SPILLS Number of spills	
	7-700 tonnes	> 700 tonnes
1970-1979	543	245
1980-1989	360	94
1990-1999	281	77
2000-2009	147	35
2010-2013	20	8
Total	1351	459
Total Reported incidents=10000		

Hence, $\alpha_M = 0.1351, \alpha_L = 0.0459.$.

3.3 Computational Study- Case Study Results

Here, we present results using a modification of the test case we described in Cho et al. (2014). While the liquefaction plant is a country in the Middle East, required depots to be served are located in North America, Europe, and South America. Data presented in Cho et al. (2014) such as the specification of LNG tankers, customer demands in each time periods and other parameters are maintained. Where applicable, data presented for

the first three customer demands in the terminals are maintained to coincide with the three customers identified. However, distance (in Nautical miles Nm) and computed raw risk data (based on section 3.2) in this case study are shown in Tables 3.4 and 3.5. In addition, uncertainties as a result of boil off gas BOG introduced in Cho et al. (2014) are excluded in the implementation presented in this section.

Table 3.4: Distance (Nautical miles Nm) between depot and liquefaction terminals

		Terminal 2	Terminal 3	Terminal 4
Depot	Route 1	9789	5028	8376
	Route 2	12597	10165	9540
Terminal 2	Route 1		4781	5663
	Route 2		5259	6229
Terminal 3	Route 1			4512
	Route 2			-

Readers should note that in this case study, only a single route option is available for voyage between Terminals 3 and 4. This means that there is no alternative (and navigable) vessel route choice between the two terminals that can accommodate the LNG vessels.

Table 3.5: Raw risk data between depot and liquefaction terminals

		Terminal 2	Terminal 3	Terminal 4
Depot	Route 1	0.000453	0.000294	0.000423
	Route 2	0.000324	0.000384	0.000268
Terminal 2	Route 1		0.000048	0.000050
	Route 2		0.000095	0.000019
Terminal 3	Route 1			0.000108
	Route 2			-

The model is implemented in GAMS and solved using CPLEX. All MIPs are solved within a relative tolerance of 3% duality gap, and all computational runs are made on a 3.00 GHz Intel Xeon machine with 400 GB of memory, running CPLEX version.

Results obtained for the case study is summarized below:

1. Irrespective of decision maker preference, choice of route between ‘the depot and terminal 3’, ‘terminal 2 and terminal 3’, ‘terminal 3 and terminal 4’ are always the same, given that such a voyage is included in the optimal delivery plan. While only a single route option exists in the latter voyage (terminal 3 and terminal 4),

distance and risk considerations favor a particular alternate route in the former voyages.

2. For all other voyages (apart from those identified above), choice of the alternate routes is dependent on the decision maker's preference. Again, this is applicable if the particular voyage is included in the optimal delivery plan returned by the model. Figure 3.1 shows a sample optimized 6 month delivery schedule/routing plan from day D+1 to day D+192. In addition, alternate choice of voyage route is indicated.

3. Figure 3.2 indicates that the appropriate choice of λ for the case study lies between 0.4 and 0.6. Neglecting either of the two constituents in the objective function doesn't give the least aggregated cost.

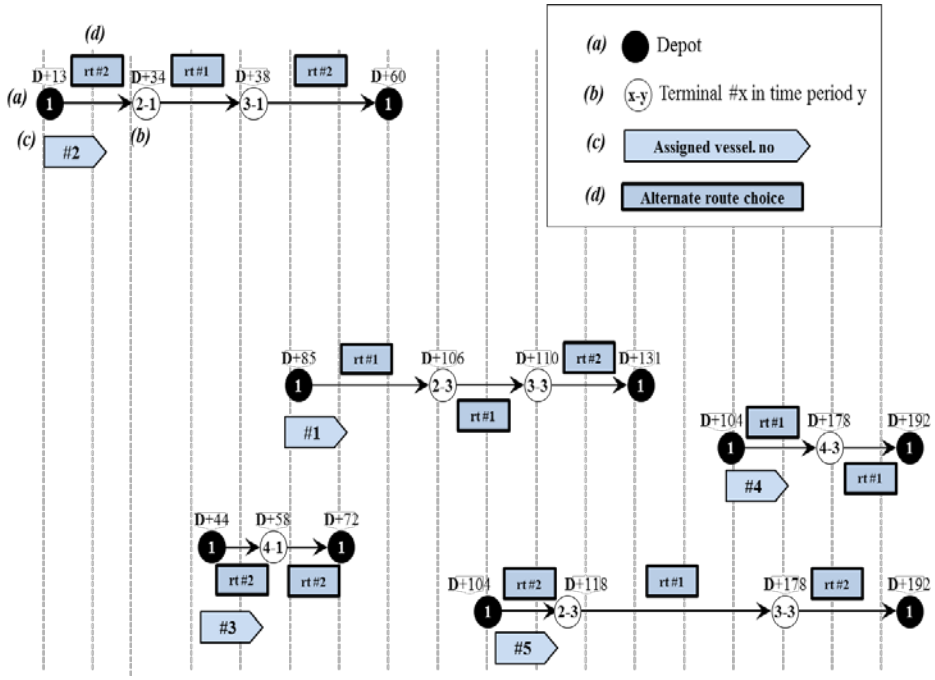

Figure 3.1: Sample Delivery Schedule

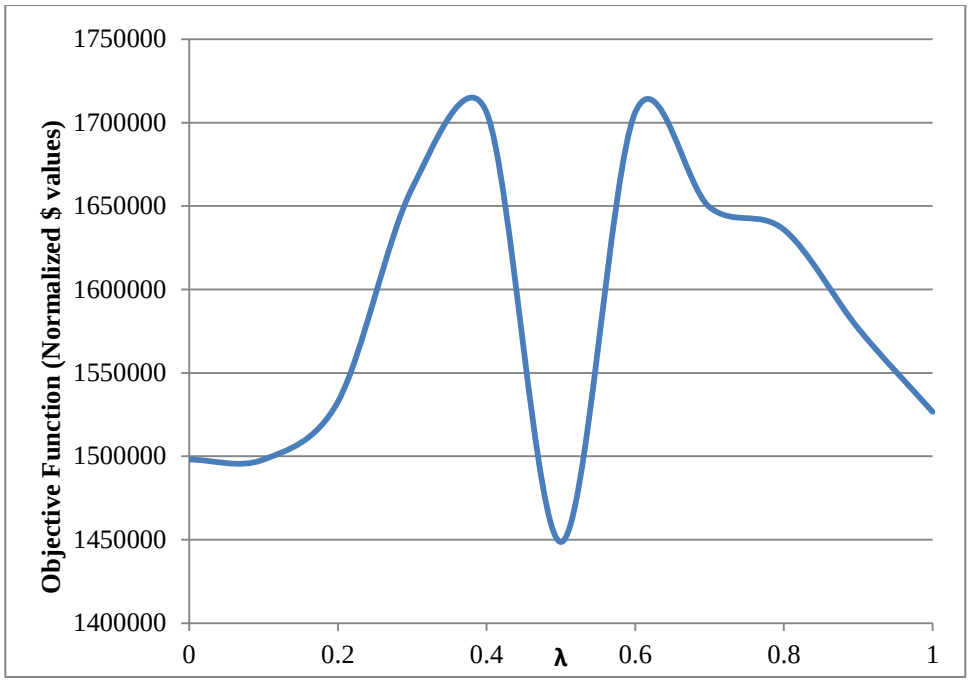

Figure 3.2: Objective function versus decision maker's preference

3.4 Conclusion

In this chapter, we identified LNG vessels (and their cargoes) as vital maritime assets that should be protected, and presented a framework for risk-based transportation of LNG vessels. The framework considers alternate voyage routes in determining an optimal cargo delivery schedule between liquefaction and re-gasification terminals. Due to lack of data as a result of the current lofty safety records in the LNG transportation industry, some parameters were estimated from Crude oil, another petrochemical energy resource. Afterwards, we integrated the described risk methodology into the model we described in Cho et al. (2014) and used our methodology to solve a realistic sample case study.

Chapter 4

Optimal Deployment of Underwater Sonar System

4.1 Introduction

The sonar placement problem described in this chapter efficiently determines the regional locations to allocate different types of sonars such that overall detection probabilities is optimized in a multi-period deployment scheme, taking criticality (regional importance) into considerations under a maritime environment.

Of the three SPP problems identified in literature (see Chapter 1), we address the Area coverage problem due to the emerging trend that terrorism, piracy and arson attacks have evolved into targeting areas of interests or regions rather than specific targets in the hope of having better odds at accomplishing their heinous goals. The coverage problem entails a sonar is able to provide coverage to its region of placement as well as surrounding regions within the limits of its coverage (in terms of detection ranges and orientations). However, due to Acoustics theory, degradation exists in these detection probabilities as we recede away from the point of placement. This degradation is known to be non-linear in nature. Some existing studies, especially in the terrestrial domain have modeled the gradual degradation in sensor strength using exponential functions with parameters determined from the specific sensor characteristics and deployment environments. While these parameters are not only difficult to estimate, the approach also increases the complexity of the problems, introducing non-linearity to model multiple-detection based on sonar range. As such, our methodology entails a division of a sonar

influence into three distinct regions: *primary* (point of sonar placement), *secondary and tertiary regions*. Our opinion is that rather than assigning a function to the detection probabilities in these regions, experts' opinion should be solicited.

Our study contributes to the literature of maritime security by proposing a new multi-objective mathematical model for placing underwater sonars to identify potential underwater threats. Using hexagonal grid-based system, the model integrates both static and mobile sensors in a placement methodology within a multi-period deployment scheme. In comparison to their terrestrial equivalents, underwater sonars are known to be quite expensive. For example, Borowski et al. (2008) reports the cost associated with a certain diver detection system based on sonar technology used by the United States coast guards to be approximately $300,000 for each system. Thus, our placement methodology is to be achieved under strict budgetary limitations.

4.2 Formulation

In this section, a formal definition of our sonar placement formulation for surveillance of maritime infrastructures is presented.

4.2.1 Model Parameters, Indices and Sets

The relative importance assigned to a section of the AOI (Area of Interest), cell (i, k) at period *t* is reflected by its criticality index h_{ikt}. Expert judgments and aid of a utility function may be used in this regard. While unit costs of static and mobile sonars are denoted by c_a and c_b respectively, *B* is the available budget and the maximum number of coverage permitted for a cell is denoted by $\bar{c}$. Detection probabilities for static

sonar type a and mobile sonar type b are denoted by ${p_a}^z$ and ${p_b}^z$ respectively, where z is an index for a sonar's coverage strength. $z \in \{p$- primary coverage, q - secondary coverage, t- tertiary coverage$\}$.

Finally, sets N_{ikaa^z} represents the set of cells in the neighborhood of cell (i,k) [which has static sonar of type a placed in it] that can be covered by cell (i,k) with detection probability p_{a^z}. N_{ikbb^z} is a similar set representing the mobile sensors. Also, the set of cells in the neighborhood of cell (i,k) within hop distance d is denoted by M_{ikd}, where d is an index describing these hop movements. The mobile sonars at period t may relocate to any member of this set in the next period $t+1$.

4.2.2 Decision Variables

Binary variables $X_{i,k}^{a}$ equal 1 if a static sonar of type a is located in cell (i,k) and binary variables $Y_{i,k}^{b,t}$ equals 1 if a mobile sonar of type b is located in cell (i,k) at period t. Otherwise, these variables will equal 0. Similarly, $Y_{i,k,d}^{b,t}$ is a dependent variable that equals 1 if mobile sonar of type b is located in a cell (i,k) at period t and within 'd' hop movements when it moves from time $t-1$; and equals 0 otherwise. This relationship exists between $Y_{i,k}^{b,t}$ and $Y_{i,k,d}^{b,t}$: $\sum_d Y_{ikd}^{b,t} = Y_{ik}^{b,t}$. Finally, $W_{i,k}^{a,a^z}$ and $W_{ik}^{b,b^z,t}$ are integer variables representing the number of times a cell (i,k) is covered by static sonar type a with coverage strength a^z; and the number of times a cell (i,k) is covered by mobile sonar type b with coverage strength b^z at period t respectively.

4.2.3 Mathematical Model

We formally define our sonar placement model in this sub-section. The multi-objective model is formulated as shown in the following equations:

$$\max_{Q\in(Qa,Qb)} \sum_i \sum_k \sum_t h_{ikt} * Qa_{ik} + \sum_i \sum_k \sum_t h_{ikt} * Qb_{ikt} , \tag{4.1}$$

$$\max_W |T| * \sum_i \sum_k \sum_a \sum_{a^z} W_{ik}^{a,a^z} + \sum_i \sum_k \sum_b \sum_{b^z} \sum_t W_{ik}^{b,b^z,t} , \tag{4.2}$$

Subject to:

$$\sum_a c_a . \sum_i \sum_k X_{ik}^a + \sum_b c_b . \sum_i \sum_k Y_{ik}^{bt} \leq B \quad \forall\, t , \tag{4.3}$$

$$\sum_a \sum_{(f,h)\,\in\, N_{ikaa^z}} X_{fh}^a + \sum_a X_{ik}^a \geq W_{ik}^{a,a^z} \quad \forall i,k,a^z , \tag{4.4}$$

$$\sum_b \sum_{(f,h)\,\in\, N_{ikbb^z}} Y_{fh}^{bt} + \sum_b Y_{ik}^{bt} \geq W_{ik}^{b,b^z,t} \quad \forall i,k,t,b^z , \tag{4.5}$$

$$\sum_a W_{ik}^{a,a^z} + \sum_b W_{ik}^{b,b^z,t} \leq \bar{c} \quad \forall\, i,k,t,a^z,b^z , \tag{4.6}$$

$$\sum_a X_{ik}^a + \sum_b Y_{ik}^{bt} \leq 1 \quad \forall\, i,k,t , \tag{4.7}$$

$$Y_{ik}^{b,t} \leq Y_{ik}^{b,t+1} + \sum_{(f,h)\,\in\, M_{ikd}} Y_{fhd}^{b,t+1}, \quad \forall\, i,k,b,d,t , \tag{4.8}$$

$$\sum_d Y_{ikd}^{b,t+1} \leq 1 \qquad \forall\, i,k,b,t , \tag{4.9}$$

$$\sum_{i,k} Y_{i,k}^{b,t} = \sum_{i,k} Y_{i,k}^{b,t+1} \qquad \forall\, b,t , \tag{4.10}$$

$$\sum_b \sum_i \sum_k Y_{ik}^{bt} \geq SR * \left(\sum_b \sum_i \sum_k Y_{ik}^{bt} + \sum_a \sum_i \sum_k X_{ik}^{a} \right) \quad \forall t \,, \tag{4.11}$$

$$-Qa_{ik} = \sum_{a^z} W_{ik}^{a,a^z} \ln(1 - p_{a^z}) \; \forall \; i, k, a \,, \tag{4.12}$$

$$-Qb_{ikt} = \sum_{b^z} W_{ik}^{b,b^z,t} \ln(1 - p_{b^z}) \; \forall \; i, k, b, t \,, \tag{4.13}$$

$$X_{ik}^{a}, Y_{ik}^{b,t} \epsilon \; B; \; W_{ik}^{a,a^z}, W_{ik}^{b,b^z,t} \epsilon \; I^{+} \,; Qa_{ik}, Qb_{ikt} \geq 0 \,. \tag{4.14}$$

Constraints (4.3) are budgetary constraints indicating available budget for sonars at each period t. Constraints (4.4) and (4.5) depict cell sonar coverage: For a cell (i, k) to be covered by detection strength a^z, a static sonar should exist to cover itself (primary coverage) and those in its neighborhood (secondary and tertiary coverages). Similar argument exists for each mobile sonar at period t. Constraints (4.6) show limitation in the total number of sonars covering a cell at any period *t*. Given that sonar detection probabilities are generally high (usually >=0.95), it is reasonable to limit the total number of sonars covering a cell to a small integer, similar to the approach in Ghafoori and Altiok (2012). An alternate approach may be to limit the total detection probabilities attained by a cell (i, k) to a certain detection probability. Constraints (4.7) provide limitation in the total number of sonars allocated to a cell at period t. Limiting the number of sonar allotted to a cell (i, k) under budget limitation to unity is well documented in literature. Constraints (4.8, 4.9, 4.10 & 4.11) portray sonar mobility: Constraints (4.8) - movement between successive periods, Constraints (4.9) - choice of a single hop distance *d* chosen if sonar movement occurs across periods, Constraints (4.10) - preservation of the total number of mobile sonar type deployed in each period and

Constraint (4.11) - sonar density. In the sensor literature, there exist different derivations for sensor density, depending on the SPP problem under consideration (e.g. in Wang et al. (2008), a derivation for the k-coverage problem is provided). Motivations behind constraints (4.12 & 4.13) are also presented afterwards. Finally, constraints (4.14) state the bounds and logical restrictions on the decision variables.

4.2.4 Objective Function (4.1): Derivation and Implied Constraints

For static sonars, the objective function can be modeled in equation (4.1),

$$\max_{W} \sum_{i}\sum_{k}\sum_{t} h_{ikt} * \left(1 - \prod_{a^z}(1 - p_{a^z} * W_{ik}^{a,a^z})\right) \quad \text{and} \tag{4.1a}$$

$$= \min_{W} \sum_{i}\sum_{k}\sum_{t} h_{ikt} * \left(\prod_{a^z}(1 - p_{a^z} * W_{ik}^{a,a^z})\right). \tag{4.1b}$$

It should be noted that equation (4.1b) is analogous to the minimization of expected consequence (risk measure of interest) in risk analysis parlance. In risk analysis terminology, h_{ikt} depicts consequence level and $\prod_{a^z}(1 - p_{a^z} * W_{ik}^{a,a^z})$ indicates the vulnerability of an infrastructure. In addition, equation (4.1b) suggests that our model implicitly assumes uniformity in threat probabilities for the infrastructures. We refer interested readers to Ghafoori and Altiok (2012) and Willis (2007) for a detailed presentation of how expected consequence and its constituents (consequence level, asset vulnerability and threat probabilities) are addressed in the risk analysis literature. Also Chapter 2 of this dissertation provides a summarized insight to these constituents.

Equating (4.1b) to an exponential function as shown in Hsieh (2003) gives:

$$e^{-Qa_{ik}} = \prod_{a^z} (1 - p_{a^z} * W_{ik}^{a,a^z}). \tag{4.1c}$$

The objective equation becomes,

$$\min_W \sum_i \sum_k \sum_t h_{ikt} * e^{-Qa_{ik}} \text{ and} \tag{4.1d}$$

$$== \max_W \sum_i \sum_k \sum_t h_{ikt} * Qa_{ik} . \tag{4.1e}$$

And constraints (4.1f ´) and (4.1f ´´) need to be added to complete the linearization:

$$e^{-Qa_{ik}} = \prod_{a^z} (1 - p_{a^z} * W_{ik}^{a,a^z}) \quad \forall\, i,k,a \text{ and} \tag{4.1f ´}$$

$$Qa_{ik} \geq 0 \qquad \forall\, i,k . \tag{4.1f´´ }$$

However, constraint $(4.1f'')$ can be linearized by taking its natural log,

$$-Qa_{ik} = \sum_{a^z} \ln(1 - p_{a^z})^{W_{ik}^{a,a^z}} \ \forall\, i,k,a \text{ and} \tag{4.1g}$$

$$-Qa_{ik} = \sum_{a^z} W_{ik}^{a,a^z} \ln(1 - p_{a^z}) \ \forall\, i,k,a \ . \tag{4.1h }$$

Equations (4.1h) are constraints (4.12) as presented earlier in Section 4.2.3. Similar derivations apply for the mobile sonars.

4.3 Numerical Experiments

This section presents experiments to highlight performance of the model. We also use the experiments to show the desirability of our proposed grid system.

4.3.1 Description of a test case

Due to inaccessibility of specific data as well as implied security concerns, we had no access to required marine data to solve a real world case study. However, we were privileged to have access to incomplete data of port operations in a busy port (We are unable to name the specific port in this dissertation due to security and confidentiality concerns). Descriptions of the test case in this chapter and data used in our experiments are to a large extent, based on actual (though incomplete/partial) real world data. Though semi-hypothetical, the example case study which involves sonar deployment in a sea route network traversed by ocean-going vessels in a port shows the applicability of the methodology. We consider a maritime environment involving routes of different types of vessels where the choice of route is determined by the cargo (The cargo we consider are LNG, Oil, Steel, Agricultural produce, and Motor vehicles).

We discretize regions into grids and assign criticality indices to all the grids. The criticality is based on the type of sea route as well as the number of sea routes passing through a cell. For example, cells or grids with vessels more vulnerable to attack such as LNG vessels are considered to be more important. Criticality indices are assigned based on this importance. Of course, criticality can also be influenced by the existence of important infrastructures or the fact that some routes may be located in close proximity to port entrances. In addition, this criticality changes with time. Considering criticalities of vessel routes based on seasonality, we use twelve discrete periods to depict monthly change in vessel routes (as a result of tidal movements, seasonal changes, weather condition, etc.).

4.3.2 Sonar Types and Coverage

For simplicity, detection ranges of the sonars chosen are limited to coincide with their coverage regions (primary/secondary/tertiary) and these regions are taken to be unit grids. Types of sonars considered (with different costs and coverage) include Omni-directional (360° coverage range) sonars with coverage strength of two grid units (primary and secondary detections), 180° Coverage sonars with coverage strength of three grid units (primary, secondary and tertiary detections): either upper hemisphere or lower hemisphere coverage range; and 90° Coverage sonars with coverage strength of three grid units (primary, secondary and tertiary detections): either 1st, 2nd, 3rd or 4th quadrant coverage range.

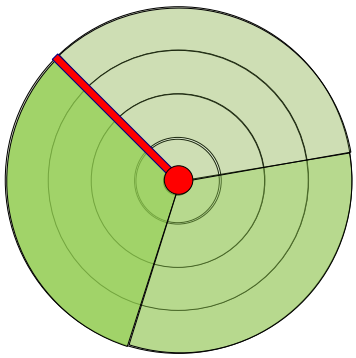

(a) Omni-directional Range

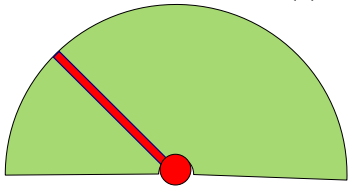

(b) 180° Coverage Range

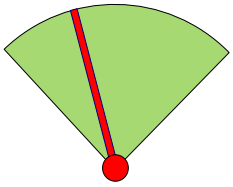

(c) 360° Coverage Ranges

Figure 4.1: Sonar Types used in test case

Also, the sonar density is taken to be a minimum of 50%. This restriction can be modified to suit various density coverage requirements based on the coverage problem being solved or it can be relaxed without having much influence on deployment solutions. It should be noted that the choice of model parameters and budget constraints are major determinants of this influence.

Table 4.1: Experiment Setting

Type	Coverage Orientation	Coverage Range	Cost (10^3 $)	Detection Probabilities		
				Primary	Secondary	Tertiary
Type 1	360°	2 Grid Units	18.00	0.99	0.78	N/A
Type 2	180°	3 Grid Units	15.00	0.99	0.65	0.45
Type 3	90°	3 Grid Units	12.00	0.99	0.50	0.35

The costs shown are for the static sonars and mobile sonars are assumed to cost twice as much as their static equivalents

Table 4.1 show major parameters used in the sample problem. It should be noted that a different set of parameters (Biobaku et al., 2014) designed to be easily solved, though with some impractical parameter choice values, was used in confirming model validity/verification. For sonar mobility, we restrict the movements of our mobile sonars to a maximum of three hops. This restriction takes into consideration that energy requirements to achieve relocation is limited. Similar to what obtains in the sensor

coverage literature; we define a 'hop' as a movement from point of deployment in period t to a new position in period $t + 1$ across neighboring regions. Hence, mobile sonars at period t can be re-positioned to neighboring regions within 1st, 2nd or 3rd hop(s) of their point of deployment at period *t+1*.

4.3.3 Experimental Setup

We designed experiments using two distinct experimental settings to capture extremities in possible allocations. Whereas an initial experimental set (referenced in Section 4.3.2) used for model validation/verification was designed to be easily solved, its parameter values are not completely practical. Conversely, the experimental set presented in this dissertation provides a more compelling attempt at practicality in its choice of parameter values but does not readily help in confirming model validity/verification. A discussion by which these parameters are estimated is beyond the scope of this dissertation.

Prior to implementing the model to include both types of sonars as well as multi-periodicity, we carry out experiments using only static sonars in a single period and optimize using only the first objective function. This simple approach permits us to establish the preference of the hexagonal grid without the complexity of the hybrid combinations of mobile and static sonars in a multi-periodic environment. Hence, the problem configurations used in this chapter are:

Problem Configuration Type #1 (SSP): Using only static sonars in a single period deployment scheme while optimizing using only the first objective function.

Problem Configuration Type #2 (SMMP): Using both static and mobile sonars in a multi-period deployment scheme while optimizing using both objective functions.

All models are implemented in GAMS and solved using CPLEX. All MIPs are solved within a relative tolerance of 3% duality gap, and all computational runs are made on a 3.00 GHz Intel Xeon machine with 400 GB of memory, running CPLEX version.

4.4 Numerical Results

This section presents results showing model features proposed. Thereafter, sensitivity analysis is provided on model parameter $\bar{c}$.

4.4.1 Numerical Results-SSP

As highlighted in Section 4.3, we restrict our optimization to only objective function (1) for this configuration. As a performance measure, numerical results are compared when deploying sonars with both the conventional and the proposed grid system.

Figure 4.2 shows the objective functions using the two grid systems. It should be noted that an unusual behavior of the solver solution time is noticed for each grid system. This is due to the branching rules the CPLEX solver uses in its implementation. This phenomenon is well documented in literature. For example, Ghafoori and Altiok (2012) reports similar behavior.

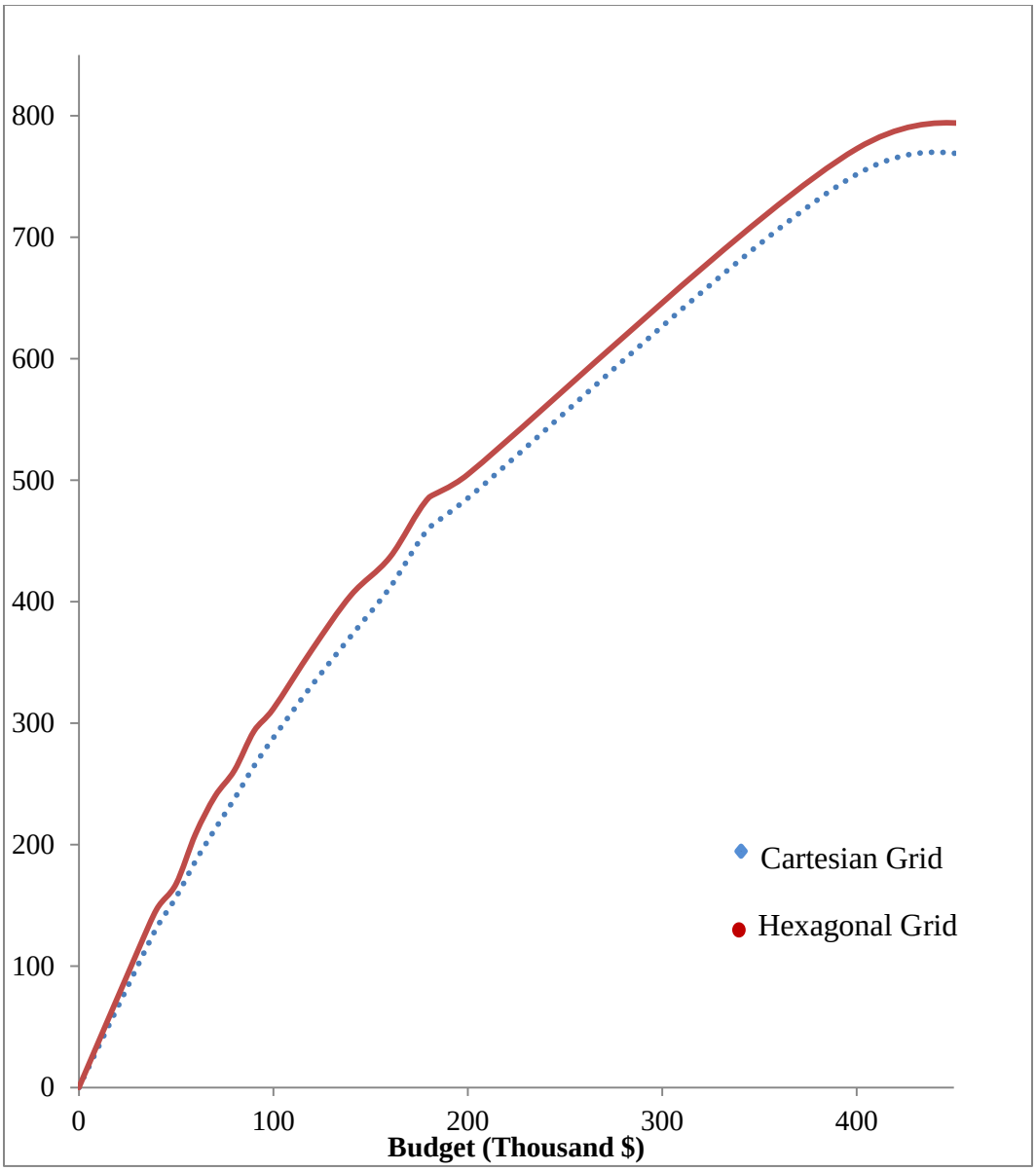

Figure 4.2: SSP: Objective Function (1) vs Budget Availability- Cartesian and Hexagonal Grids

4.4.2 Numerical Results-SMMP

Since we place more importance on objective (4.1) in comparison to objective (4.2), we use the lexicographic multi-objective approach in our solution methodology. In

contrast to the latter objective, the former objective incorporates criticality, a concept widely adopted in risk management methodology. Hence, our solution approach places more emphasis on objective (4.1).

Lexicographic Optimization for two objective functions

Given an optimization problem with two objective functions such that objective function, f1 is accorded more priority in comparison to objective function f_2:

$$Max\ [f_1,\ f_2]$$

$$s.t: Ax \leq b, x \geq 0$$

The lexicographic multi-optimization can be carried out in two stages:

Stage 1:

$$Max\ f_1$$

$$s.t: Ax \leq b, x \geq 0$$

Stage 2:

$$Max\ f_2 - \alpha * \beta$$

$$s.t: Ax \leq b, f_1 \geq z1^* - \beta, x \geq 0$$

where, $\alpha\ and\ \beta$ are parameter weight and deviation variable respectively; and $z1^* = \max f_1$ is the optimal objective function from stage 1.

The choice of an appropriate α can be determined by rule of thumb or by experimentation. For our purpose, we determine an appropriate value by using different

values of α and then comparing the values of the objective function f_1 obtained from both the multi-optimization and single optimization instances. A slight deviation from these values indicates an appropriate choice of α. This approach is adopted since we consider (4.1) to be the objective function of higher priority. Clearly, other approaches at choosing a value of α will be applicable.

4.4.3 Discussion: Objective functions vs. budget availability

Figure 4.3 shows the objective functions in SMMP for some budgetary limitations using our chosen choice of α. Based on our highlighted approach in the choice of an appropriate value for α in the multi-optimization scheme, choosing $\alpha \geq 1$ gives objective function (4.1) close to that obtained in the single optimization scheme. Specifically, we find $\alpha = 1$ to be appropriate for our purpose.

While objective (4.1) is expectedly monotonically non-decreasing as available budget increases, objective (4.2) is not due to the adopted multi-optimization methodology. In the case of (4.1), even if an incremental increase in budget is not enough to procure additional sonars, the worst case is that an existing optimal solution before a budget increase is still maintained after the increment. In contrast, the new optimal value of objective function (4.2) after the budget increment may in fact be degraded if the budget increment permits purchase of more sonars that can improve the value of objective (4.1) at the expense of Objective function (4.2). Of course, it is expected that with *'enough'* budget, this behavior in the value of objective function (4.2) will become non-existent. Figure 4.3 clearly indicates this expectation.

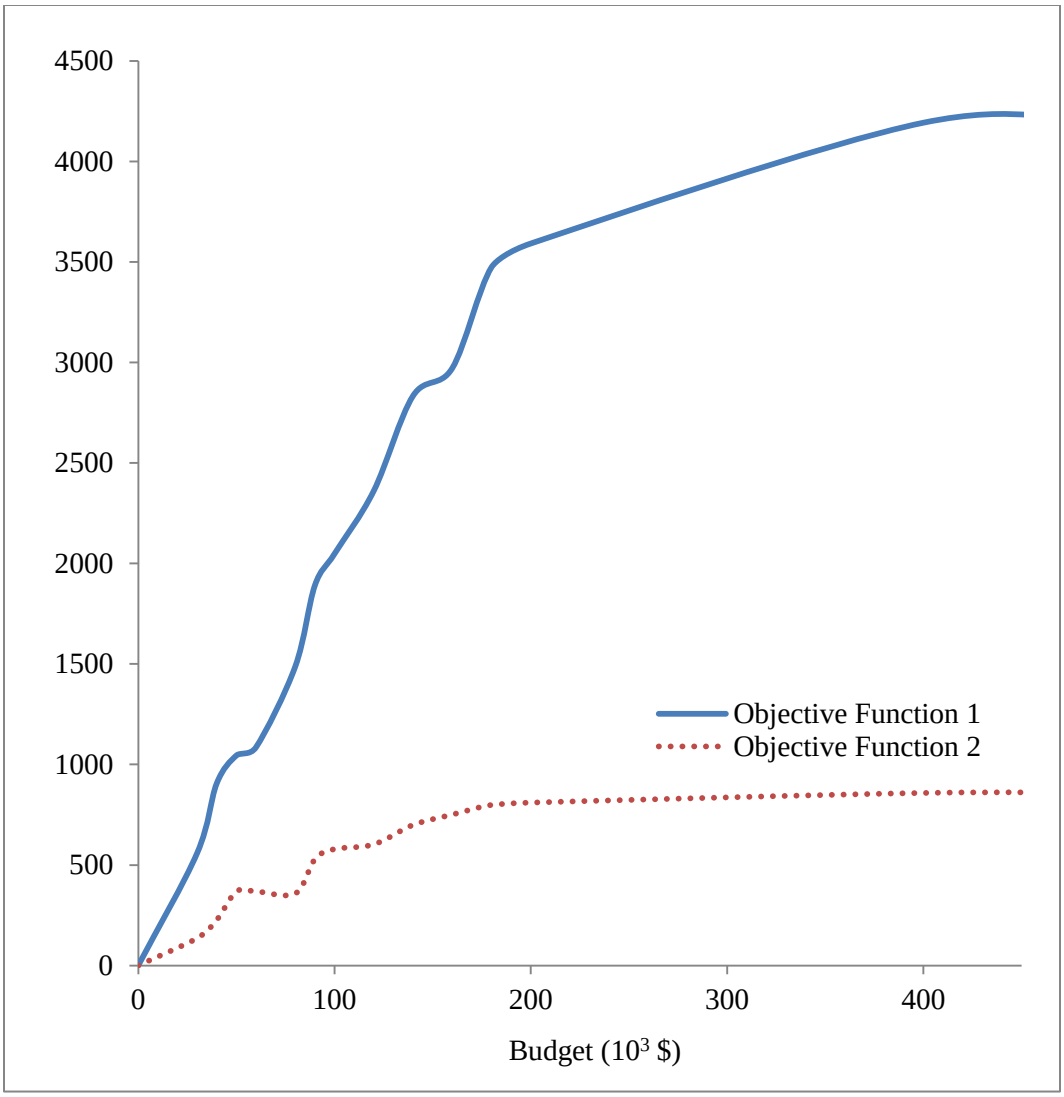

Figure 4.3: SMMP: Objective Functions vs Budget Availability

4.4.4 Sensitivity Analysis

We carry out sensitivity analysis based on one of the identified constraints: maximum number of coverage allowed per region in each time period. Although we present results using a specific value for this parameter in prior sections above, sensitivity analysis permits us to visualize the compromise between obtaining best possible

objective value functions and providing adequate coverage (based on literature definition and our definition) to sub-regions within the AOI.

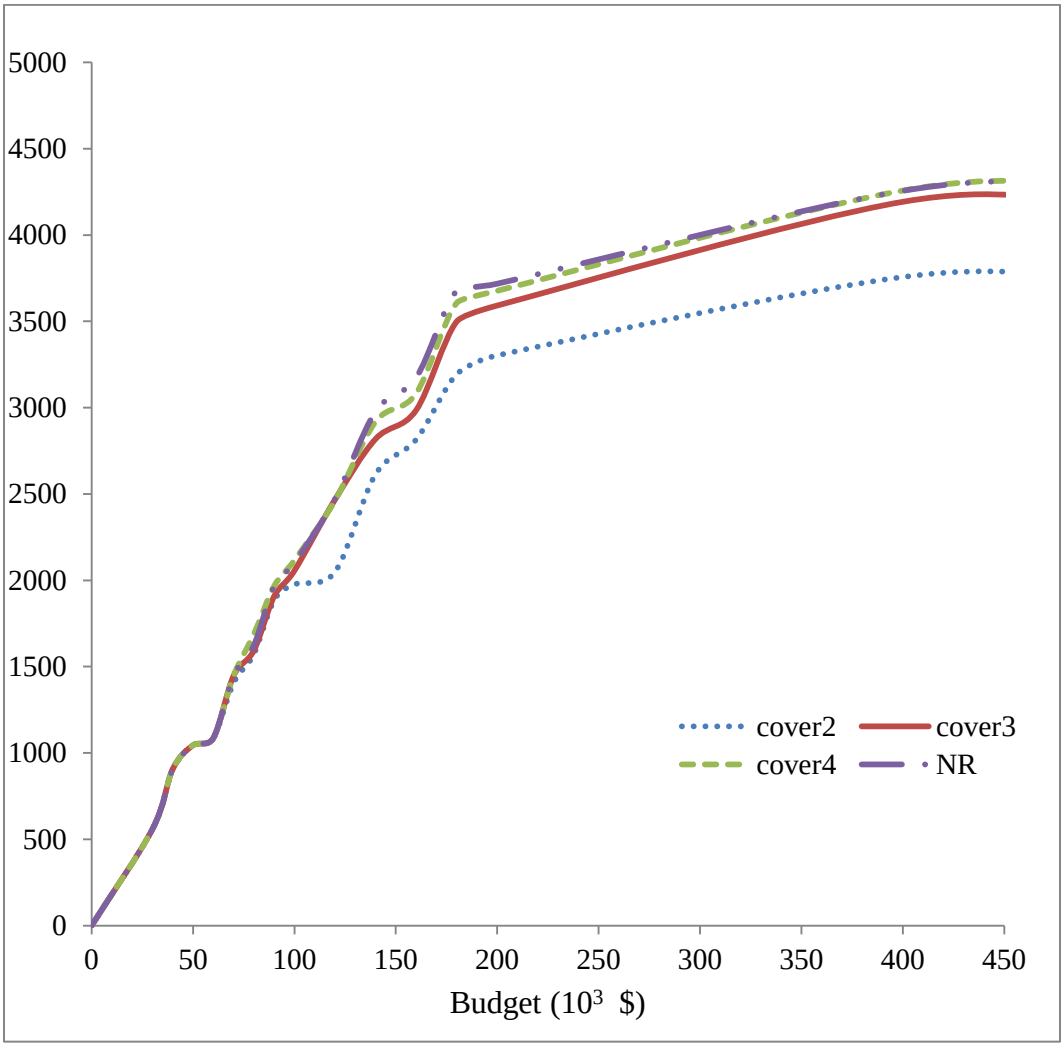

Figure 4.4a**:** Sensitivity Analysis: Objective Function (1)

As noted in Section 4.1, unlike terrestrial coverage problems, our coverage problem deals with partial coverage. Despite this, we are interested in how our deployment strategy performs. Hence, we introduce the *'pn-coverage'* analysis in our discussions.

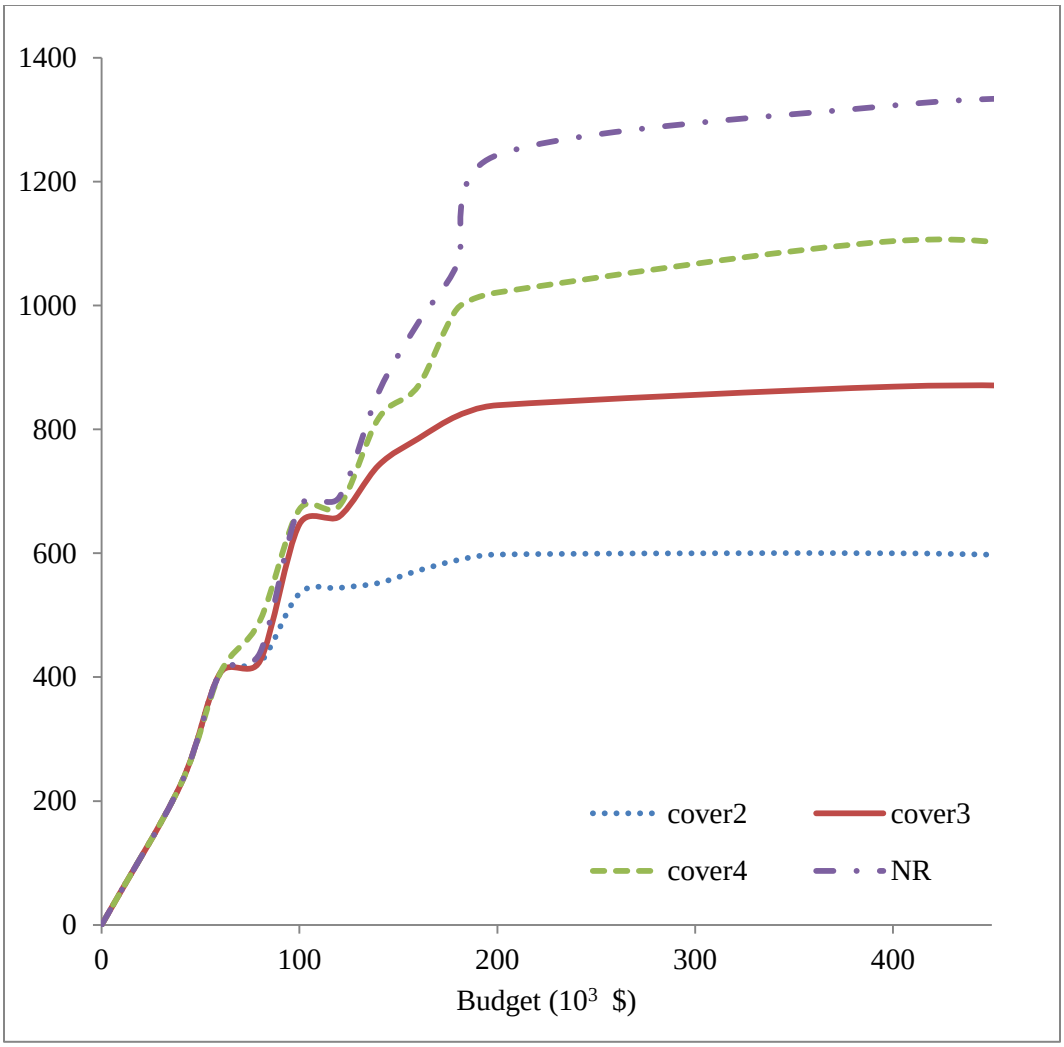

Figure 4.4b: Sensitivity Analysis: Coverage

Definition 4.1*:* For SMMP, we formally define the *'pn-coverage'* as the percentage of the AOI that is covered by at least n-sonars across the entire deployment periods.

Figure 4.5 shows the *'pn-coverage'* attained for some chosen parameter values of the maximum number of coverage allowed per region. Since the *'p1-coverage'* case is trivial (its percentages are expected to be high irrespective of the chosen parametric values), only both the *'p2- and p3-coverages'* cases are shown.

As shown in Figure 4.4a and Figure 4.4b, increasing the maximum cover per grid tends to bring a desirable increase in both objective function (4.1) and the coverage. However, Figure 4.5a and Figure 4.5b also indicate that doing this erodes the performance of *pn-coverage* as we have defined it. Restricting maximum cover per period to 3 seems to provide a more consistent coverage per budget availability. This is more apparent at lower to medium budget availability.

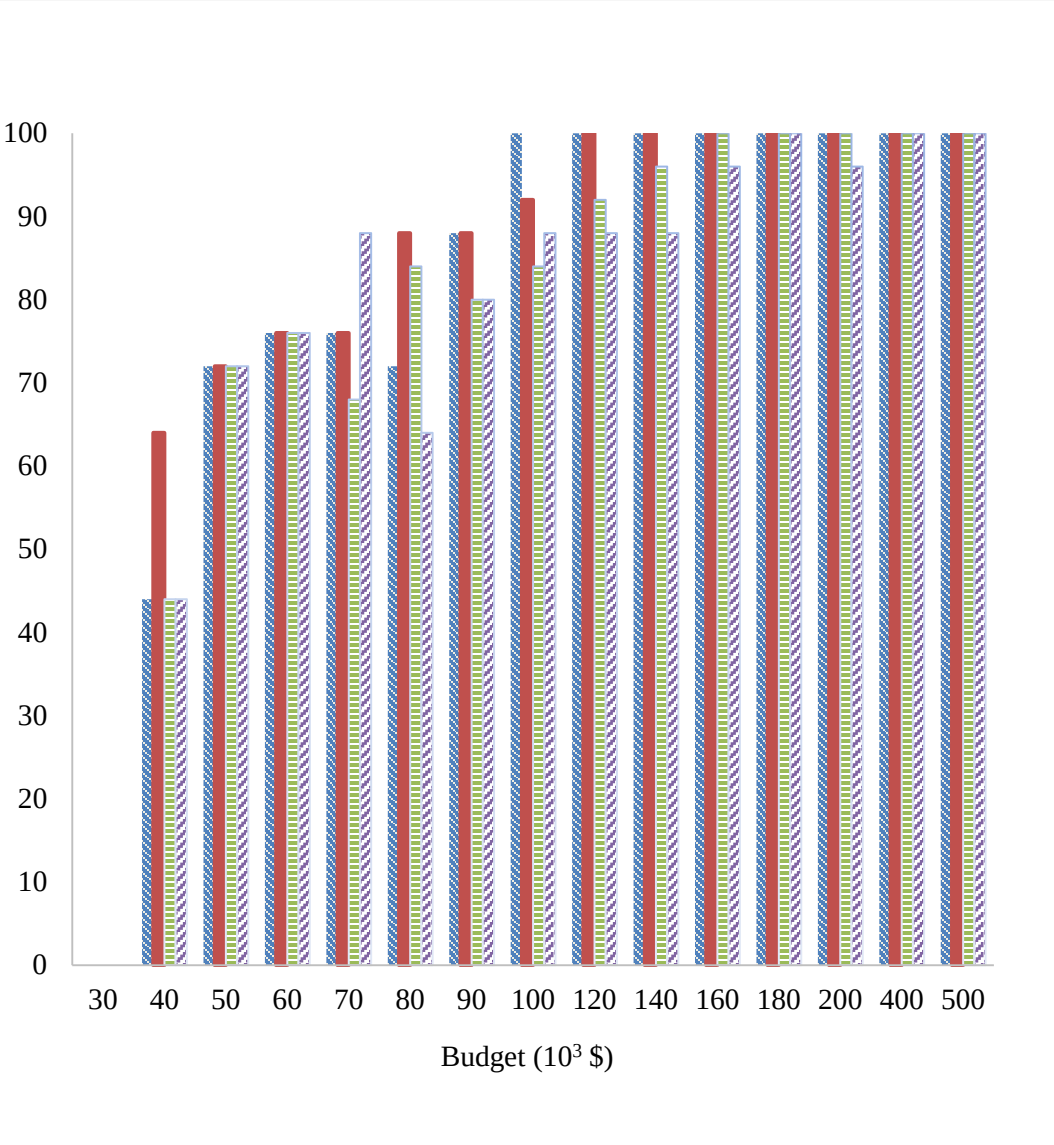

Figure 4.5a: Sensitivity Analysis: *p2- Coverage*

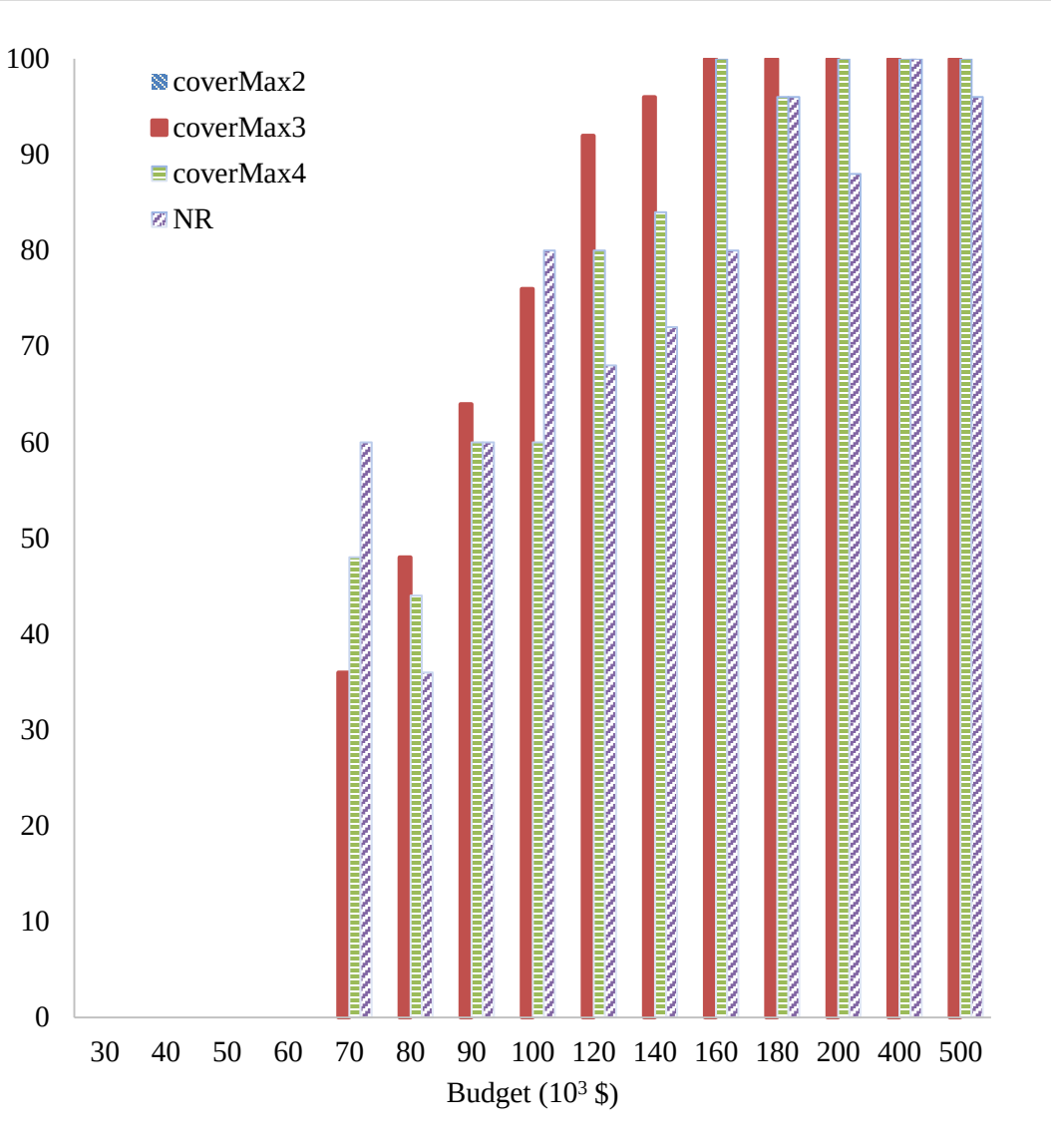

Figure 4.5b: Sensitivity Analysis: *p3-Coverage*

4.5 Discussions and Conclusions

In this chapter, we presented an optimization model with a hybrid combination of static and mobile sonars. We implemented the model to solve a semi-hypothetical, yet practical problem in the maritime domain (relying on partial/incomplete data due to security and confidentiality concerns) within a multi-period placement methodology. The

desirability of having a hybrid deployment of both static and mobile sensor in any generic sensor deployment has already been established in literature. As such, we have restricted ourselves to the observation that our sonar placement methodology not only improves the objective functions but also permits other regions in the area of interest which may never have been covered by sonars due to budgetary constraints to be eligible for coverage at other periods. To illustrate this observation, we introduced the *'pn-coverage'* criteria in the chapter. The placement methodology we adopted increases the possibility that all regions within the AOI are covered at some period. For our test case problem, this ensures minimization of un-covered regions for exploitation by terrorists, smugglers, arsonist, etc., even on a limited budget.

In addition, from our results, we lay claim to the following: Hexagonal grids generally outperform the conventional Cartesian grids; our approach of a multi-objective optimization rather than single-optimization technique is appropriate; sensitivity analysis suggests the desirability of restricting maximum cover per grid to a small integer (say, 3 as shown in Section 4.4).

Chapter 5

A fortification approach to the underwater sonar placement problem

5.1 Introduction

A tri-level defender–attacker–defender model involves three agents acting sequentially (See Chapter 1). In a fortification model we propose for the Sonar placement problem, the top level corresponds to the *defender*'s decision on allocating defensive resources (sonars) to protect maritime infrastructures before any attack is initiated. The middle-lower level is a typical bi-level interdiction problem. The middle level decisions are made by the '*attacker'*, who attempts to maximize the overall probability of non-detection by deploying its resources to unprotected (or inadequately protected) part of the maritime area of interest. Afterwards, actions of the *'attacker'* are appraised, and the '*defender'* reacts to that disruption by solving an optimal sonar placement problem to minimize the overall probability of non-detection. Figure 5.1 shows the interraction between the agents.

Compared to a Game-theoretic based approach where only two level of interactions are considered in a strategic planning framework, the D-A-D model produces a superior protection plan because it considers an additional third level of interaction between the *defender* and the *attacker*, and thereafter selects the optimal strategy to thwart the attacker's efforts based on the optimal strategic plan adopted by the latter.

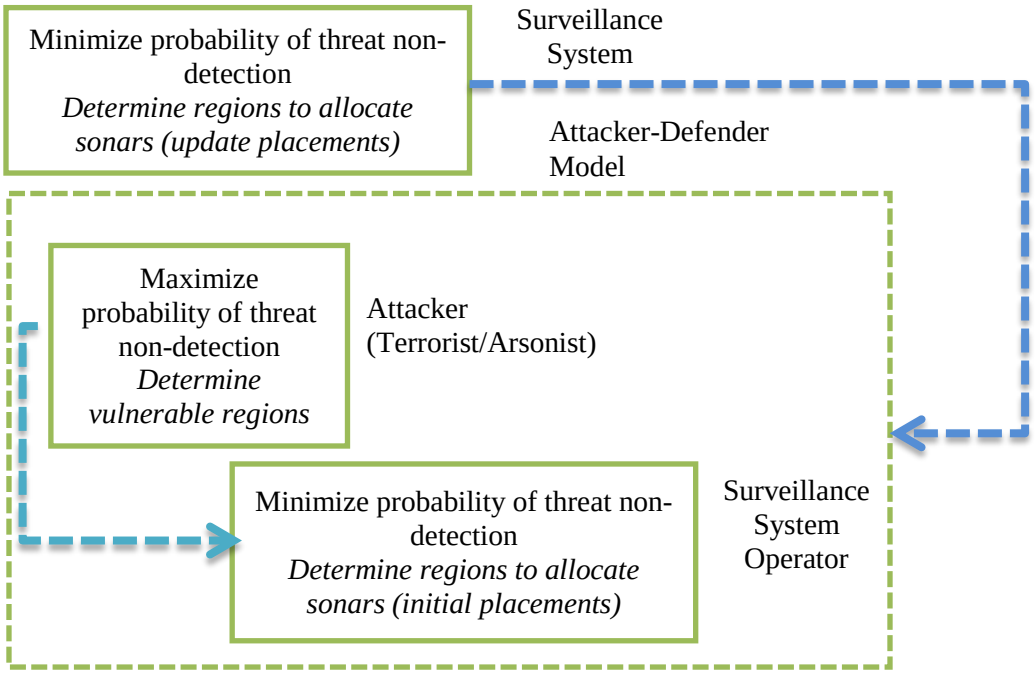

Figure 5.1- D-A-D (Fortification) framework-Underwater Protection

5.2 Problem Formulation

This section presents the mathematical formulation of a *'Defender-Attacker-Defender'* model used for the underwater sonar placement problem. Based on the model introduced in Chapter 4, the formulation describes interactions between the protector of the maritime infrastructures, *'Defender'* and an intelligent *'Attacker'* who attempts to frustrate the effort(s) of the defender.

The optimal sonar placement problem in the lower level is the MIP problem presented in Chapter 4 where sonar placement is influenced by coverage requirements and budget limitations. However, in order to properly analyze/investigate interactions between *'Attacker'* and *'Defender'*, the resource availability in terms of budget limitation is now in terms of cardinality i.e. resource availabilities are dictated in terms of integer parameters. The approach enables the model to be generic enough because the defender resources for evading intrusion could be torpedoes, submarines, or even swimmers. It

would have been difficult to provide practical/realistic dollar equivalents to these resources without losing generality in the model. Also, due to insights from the results obtained in Chapter 4, the objective function in the tri-level model is based on the first objective function, as introduced in Section 4.2.4 of Chapter 4.

In this chapter, $\bar{\boldsymbol{x}}$ denotes a fixed decision variable $\boldsymbol{x}$ and other model declarations follow standard notations. The new nomenclature introduced is shown in Section 5.2.1. For those not shown, the same nomenclature introduced in Chapter 4 remains applicable.

5.2.1 Nomenclature

Sets and Indices

N_{Vik}	Set that contains a point of attack i, k and other cells in its neighborhood affected by the attack/intrusion.
$G_{X,Y}$	Set that contains binary variables X_{ik}^{a} and Y_{ik}^{bt}

Parameters

q_{max}	Cardinality budget for the Attacker
B	Cardinality budget for the Defender
$attackLevel$	Level at which attacker's intrusion is felt: Point of attack and neighbors to this point of attack.
$p_{attackLevel}$	Depicts the extent of destruction depending on proximity to point of attack i, k and is expressed as a probability, with the point of attack having the highest probability.
M	Big M- A relatively very large number.

Decision Variables

V_{ikt}	Binary attack decision: 1 if grid i, k is attacked at period t,

and 0 otherwise.

5.2.2 Tri-level Model ($M_{DAD-tri}$)

The defender-attacker-defender model is presented in this section. The mathematical model is described by the following equations:

(Model $M_{DAD-tri}$)

$$\underset{X,Y}{\text{Min}}\ \underset{V}{\text{Max}}\ \underset{W,Q}{\text{Min}} - \sum_i \sum_k \sum_t h_{ikt} * (Qv_{ikt} + Qa_{ik} + Qb_{ikt}) , \tag{5.1}$$

Subject to:

$$\sum_a c_a . \sum_i \sum_k X_{ik}^a + \sum_b c_b . \sum_i \sum_k Y_{ik}^{bt} \leq B \quad \forall\, t , \tag{5.2}$$

$$\sum_a \sum_{(f,h) \in N_{ikaa^z}} X_{fh}^a + \sum_a X_{ik}^a \geq W_{ik}^{a,a^z} \quad \forall i,k,a^z , \tag{5.3}$$

$$\sum_b \sum_{(f,h) \in N_{ikbb^z}} Y_{fh}^{bt} + \sum_b Y_{ik}^{bt} \geq W_{ik}^{b,b^z,t} \quad \forall i,k,t,b^z , \tag{5.4}$$

$$\sum_{a,a^z} W_{ik}^{a,a^z} + \sum_{b,b^z} W_{ik}^{b,b^z,t} \leq \bar{c} \quad \forall\, i,k,t , \tag{5.5}$$

$$\sum_a X_{ik}^a + \sum_b Y_{ik}^{bt} \leq 1 \quad \forall\, i,k,t , \tag{5.6}$$

$$Y_{ik}^{b,t} \leq Y_{ik}^{b,t+1} + \sum_{(f,h) \in M_{ikd}} Y_{fhd}^{b,t+1}, \quad \forall\, i,k,b,d,t , \tag{5.7}$$

$$\sum_d Y_{ikd}^{b,t+1} \leq 1 \qquad \forall\, i,k,b,t , \tag{5.8}$$

$$\sum_{i,k} Y_{i,k}^{b,t} = \sum_{i,k} Y_{i,k}^{b,t+1} \qquad \forall\, b,t , \tag{5.9}$$

$$\sum_{b}\sum_{i}\sum_{k} Y_{ik}^{bt} \geq SR * \left(\sum_{b}\sum_{i}\sum_{k} Y_{ik}^{bt} + \sum_{a}\sum_{i}\sum_{k} X_{ik}^{a}\right) \quad \forall t\,, \tag{5.10}$$

$$-Qa_{ik} = \sum_{a^z} W_{ik}^{a,a^z} \ln(1 - p_{a^z}) \; \forall\, i,k,a\,, \tag{5.11}$$

$$-Qb_{ikt} = \sum_{b^z} W_{ikt}^{b,b^z} \ln(1 - p_{b^z}) \; \forall\, i,k,b,t\,, \tag{5.12}$$

$$\sum_{i,k} V_{ikt} \quad \leq q_{max} \qquad\qquad \forall\, t\,, \tag{5.13}$$

$$\sum_{a,a^z} W_{ik}^{a,a^z} + \sum_{b,b^z} W_{ik}^{b,b^z,t} \leq M(1 - V_{ikt} \quad) \qquad \forall i,k,t\,, \tag{5.14}$$

$$\sum_{(f,h)\,\in\, N_{Zik}} V_{fht} \quad \geq V_{ikt}^{attackLevel} \qquad \forall i,k,t,attackLevel\,, \tag{5.15}$$

$$Qv_{ikt} = \sum_{attackLevel} V_{ikt}^{attackLevel} \ln(1 - p_{attackLevel}) \; \forall\, i,k,t\,, \tag{5.16}$$

$$X_{ik}^{a}, Y_{ik}^{b,t}, V_{ikt}^{attack}, V_{ikt} \quad \epsilon\, B,\; W_{ik}^{a,a^z}, W_{ikt}^{b,b^z}, V_{ikt}^{attackLevel} \epsilon\, I^{+}\,, Qa_{ik}, Qb_{ikt} \geq 0, \tag{5.17}$$

$$Qv_{ikt} \leq 0\,.$$

As in Chapter 4, we assume if an infrastructure is defended by sonar, then it becomes invulnerable to destruction. Objective function (5.1) and constraints (5.2-5.12) are as described in Chapter 4. In addition, Constraints (5.13) depicts limitation in attacker resources during period t. While equations (5.14) implies the *'Attacker'* only attempts to intrude on sections of the AOI that are left unprotected (The assumption is that the 'attacker' has 'intelligence' about the resources available to the defender and is also aware of the initial protection procedure), equations (5.15) and (5.16) are coverage equations related to the extent of damage to a point of attack and its neighboring areas. Their derivations are similar to that developed for coverage of detection probabilities as

presented in Section 4.2.4 of Chapter 4. And finally, Constraints (5.17) indicate the type of decision variables.

Combining equations (5.5) and (5.14),

$$\sum_{a,a^z} W_{ik}^{a,a^z} + \sum_{b,b^z} W_{ik}^{b,b^z,t} \leq \bar{c} \quad \leq M(1 - V_{ikt} \;) \qquad \forall i,k,t\,.$$

Hence, constraints (5.5) can be dropped from the model and M in constraints (5.14) can be set to $\bar{c}$. Whenever a sub-section of the AOI is protected, binary variable V_{ikt} is 0 and $\bar{c}$ is thus a tighter bound under this scenario.

The entire model is a mixed-integer linear tri-level programming problem. Like in most tri-level problems of this nature, the presence of binary decision variables in the middle level does not permit reduction to an equivalent single-level problem (Brown et al., 2006 and Alguacil et al., 2014). In the interactions between the *'Attacker'* and the *'Defender'*, the former tries to minimize the overall probability of non-detection by manipulating decision variables in the first and third levels, while the latter attempts to maximize the overall probability of non-detection by controlling decision variables in the second level. To solve the problem, a decomposition-based approach is proposed and is fully discussed in Section 5.3.

5.3 A decomposition procedure of the tri-level sonar placement problem

To solve $\boldsymbol{M_{DAD-tri}}$, we propose to decompose the problem into sub-problems and then solve using standard techniques. Without loss of generality, we further assume in our model that only a single grid is affected in the advent of a successful intrusion.

Hence, constraints (5.15) can be dropped and $V_{ikt}^{attackLevel}$ in constraints (5.16) is replaced by V_{ikt}. Constraints (5.16) are then rewritten as constraints (5.16a).

5.3.1 Bi-level optimization equivalent of the tri-level sonar placement problem (Model M_{AD-bi})

For the Attacker sub-problem (Model M_{AD-bi}), we re-formulate the problem based on Model $\boldsymbol{M_{DAD-tri}}$ by fixing the protection variables X and Y. Hence, Model M_{AD-bi} is a bi-level Attacker-Defender model where X and Y variables are treated as parameters. The model is shown in the following equations:

(Model M_{AD-bi})

$$\underset{V}{\text{Max}} \underset{W,Qa,Qb}{\text{Min}} -\sum_{i}\sum_{k}\sum_{t} h_{ikt} * (Qv_{ikt} + Qa_{ik} + Qb_{ikt}) , \tag{5.1a}$$

Subject to:

$$\sum_{a} \sum_{(f,h) \in N_{ikaa^z}} \overline{X_{fh}^{a}} + \sum_{a} \overline{X_{ik}^{a}} \geq W_{ik}^{a,a^z} \quad \forall i,k,a^z , \tag{5.3a}$$

$$\sum_{b} \sum_{(f,h) \in N_{ikbb^z}} \overline{Y_{fh}^{bt}} + \sum_{b} \overline{Y_{ik}^{bt}} \geq W_{ik}^{b,b^z,t} \quad \forall i,k,t,b^z , \tag{5.4a}$$

$$\sum_{a,a^z} W_{ik}^{a,a^z} + \sum_{b,b^z} W_{ik}^{b,b^z,t} \leq \bar{c}(1 - V_{ikt} \quad) \qquad \forall i,k,t , \tag{5.14a}$$

$$Qv_{ikt} = V_{ikt} \quad \ln(1 - p_{attackLevel}) \, \forall \, i,k,t , \tag{5.16a}$$

Constraints $(11), (12), (13)$ from Model $\boldsymbol{M_{DAD-tri}}$, and

$$W_{ik}^{a,a^z}, W_{ikt}^{b,b^z} \epsilon\, I^+ , V_{ikt}, Qa_{ik}, Qb_{ikt} \geq 0, Qv_{ikt} \leq 0. \tag{5.17a}$$

5.3.2 Single level optimization equivalent to the tri-level sonar placement problem (Model M_{D-s})

Using standard reformulation, we convert Model $M_{AD-bi}$to an equivalent integer programming problem by using an attack plan V_{ikt}. For fixed attack and defense plans, we have model M_{D-S} , where the variables X, Y and V are treated as parameters.

(Model M_{D-s})

$$\underset{W,Qa,Qb}{\text{Min}} \left(-\sum_i \sum_k \sum_t h_{ikt} * (Qv_{ikt} + Qa_{ik} + Qb_{ikt}) \right), \tag{5.1b}$$

Subject to:

Constraints $(5.3a, 5.4a, 5.11, 5.12, 5.14a$ &$5.16a)$ from Models $M_{DAD-tri}$

and M_{AD-bi},

$$W_{ik}^{a,a^z}, W_{ikt}^{b,b^z} \epsilon\, I^+ , Qa_{ik}, Qb_{ikt} \geq 0,\ Qv_{ikt} \leq 0. \tag{5.17b}$$

5.3.3 A dual formulation of model M_{D-s} (Model M_{A-dual})

To iteratively solve the sonar placement problem, we desire to obtain a sub-problem. Using the LP relaxation of $\boldsymbol{M_{D-s}}$, we transform the relaxed model to a maximization problem (model $\boldsymbol{M_{A-dual}}$) by taking its primal dual and thereafter transform attack parameters back to decision variables. In line with standard decomposition procedures (e.g. Benders' decomposition), model $\boldsymbol{M_{A-dual}}$ is referred to as a sub-problem of our tri-level model. Since the feasible region of the LP relaxation in a

standard IP optimization problem is often larger than the feasible region of the IP, the optimal value of the former latter is no better than the optimal value of the former. In fact, the objective function values of a feasible IP solution and the optimal LP solution, respectively, yields a pair of upper and lower bounds (Yelbay et al. 2015). For a minimization problem like model $\boldsymbol{M_{D-s}}$, the optimal objective value of the LP relaxation is no higher than that of the original problem (Readers should note this is due to the negative sign in the objective function of model $\boldsymbol{M_{D-s}}$).

To formulate model $\boldsymbol{M_{A-dual}}$, we define the dual variables below:

$\mu_{ik}^{a^z}$ Dual Variables corresponding constraints (5.3a) in the LP relaxed model of M_{D-s}

$\Pi_{ik}^{b^z}$ Dual Variables corresponding constraints (5.4a) in the LP relaxed model of M_{D-s}

Ψ_{ik}^{a} Dual Variables corresponding constraints (5.11) in the LP relaxed model of M_{D-s}

Ω_{ik}^{bt} Dual Variables corresponding constraints (5.12) in the LP relaxed model of M_{D-s}

γ_{ik}^{t} Dual Variables corresponding constraints (5.14) in the LP relaxed model of M_{D-s}

τ_{ik}^{t} Dual Variables corresponding constraints (5.16a) in the LP relaxed model of M_{D-s}

Afterwards, we carry out the following:

1. Re-transform attack parameters $\bar{V}$ back to decision variables V
2. Include attacker cardinality constraints (constraints 5.13)

Model $\boldsymbol{M_{A-dual}}$ (A dual formulation of model M_{D-s}) is formulated in the following equations:

$(\boldsymbol{M_{A-dual}})$

$$\underset{V,\mu,\Pi,\Psi,\Omega,\gamma,\tau}{\text{Max}} -\left(\sum_i \sum_k \sum_{a^z} \mu_{ik}^{a^z} \left\{\sum_a \sum_{(f,h)\in N_{ikaa^z}} \overline{X_{fh}^a} + \sum_a \overline{X_{\imath k}^a}\right\}\right) \tag{5.18}$$

$$-\left(\sum_i \sum_k \sum_{b^z} \sum_t \Pi_{ik}^{b^z t} \left\{\sum_b \sum_{(f,h)\in N_{ikbb^z}} \overline{Y_{fh}^{bt}} + \sum_b \overline{Y_{\imath k}^{bt}}\right\}\right)$$

$$+\sum_i \sum_k \sum_a \Psi_{ik}^a\, 0 + \sum_i \sum_k \sum_b \sum_t \Omega_{ik}^{bt}\, 0$$

$$-\sum_i \sum_k \sum_t \gamma_{ik}^t \times M(1 - V_{ikt}\ \ ) + \sum_i \sum_k \sum_t \tau_{ikt}$$

$$\times V_{ikt}\ \ \ln(1 - p_{attack})\ \text{, and}$$

$$\underset{V,\mu,\Pi,\Psi,\Omega,\gamma,\tau}{= \text{Max}} -\left(\sum_i \sum_k \sum_{a^z} \mu_{ik}^{a^z} \left\{\sum_a \sum_{(f,h)\in N_{ikaa^z}} \overline{X_{fh}^a} + \sum_a \overline{X_{\imath k}^a}\right\}\right) \tag{5.18a}$$

$$-\left(\sum_i \sum_k \sum_{b^z} \sum_t \Pi_{ik}^{b^z t} \left\{\sum_b \sum_{(f,h)\in N_{ikbb^z}} \overline{Y_{fh}^{bt}} + \sum_b \overline{Y_{\imath k}^{bt}}\right\}\right)$$

$$-\sum_i \sum_k \sum_t \gamma_{ik}^t \times M(1 - V_{ikt}\ \ ) + \sum_i \sum_k \sum_t \tau_{ikt}$$

$$\times V_{ikt}\ \ \ln(1 - p_{attack}).$$

Subject to:

$$-\mu_{ik}^{a^z} - \Psi_{ik} \ln(1 - p_{a^z}) - \gamma_{ik}^t \leq 0\ \forall\ i, k, a, a^z, t\ , \tag{5.19}$$

$$-\Pi_{ik}^{b^z t} - \Omega_{ik}^t \ln(1 - p_{b^z}) - \gamma_{ik}^t \leq 0\ \ \forall\ i, k, b, b^z, t\ , \tag{5.20}$$

$$-\Psi_{ik} \leq -h_{ikt}\ \ \forall\ i, k, t\ , \tag{5.21}$$

$$-\Omega_{ik}^t \leq -h_{ikt}\ \forall\ i, k, t\ , \tag{5.22}$$

$$\tau_{ik}^{t} \geq \quad -h_{ikt} \; \forall \; i,k,t \; , \tag{5.23}$$

$$\sum_{ik} V_{ikt} \quad \leq q_{max} \quad \forall \; t \; , \tag{5.13}$$

$$\mu_{ik}^{a^z} \geq 0, \Pi_{ik}^{b^z t} \geq 0, \Psi_{ik} \; free, \Omega_{ik}^{t} \; free, \tau_{ik}^{t} free, \gamma_{ik}^{t} \geq 0 \; . \tag{5.24}$$

To establish linearized equivalence of non-linear terms in the objective function of $\boldsymbol{M_{A-dual}}$, we consider two optimization models, $\boldsymbol{D_1}$ and $\boldsymbol{D_2}$:

$\boldsymbol{D_1}$: $\min\{f_1(x,y)|(x,y)\epsilon \; S_1\}$,

where $S_1 = \{(x,y)|h_1(x,y) \leq b_1, g_1(x,y) = b_2, x \; \epsilon \; \mathcal{B}^n, y \; \epsilon \; \mathbb{Z}_+^n\}$

$\boldsymbol{D_2}$: $\min\{f_2(x,y)|(x,y)\epsilon \; S_2\}$,

where $S_2 = \{(x,y)|h_2(x,y) \leq d_1, g_2(x,y) = d_2, x \; \epsilon \; \mathcal{B}^n, y \; \epsilon \; \mathbb{Z}_+^n\}$

Definition 5.1 (*Baharnemati, 2011)* Two optimization models, $\boldsymbol{D_1}$ and $\boldsymbol{D_2}$, are considered equivalent if they have the same objective function, i.e., $f_1(x,y) = f_2(x,y)$ and the feasible solutions of the models have one-to-one correspondence, i.e., for each $(x,y)\epsilon \; S_1$ there is only one $(x',y')\epsilon \; S_2$ and vice versa.

Proposition 5.1 *Given that β is a binary variable and α is a positive integer variable with an upper bound $\bar{\alpha}$. Then, the non-linear term, $\alpha\beta$ can be linearized by defining a new positive real variable, $\rho = \alpha\beta$ and introducing the following constraints:*

$$\rho \leq \alpha\beta \; ,$$

$$\rho \leq \alpha \; ,$$

$$\rho \geq \alpha + \bar{\alpha}(\beta - 1) \; ,$$

Proof. See Glover (1975) and Adams et al. (2004) for details.

Corollary 5.1. *An equivalent linear MIP formulation to Model* $\boldsymbol{M_{A-dual}}$ *is obtainable by replacing the non-linear components of the objective function (18a) i.e.* $(1 - V_{ikt}\ ) \times \gamma_{ik}^{t}$ *and* $V_{ikt}\ \times \tau_{ik}^{t}$ *with continuous variables* ζ_{ik}^{t1} *and* ζ_{ik}^{t2} *respectively, and subsequently introducing constraints (25-28) to the model formulation as additional constraints:*

$$\zeta_{ik}^{t1} \leq \overline{\gamma_{ik}^{t}} \times (1 - V_{ikt}\ ), \tag{5.25a}$$

$$\zeta_{ik}^{t1} \leq \gamma_{ik}^{t}, \tag{5.26a}$$

$$\zeta_{ik}^{t1} \geq \gamma_{ik}^{t} - \left(V_{ikt}\ \times \overline{\gamma_{ik}^{t}}\right), \tag{5.27a}$$

$$\zeta_{ik}^{t1} \geq 0, \tag{5.28a}$$

$$\min\left\{0, \underline{\tau_{ik}^{t}}\right\} \leq \zeta_{ik}^{t2} \leq \overline{\tau_{ik}^{t}}, \tag{5.25b}$$

$$\underline{\tau_{ik}^{t}} \times V_{ikt}\ \leq \zeta_{ik}^{t2} \leq \overline{\tau_{ik}^{t}} \times V_{ikt}\ , \tag{5.26b}$$

$$\tau_{ik}^{t} - (1 - V_{ikt}\ ) \times \overline{\tau_{ik}^{t}} \leq \zeta_{ik}^{t2} \leq \tau_{ik}^{t} - (1 - V_{ikt}\ ) \times \underline{\tau_{ik}^{t}}, \tag{5.27b}$$

$$\zeta_{ik}^{t2} \leq \tau_{ik}^{t} - (1 - V_{ikt}\ ) \times \overline{\tau_{ik}^{t}}\ . \tag{5.28b}$$

With γ_{ik}^{t} bounded below by 0 and above by $\overline{\gamma_{ik}^{t}}\ i.e, [0, \overline{\gamma_{ik}^{t}}]$, where in the absence of further information, the upper bound $\overline{\gamma_{ik}^{t}}$ can be reasonable set to *M* (Big-M, a considerably large number). Hence, the term $\gamma_{ik}^{t} \times (1 - V_{ikt}\ )$ in the objective function can be replaced by ζ_{ik}^{1t} and Constraints (25a-28a) are added to complete the linearization of $(1 - V_{ikt}\ ) \times \gamma_{ik}^{t}$. Here, τ_{ik}^{t} is a free dual variable and it is thus not bounded by 0, but by $[\underline{\tau_{ik}^{t}}, \overline{\tau_{ik}^{t}}]$. Again, without access to more information, these bounds can be set to [-M, +M]. Non-linear components, $V_{ikt} \times \tau_{ik}^{t}$ in the objective function can then be replaced by ζ_{ik}^{t2} and Constraints (25b-28b) are added to complete the linearization of $V_{ikt} \times \tau_{ik}^{t}$.

Constraints (25-28) help to linearize the non-linear terms in equation (18a). For example, Constraints (26b) ensures that if $V_{ikt} = 0$, then ζ_{ik}^{t2} is forced to be 0 as well. Likewise, Constraints (27b) enforce that if $V_{ikt} = 1$, then ζ_{ik}^{t2} has to be equal to τ_{ik}^{t}. Although Constraints (25b and 28b) may be redundant under some instances, they ensure feasibility is attained in all situations. An instance that shows their usefulness is when the lower bound $\underline{\tau_{ik}^{t}}$ happens to be non-positive.

5.3.4 Master problem formulation of the tri-level sonar placement problem (Model $\boldsymbol{M_{D-MP}}$)

To complete the decomposition procedure, we follow general decomposition procedures (e.g. Benders, 2005, Alguacil et al., 2014, etc.) by formulating a master problem. We introduce model $\boldsymbol{M_{D-MP}}$, which is a lower bound on our tri-level model, includes a subset of possible attacks and keeps track of the attack positions returned by the sub-problem (model $\boldsymbol{M_{A-dual}}$) at each iteration j. The model is shown below:

(Model $\boldsymbol{M_{D-MP}}$)

$$\min_{XY\in(X,Y),Wj,Qj\in(Qaj,Qbj)} \varsigma \ , \tag{5.29}$$

Subject to:

$$\varsigma \geq -\sum_{i}\sum_{k}\sum_{t} h_{ikt} * \left(Qv_{iktj} + Qa_{ikj} + Qb_{iktj}\right) \quad \forall\, j \ , \tag{5.30}$$

$$\sum_{a} c_a . \sum_{i}\sum_{k} X_{ik}^{a} + \sum_{b} c_b . \sum_{i}\sum_{k} Y_{ik}^{bt} \leq B \quad \forall\, t \ , \tag{5.2}$$

$$\sum_{a} \sum_{(f,h) \in N_{ikaa^z}} X_{fh}^{a} + \sum_{a} X_{ik}^{a} \geq W_{ikj}^{a,a^z} \quad \forall i,k,a^z,j\,, \tag{5.3b}$$

$$\sum_{b} \sum_{(f,h) \in N_{ikbb^z}} Y_{fh}^{bt} + \sum_{b} Y_{ik}^{bt} \geq W_{ikj}^{b,b^z,t} \quad \forall i,k,t,b^z,j\,, \tag{5.4b}$$

$$\sum_{a,a^z} W_{ikj}^{a,a^z} + \sum_{b,b^z} W_{ikj}^{b,b^z,t} \leq \bar{c} \quad \forall\, i,k,t\,,j\,, \tag{5.5a}$$

$$\sum_{a} X_{ik}^{a} + \sum_{b} Y_{ik}^{bt} \leq 1 \quad \forall\, i,k,t\,, \tag{5.6}$$

$$Y_{ik}^{b,t} \leq Y_{ik}^{b,t+1} + \sum_{(f,h) \in M_{ikd}} Y_{fhd}^{b,t+1}, \quad \forall\, i,k,b,d,t\,, \tag{5.7}$$

$$\sum_{d} Y_{ikd}^{b,t+1} \leq 1 \qquad \forall\, i,k,b,t\,, \tag{5.8}$$

$$\sum_{i,k} Y_{i,k}^{b,t} = \sum_{i,k} Y_{i,k}^{b,t+1} \qquad \forall\, b,t\,, \tag{5.9}$$

$$\sum_{b}\sum_{i}\sum_{k} Y_{ik}^{bt} \geq SR * \left(\sum_{b}\sum_{i}\sum_{k} Y_{ik}^{bt} + \sum_{a}\sum_{i}\sum_{k} X_{ik}^{a} \right) \quad \forall t\,, \tag{5.10}$$

$$-Qa_{ik} = \sum_{a^z} W_{ik}^{a,a^z} \ln(1 - p_{a^z})\, \forall\, i,k,a\,, \tag{5.11}$$

$$-Qb_{ikt} = \sum_{b^z} W_{ikt}^{b,b^z} \ln(1 - p_{b^z})\, \forall\, i,k,b,t\,, \tag{5.12}$$

$$Qv_{iktj} = V_{iktj}\, \ln(1 - p_{attackLevel})\, \forall\, i,k,t,j\,, \tag{5.16a}$$

$$\varsigma\ free; X_{ik}^{a}, Y_{ik}^{b,t} \epsilon\, B;\ W_{ikj}^{a,a^z}, W_{iktj}^{b,b^z} \epsilon\, I^{+}\,; Qa_{ikj}, Qb_{iktj} \geq 0\,, \tag{5.17}$$

where:

W_{ikj}^{a,a^z} Number of times a cell i,k is covered by static sonar type a with coverage strength a^z at iteration j

W_{iktj}^{b,b^z} Number of times a cell i,k is covered by mobile sonar type b with coverage strength b^z during time t at iteration j

Qa_{ikj} Linearization variable Qa at iteration j

Qb_{iktj} Linearization variable Qb during time t at iteration j

Qv_{iktj} Linearization variable Qv during time t at iteration j

The objective function (5.29) represents non-detection probability as a result of the worst-case actions undertaken by the attacker and the cut constraints (5.30) give a bound on the worst-case objective with respect to an attack plan from the attacker. Other constraints are as presented in $\boldsymbol{M_{DAD-tri}}$, with the added intuition (where necessary as indicated by iteration j) that the constraints are for each attack plan j.

Proposition 5.2. *The tri-level programming model (model $\boldsymbol{M_{DAD-tri}}$) is equivalent to the single optimization model described in Model $\boldsymbol{M_{D-MP}}$.*

Proof. The tri-level program of model $\boldsymbol{M_{DAD-tri}}$ is equivalent to the model below:

$$\min_{W_j, Qa_j, Qb_j} \varsigma \,,$$

Subject to:

$$\varsigma \geq \max_{V} \min_{W,Qa,Qb} \sum_{i} \sum_{k} \sum_{t} -h_{ikt} \times \left(Qv_{iktj} + Qa_{ikj} + Qb_{iktj}\right) \quad \forall\, j \,,$$

Constraints (5.2-5.17) from model $M_{DAD-tri}$.

We observe that the attacker decision set $\boldsymbol{V}$ is a finite discrete set that comprises of all attack decisions. Also, W and Q are dependent variables that depend on the values attained by finite discrete sets $\boldsymbol{X}$ and $\boldsymbol{Y}$, which in turn describe all defensive decisions.

Moreover, removal of the minimization function in the first constraint set has no effects on optimality. Thus, by enumeration, the model shown above is equivalent to model $\boldsymbol{M_{DAD-tri}}$. This completes the proof.

5.4 A solution algorithm for solving the tri-level sonar placement problem (ASPP-d)

Using a decomposition procedure similar to column-and-constraint generation (C&CG), the models presented in the prior sections are used in an algorithm to achieve optimal placement of sonars, taking into consideration the expected actions of an *'intelligent'* attacker or adversary. The algorithm is implemented at two levels, i.e., a master problem and a sub-problem and is shown below:

Step 0: Initialization
Set $DAD_{lb} = -\infty$ and $DAD_{ub} = +\infty$. Set attack plan vector $\bar{\mathbf{V}} = \mathbf{0}$ Set iteration index, j =1
While $DAD_{ub} - DAD_{lb} > \varepsilon * DAD_{lb}$
Step 1 Solve Model $\boldsymbol{M_{D-MP}}$ Update $DAD_{ub} = \varsigma$ Update defense vectors $\mathbf{X_{current}} = \bar{\mathbf{X}}, \mathbf{Y_{current}} = \bar{\mathbf{Y}}$
Step 2: Solve Model $\boldsymbol{M_{A-dual}}$ for $\mu, \Pi, \Phi, \Psi, \Omega, \tau$, V and assign $Soln_{A-dual}$ as its objective function Update attack vectors $\mathbf{V_{current}}$ Update $DAD_{ub} = \min(DAD_{ub}, Soln_{A-dual})$
Step 3: Set j=$j+1$

where,

DAD_{ub} Solution to DAD Model-Upper bound

DAD_{lb}	Solution to DAD Model-Lower bound
$X_{current}$	Present defense deployment plan X
$Y_{current}$	Present defense deployment plan Y
$V_{current}$	Attacker's response to the present deployment plan
ε	Tolerance for the DAD model

While the master problem gives a lower bound to the tri-level problem, the sub-problem returns an upper bound and provides the worst intrusion/attack plan for a given set of protection decisions. Theoretically, an optimal solution is attained when the duality gap is within a small threshold value $\varepsilon > 0$.

Proposition 5.3. *Algorithm* ***ASPP-d*** *converges to the optimal value of tri-level Model* $\boldsymbol{M_{DAD-tri}}$ *in* $O(q')$ *iterations, where* q' *is the number of elements in sets* $\boldsymbol{X}$ and $\boldsymbol{Y}$.

Proof. At optimality, $DAD_{lb} = DAD_{ub}$. Let $\boldsymbol{u}$ represent the set of all dual variables in Model $\boldsymbol{M_4}$. Let (X^*, Y^*) and (V^*, u^*) be the optimal values of Model $\boldsymbol{M_{D-MP}}$ and Model $\boldsymbol{M_{A-dual}}$ respectively obtained in iteration $j + 1$.

Step 3 of the algorithm indicates that:

$$DAD_{ub} \leq \sum_i \sum_k \sum_t -h_{ikt} * (Qv_{ikt} + Qa_{ik} + Qb_{ikt}).$$

Since initial decision variables of the *'Defender'* are determined in Step 2 from sets $\boldsymbol{X}$ and $\boldsymbol{Y}$**.** These are consequently used as parameters in the optimization problem of model $\boldsymbol{M_{A-dual}}$, this indicates that optimal solution (X^*, Y^*) are determined prior to iteration $j + 1$ (perhaps at iteration $j, j - 1, j - 2, \ldots\ldots$). Hence, the number of iterations

before attaining convergence with the algorithm is dependent on the cardinality of the union of sets $\boldsymbol{X}$ and $\boldsymbol{Y}$, assuming the set is finite. It should be noted that the number of operations executed by loops in the algorithm is the sum of the individual loop efficiencies. Hence, the efficiency is $q' + q''+$, i.e. $O(q')$, where q'' is the number of elements in the set of dual variables and q' is as defined in the proposition. This is because, unlike an alternate procedure such as the Benders decomposition approach, the loops in algorithm *ASPP-d* are not nested. This completes the proof.

5.5 Theoretical Insights and Discussions on Models $\boldsymbol{M_{DAD-tri}}$ and $\boldsymbol{M_{A-dual}}$

5.5.1 Theoretical Insights and Discussions- $\boldsymbol{M_{DAD-tri}}$

Based on the solution concept of multi-level programming in Bard (1998) and Zhang et al. (2010), we give definitions to sets in reference to $\boldsymbol{M_{DAD-tri}}$, which will assist in developing a theoretical basis for an optimal solution of the tri-level model. In the following definitions, $(x\epsilon\, \boldsymbol{X}, y\,\epsilon\, \boldsymbol{Y})$ **,** and $(x'\epsilon\, \boldsymbol{X'}, y'\epsilon\, \boldsymbol{Y'})$ indicate the *Defender*'s top and bottom level decision variables, respectively; and $z\,\epsilon\, \boldsymbol{Z}$ indicates the *Attacker* mid-level decision variables. In addition, function F refers to the objective function of model $\boldsymbol{M_{DAD-tri}}$.

Definition 5.2

1. Feasible region of $M_{DAD-tri}$

$$S = \{(q, z, r) | q\epsilon\, \boldsymbol{X} \cup\, \boldsymbol{Y}, z \in \boldsymbol{Z}, r\epsilon\, \boldsymbol{X'} \cup\, \boldsymbol{Y'}\,, Constraints\ (5.2 - 5.17)\}$$

2. Attacker's *(Mid-level Decisions)* feasible region for each fixed defense plan $q\epsilon\ \boldsymbol{X} \cup\ \boldsymbol{Y}$

$$S(q) = \{z, r\ \epsilon\ \boldsymbol{Z} \times (\boldsymbol{X}' \cup\ \boldsymbol{Y}')\ |Constraints\ (5.2 - 5.17)\}$$

3. Defender's *(Bottom-level Decisions)* feasible set for each fixed defense plan (*Top-level Decisions*) $q\epsilon\ \boldsymbol{X} \cup\ \boldsymbol{Y}$ and attack plan $z\ \epsilon\ \boldsymbol{Z}$

$$S(q, z) = \{r\epsilon\ \boldsymbol{X}' \cup\ \boldsymbol{Y}'|Constraints\ (5.2 - 5.17)\}$$

4. Reaction set (Rational) of the Defender: *Bottom-level Decisions*

$$P(q, z) = \{r|r\epsilon\ \text{argmin}\ F[(\bar{q}, \bar{z}, r)|r\ \epsilon\ S(q, z)]\}$$

5. Reaction set (Rational) of the Attacker: *Middle-level Decisions*

$$P(q) = \{(z, r)|(z, r) \in \text{argmin}\ [F(\bar{q}, z, r)|(z, r)\ \epsilon\ S(q), r\epsilon\ P(\bar{q}, z)\}$$

6. Inducible Region IR (This represents the set over which the *Defender* may optimize the objective function of Model $M_{DAD-tri}$)

$$IR =\ \{(q, z, r)|(p, z, r)\epsilon\ S; (z, r)\ \epsilon\ P(q)\}$$

It should be noted that prior sections of this chapter make no distinction between $\boldsymbol{X} \cup \boldsymbol{Y}$ and $\boldsymbol{X}' \cup \boldsymbol{Y}'$ because the sets are controlled by the same agent (i.e. the '*Defender'*).

Remark 5.1 $M_{DAD-tri}$ is equivalent to the optimization problem:

$$\min\{F(q, z, r)|(q, z, r)\ \epsilon\ IR\}$$

Proposition 5.4. *Given that set S is non-empty and compact, and that set IR is non-empty, then an optimal solution to* $M_{DAD-tri}$ *exists.*

Proof. The assumptions that both S and IR are non-empty indicates that $P\ (q^*) \neq \emptyset$ and that there exists at least an optimal $q^* \epsilon \boldsymbol{X} \cup \boldsymbol{Y}$. We further assume a sequence of decision variables $\{(q^m, z^m, r^m)\}_{m=1}^{\infty}$as a subset of IR converges to an optimal solution(q^*, z^*, r^*). From parametric-optimization $(z^*, r^*)\ \epsilon\ P\ (q^*)$. Thus, IR is also closed. In addition, IR is also bounded because $IR\ \epsilon\ S$. Since IR is non-empty, $M_{DAD-tri}$ involves minimization of a continuous/integer function over a compact non-empty set, showing that an optimal solution exists for the model. This completes the proof.

5.5.2 Theoretical Insights and Discussions- M_{A-dual}

Consider a large scale mixed integer linear programming (MILP) problem:

$$\min_{x,y}\{f(x,y)|Ax + By\ \geq b, x\epsilon R_+^n, y\epsilon Z_+^m\}, \qquad \textit{(MILP1)}$$

where $f(x,y)$ represents the model's objective function; and $A\epsilon R^{j*n}$ and $B\epsilon R^{j*m}$ respectively represent coefficient matrices for $x\epsilon R_+^n$ and $y\epsilon Z_+^m$ per constraint j; and $b\epsilon R^j$ is a vector for constraint j. Also, we assume all data are rational and that all variables are non-empty and finite.

L-P based approaches for solving MIPs such as Branch and Bound, and Branch and Cut, attempt to arrive at an optimal solution by solving several sub-problems of *(MILP1)* and then choosing the best solution, $f(x*, y*)$ from a solution pool of the sub-problems. The problem is said to be infeasible if all the generated sub problems of *(MILP1)* are infeasible. Unlike an L-P problem, it is difficult to develop a standard dual problem for MILP with properties similar to those observed in the LP case. Generally, such dual problems are neither strong nor computationally tractable (Guzelsoy and

Ralphs, 2007). However, Proposition 5.5 and Remark 5.2 show how duality can be used to solve the decomposition problem in our tri-level problem. In order to present Proposition 5.5, we introduce the following definitions:

Definition 5.3

1. Let $\boldsymbol{\pi_i}$ be a set of decision variables corresponding to primal constraints and the extra integer constraints ($\leq$ and/or $\geq$) introduced in each sub-problem (branching) $i$of set $\boldsymbol{G}$.
2. Let $\boldsymbol{\pi_{i'}}$ be a set of decision variables corresponding to primal constraints and the extra integer constraints ($\leq$ and/or $\geq$) introduced in each sub-problem (branching) i' of set $\boldsymbol{G'} \subseteq \boldsymbol{G}$.
    i. $\boldsymbol{G'}$ is a subset of $\boldsymbol{G}$, $\boldsymbol{G'} \subseteq \boldsymbol{G}$.
    ii. $\boldsymbol{G'}$ is a set of the duals of sub-problems, $g_{i'}$ whose corresponding primal sub-problems return integer solutions for $\boldsymbol{y}$.
3. Let $g_i(Ax + By)$ be the dual feasible function for sub-problem i in *(MILP1)* and $\boldsymbol{G}$ be a set of such dual feasible function. Also, let $H_{i'}(\pi_{i'})$ be the corresponding dual function of i'.

Proposition 5.5 *Given definition 5.3, the dual constraint equation of sub-problem* i *is:*

$$g_i(Ax + By) \leq f(x, y) \ \forall \ g_i \in \boldsymbol{G}$$

Then, dual feasible solution π *for (MILP1) is obtained by solving the model*:

$$\max_{\pi_i} \{H_{i'}(\pi_{i'}) | g_i(Ax + By) \leq f(x, y) \ \forall \ x \epsilon R \ \forall \ y \epsilon Z^+ \forall \ g_i \in \boldsymbol{G}\}$$

And the optimal dual feasible solution for (MILP1) is obtained by solving the model,

$$\max_{i'}\left(\max_{\pi_{i'}} H_{i'}(\pi_{i'}) \,\middle|\, g_i(Ax+By) \le f(x,y) \forall\ x \epsilon R\ \forall\ y \epsilon Z^{+} \forall\ g_{i'} \in \boldsymbol{G'}\right).$$

Proof. From Duality Theory, $H_{i'}(\pi_{i'}) \le H_i(\pi_i) \le f(x,y)\ \forall\ i, i'$ and $g_{i'}(Ax+By) \le g_i(Ax+By) \le f(x,y)\ \forall\ g_i \in \boldsymbol{G}, g_{i'} \in \boldsymbol{G'}, \boldsymbol{G'} \subseteq\ \boldsymbol{G}$. Also, from generation of sub-problems,

$g_i(Ax+By) \le g_{i'}(Ax+By) \le g(Ax+By)\ \forall\ g_i \in \boldsymbol{G}, g_{i'} \in \boldsymbol{G'}, \boldsymbol{G'} \subseteq\ \boldsymbol{G}$. Then,

$f(x,y) \ge g(Ax+By) \ge\ g_{i'}(Ax+By)\ \ge g_i(Ax+By)\ \forall\ g_i \in \boldsymbol{G}, g_{i'} \in \boldsymbol{G'}, \boldsymbol{G'} \subseteq\ \boldsymbol{G}$.

Thus, g is the dual feasible constraint function for *(MILP1)* with an equivalent objective function $H_i(\pi_i)$. Clearly, Strong duality suggests that at optimality, the dual feasible solution of sub-problem i corresponds to its primal equivalent. However, to obtain a valid solution to *(MILP1)*, the corresponding primal solution must return integrality in the $\boldsymbol{y}$ variables. This completes the proof.

Remark 5.2 *Let $y^r \epsilon\ R$ be a relaxation of $y\ \epsilon\ Z$. Then, the relationship between the optimal solutions of (MILP1) and its LP relaxation is:* $f(x^*, y^*) \le f(x^*, y^{r*})$. This relationship holds because the optimal value of the LP relaxation is no smaller than that of *(MILP1).* Thus feasible solutions to the dual of the LP relaxation correspond to upper bounds in *(MILP1).* At optimality, $f(x*, y'*) = H(\pi_r{}^*)$ where $\pi_r{}^*$ is the optimal set of decision variables corresponding to primal constraints in the LP relaxation of *(MILP1).*

From proposition 5.5,

$H(\pi^*) = \max_{i'} \max_{\pi_{i'}} H_{i'}(\pi_{i'})$,

Hence,

$H(\pi_r{}^*) \geq \max_{i'} \max_{\pi_{i'}} H_{i'}(\pi_{i'})$.

Thus, in general, the dual solution of the LP relaxation gives only an upper bound on the dual solution of the MIP i.e., bounds using LP relaxation may not be as tight as desired. As a caveat, due to this observation, convergence of ASPP-d as discussed in Section 5.3 is not expected to be as fast as desired since Model M_{A-dual} is not an LP.

5.6 Computational Results

Using ASPP-d, computational results presented in this section are based on data introduced in Chapter 4. All models are implemented in GAMS and solved using CPLEX (GAMS 2013). All MIPs are solved within a relative tolerance of 3% duality gap and all computational runs are made on a Linux server equipped with dual 3.00 GHz AMD processors (24 cores) and 256 GB memory running on Ubuntu 64bit operating system.

Table 5.1 shows results of the objective functions when we set $\bar{c} = 3$ in equations (5). In the non-collaborative interaction between the '*Attacker'* and the '*Defender'*, the table indicates that, with no resources available to neither the attacker nor the defender, the objective value will always be 0. Under this situation, there is no effect on the objective function. The observation is expected and serves to validate solution results. The table also indicates that as more resources become available to the *'Defender'*, the objective function tends to become monotonically non-increasing (readers should note

the negative signs in the objective functions and that the *'Defender'* is interested in minimizing overall non-detection probabilities). In contrast, as more resources become available to the *'Attacker'*, the objective function tends to become monotonically non-decreasing (readers should note the negative signs in the objective functions and that the Attacker's interest is in maximizing overall non-detection probabilities). All these are in agreement with expected model behavior in the interface relationships between the *'Defender'* and the *'Attacker'*.

Table 5.1: Objective Function: Resources available to Defender vs Resources available to Attacker

q_{max}	B					
	0	1	2	3	4	5
0		-503.69	-811.572	-1103.29	-1379.37	-2269.68
1	317.757	-110.867	-394.6	-698.411	-969.377	-1534.9
2	635.13	273.946	-33.531	-313.707	-583.673	-1379.37
3	948.665	620.609	310.652	54.702	-20.728	-103.21
4	1257.211	952.09	624.941	386.46	161.681	-66.168
5	1567.58	1237.89	919.86	713.688	503.91	-299.77

Figures 5.2-5.5 show objective values for different values of parameter $\bar{c}$. As indicated in the figures, without any resources (sonars) available to the *'Defender'*, the objective function remains unchanged irrespective of the value of parameter $\bar{c}$ when *"Attacker'* resources remains the same. This is because only the latter's influence is active in the objective function when the former has no resources (sonars) at its disposal.

The figures indicates that optimum value is often attained when constraints (5.5) is relaxed. Specifically, with medium to large resource availability (3-5 units) to the *'Defender'*, optimal values are observed when constraints (5.5) are relaxed. In some instances, optimal values are the same under both scenarios (i.e., when $\bar{c} = 3$ and when constraints (5.5) is relaxed) but never worse. This observation is due to the fact that constraints (5.5) restrict the solution space of the non-convex set. Since partial coverage entails that coverage in the entire AOI is related to the criticalities of sub-regions in the AOI, it is expected that with medium to large budget scenarios and relaxation of constraints (5.5), coverage will have a bias for sub-regions of the AOI with higher criticalities, thus improving the objective functions. However, when no resource is available to the *'Attacker'*, there is no difference in the optimal values when $\bar{c} = 3$ and when constraints (5.5) are relaxed.

Conversely, with low (0-2 units) resources available to the *'Defender'*, the optimal value is indistinguishable between when $\bar{c} = 3$ and when constraints (5.5) are relaxed. This is because with less budgetary resources available to the *'Defender'*, multiple sonar coverage of the subsections of the AOI with higher criticalities is negligible due to low budgets, even when constraints (5) are relaxed.

All of the above observations suggest the model provides the 'best' optimal values whenever Constraints (5) are relaxed as the Defender's allotted budget increases. However, the fundamental plan in the placement study under review in the sonar placement problem is *'Partial Coverage'*, where due to high costs of underwater sonars, procuring *'enough'* sonars to cover the entire AOI is neither economical nor practicable. In addition, the performance of the model in terms of the concepts of *'pn-coverage'*

introduced in Chapter 4 accentuates the need and importance of constraints (5.5). Although improvements (ranging from marginal to significant) in the objective function of the model is observed when constraints (5.5) is relaxed under medium to large resource availability (3-5 units) to the *'Defender'* , the portion of the AOI that is effectively covered by sonars (as represented by the *pn-Coverage* benchmark) is adversely affected. Hence, the need to maintain the multiple coverage restriction imposed by constraints (5.5) is also justified for the Tri-level programming approach in this chapter.

Essentially, we observe the same trend (in objective functions) for different values of $\bar{c}$ in constraints (5.5) and when the constraints are relaxed. In the majority of all the cases (with different resource limitations to each agent), the only difference is the magnitude of these objective functions. The only exception observed in the trend is when five units of resources are available to the '*Defender'* and none is available to the *'Attacker'* when $\bar{c}$ in constraints (5.5) is set to one unit. The reason behind this exception is that, though the '*Defender'* has adequate resources available to it, the restriction imposed on the solution space by $\bar{c} = 1$ in constraints (5.5) ensures that the objective function remains un-changed compared to when it had less than one resource available to it (i.e. when it had four units of resources available).

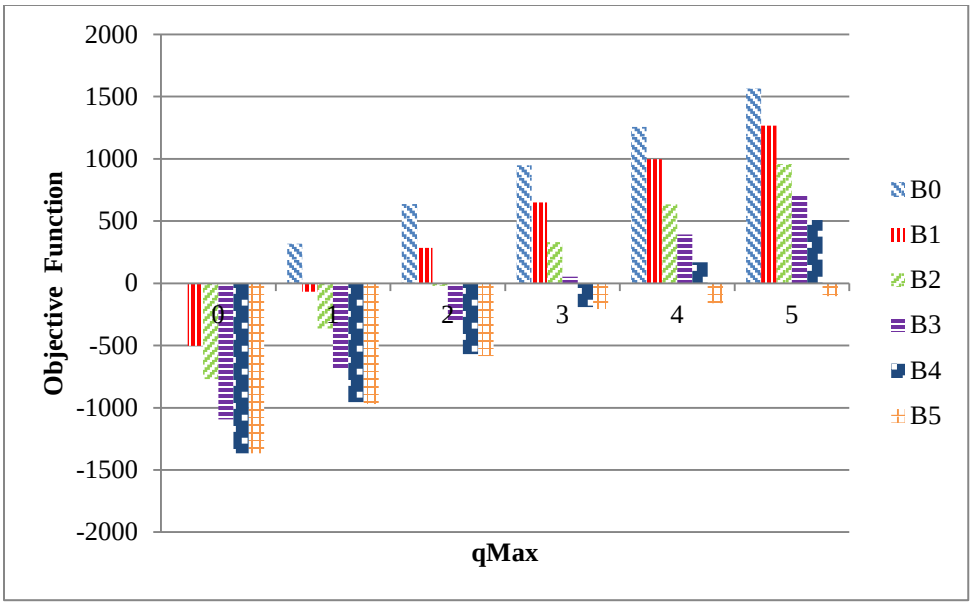

Figure 5.2: Objective Functions: Resources available to Defender vs Resources available to Attacker ($\bar{c}$=1)

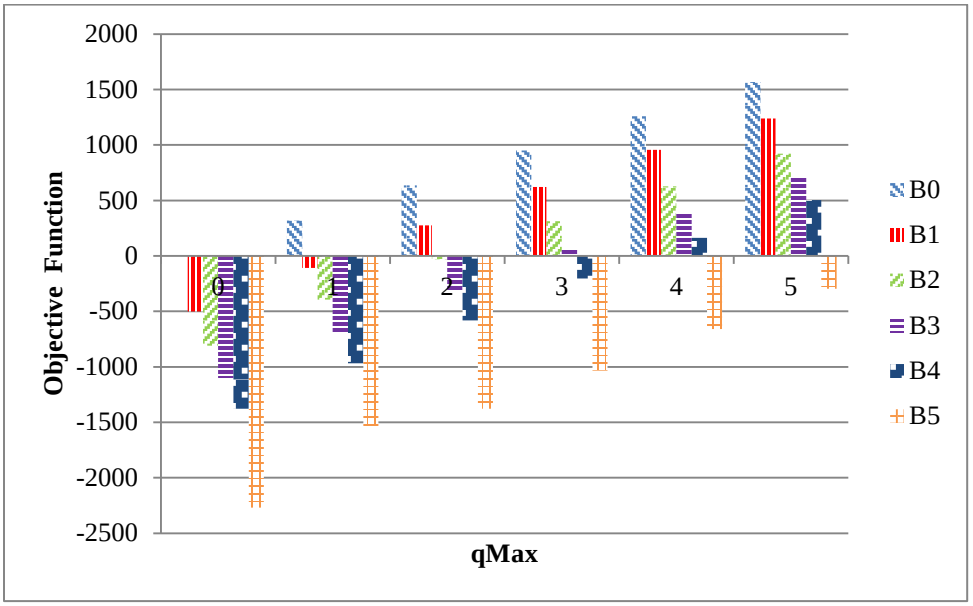

Figure 5.3: Objective Functions: Resources available to Defender vs Resources available to Attacker ($\bar{c}$=2)

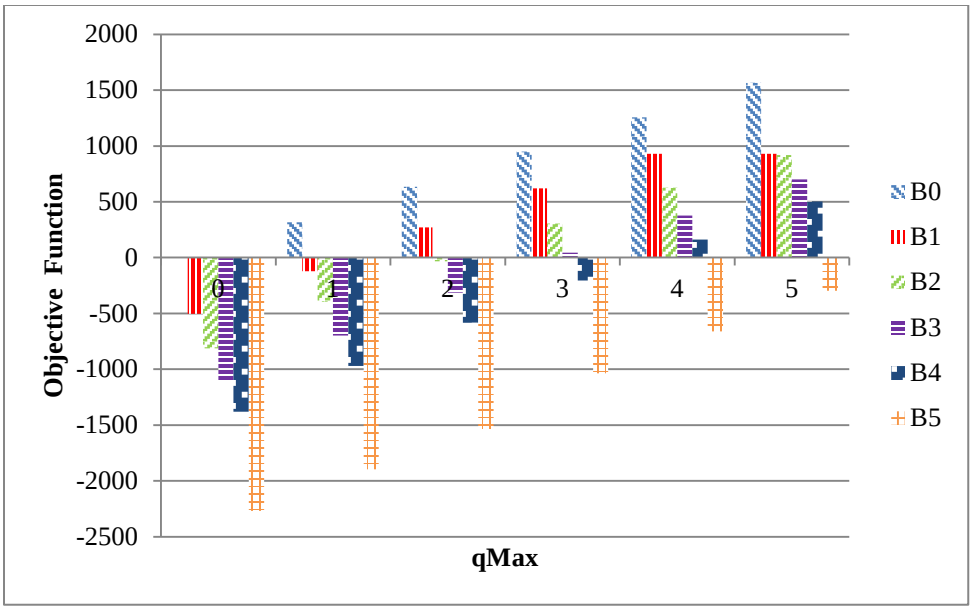

Figure 5.4: Objective Functions: Resources available to Defender vs Resources available to Attacker ($\bar{c}$=3)

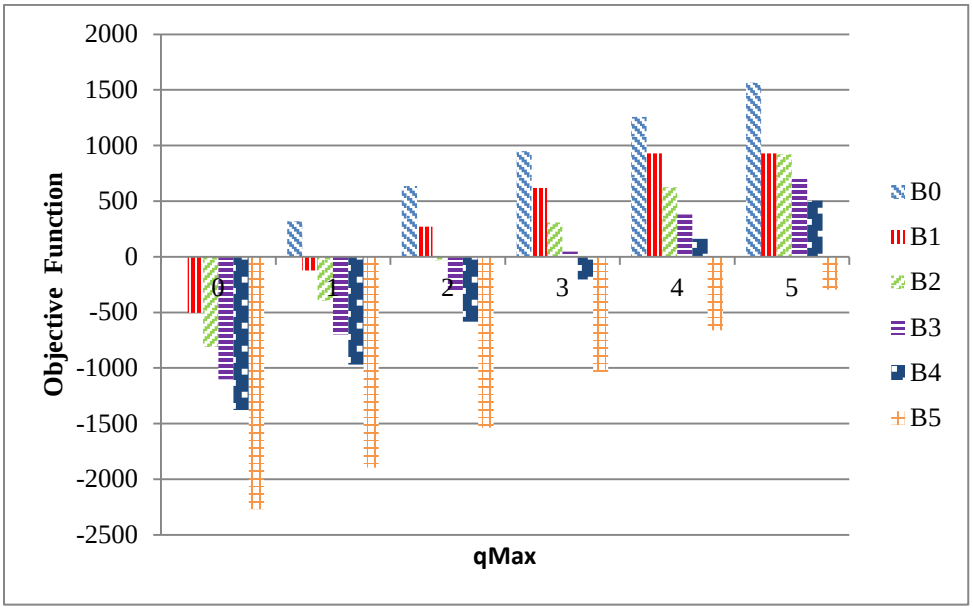

Figure 5.5: Objective Functions: Resources available to Defender vs Resources available to Attacker ($\bar{c}$=No restriction (NR) i.e. equation (5.5) is relaxed)

As shown in Figures 5.6 and 5.7, the percentage of the AOI that is protected by sonars helps to visualize vulnerability in the case of a successful intrusion by attacker(s). It is imperative to analyze the trade-off between the defense cost incurred by adding

defensive resources and the gain in vulnerability mitigation. From the figures (though with few outliers), we infer that for limited sonar resources to the *'Defender'* (1-2 units), *'p1-Coverage'* values correspond to equivalent optimal objective values in all cases (i.e. as optimal objective values improve, *'p1-Coverage'* also increases). However, with the availability of more resources to the *'Defender'* (3-5 units), '*p1-Coverage'* values do not necessarily correspond to equivalent optimal objective values. The reason behind this is that multiple coverage of subsections of the AOIs with higher criticalities improve the objective functions but have no effects on the equivalent *'p1-Coverage'* value. Also, with limited sonar resources (1-2 units) available to the *'Defender'*, relaxation of Constraints (5.5) or active use of the constraints only has marginal differences in *'p1-Coverage'* values. On the contrary, with availability of more resources (3-5 units), *'p1-Coverage'* values reduce significantly when Constraints (5.5) are relaxed in comparison to when the constraints active.

Similar explanations given in the observation related to optimal objective values also hold true. In general, as more resources become available to the *'Defender'*, setting $c = 3$ gives little or no improvement in *'p1-Coverage'* when Constraints (5) are active. However, this choice of parameter value is not outperformed by any other choice. Most of the defense benefit is achieved with a maximum of three or four resources (sonars). Larger defense investments produce progressively lower incremental vulnerability reductions. Results for *'p2-Coverage'* and *'p3-Coverage'* also follow similar trends, although with comparatively lower values, including 0 for the latter (i.e. no portion of the AOI is covered by at least three sonars across the entire deployment periods).

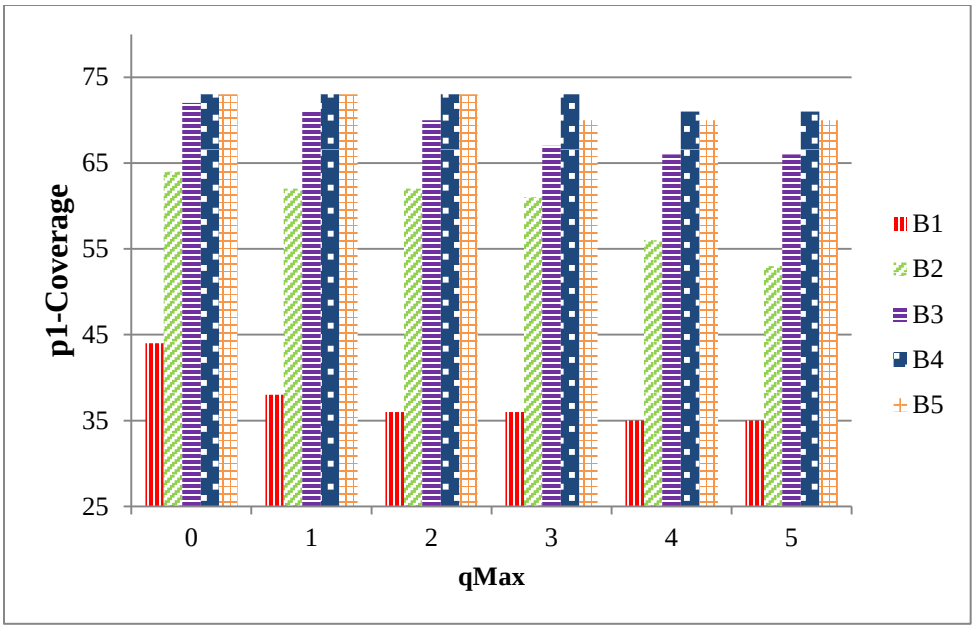

Figure 5.6: *'p1-Coverage'*: Resources available to Defender vs Resources available to Attacker ($\bar{c}$=3)

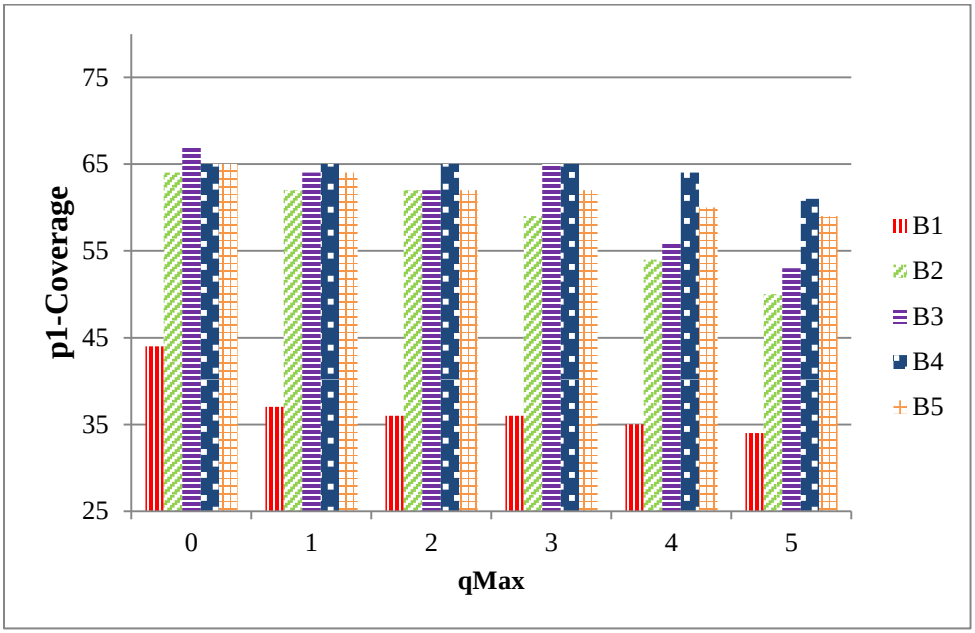

Figure 5.7: *'p1-Coverage'*: Resources available to Defender vs Resources available to Attacker ($\bar{c}$=No restriction, NR)

Results for *'p2-Coverage'* and *'p3-Coverage'* do not convey additional inferences different from those presented for the *'p1-Coverage'* case and are thus, not shown in this section.

5.7 Conclusions

In this chapter, we presented a tri-level optimization model and an algorithm to solve the sonar placement problem where optimal partial coverage is desired. Partial coverage is due to limitations imposed by budget limitations. Typically, a game-theoretic approach is often adopted in a problem of this nature where competing rational agents with conflicting interests are the decision makers. In comparison to the game theoretic approach, where only two levels of interface relationships (whether collaborative or non-collaborative) are considered in a strategic planning framework, our fortification model produces a superior protection plan because it considers an additional third level of non-collaborative relationship between the *'Defender'* and the *'Attacker'*, and thereafter selects the optimal strategy to thwart the attacker's efforts based on the optimal strategic plan adopted by the latter. Using practical data, we implemented the algorithm to solve the tri-level problem. In contrast to other approaches such as the traditional Benders-dual algorithm, which requires the sub-problem to be an LP problem, our algorithm is indifferent to such limitations. Although non-traditional methods using heuristics have been proposed to address this issue with the Benders approach, there are no guarantees the sub problem can be solved to integer optimality.

We emphasize that though protection is desirable, its desirability in terms of reducing vulnerability of the AOI should be dependent on the maximum resource

capability of the *'Attacker'*. With small attack budgets, benefits of providing protection are often minimal and investment in providing protection may be regarded as unnecessary. However, with increased resource availabilities to the attacker(s) and a consequent ability to intrude in the AOI, the significance of investing in protection resources becomes apparent. As such, decision-makers (system planners) can adopt a protection plan after reviewing costs and inherent benefits associated with the protection plan.

Chapter 6

Algorithms for the Sonar Placement Problem

6.1 Introduction

Computational complexity of the generic sensor placement problem has been proven to be *NP-hard* (See Chapter 2). To address the computational challenges posed by coverage problems, efficient algorithms to solve the Sonar placement problem (SPP) need to be developed to ensure that near-optimal solutions can be found quickly. This is especially relevant when decisions have to be made in real-time situations.

In this chapter, we propose simple and efficient algorithms (based on greedy approach) for placing sonars to satisfy coverage requirements within budgetary limitations. Essentially, the greedy technique is based on the principle of identifying optimal local solutions at each step of an algorithm with the expectation that the global (or near global) optimum of the objective function is attained at the end of the procedure.

6.2 Greedy-based Algorithms for the Sonar Placement Problem

In this section, we describe procedures of the three greedy-based algorithms we have developed to arrive at fast (even if sub-optimal) solutions. The algorithms exploit the structure of the SPP to arrive at efficient solutions.

Starting from an empty set and choosing from among eligible candidate placement positions, the greedy policy iteratively selects the sonar type- placement position pair that maximizes the expected overall increase in value of the measure metric

($\frac{v_{i,k,t}^{m}}{d_m}$), conditioned on the observed states of sonar type- placement positions it had already selected in prior iterations, thus increasing the expected total marginal benefit of the measure metric. In essence, at each iteration, the greedy policy tries to increase the expected objective value (mirrored by the equivalent measure $\frac{v_{i,k,t}^{m}}{d_m}$), given its current observations.

Sonar type- placement position pairs continue to be selected within coverage limitations until available budget is expended. If solving the SPP using mixed integer programming proves to be intractable, our greedy-based algorithms can be used to find a good initial solution. Afterwards, we can improve on this solution using any local search technique.

Pseudocodes of the greedy-based algorithms are described in Figures 6.1- 6.3. The algorithms we presented are simple and fast computational heuristics for underwater sensor placement. Our algorithms start with a null solution, i.e., an empty sequence. They evaluate all *N* candidate placement positions/sites across the entire deployment periods but only choose a deployment period t whose function $\frac{v_{i,k,t}^{m}}{d_m}$ maximizes detection probabilities of the entre AOI. To break a tie (if any), we simply choose deployment period/deployment position chronologically. Thereafter, an MIP is used to determine relocations across the other periods.

Step 0: Sets, parameters and variables: Initialization

$$Place(i,k) = no, Placement(i,k,t) = \emptyset, , numCover(i,k,t) = 0;$$

Step 1:

Compute un-expended budget $b(e) \geq 0$ for all combinations e of available sonars:

$$b(e) = B - \sum_{m} d_m r_m^e \; \forall \; r_m^e \in R_m^e$$

where d_m is the dollar cost of available sonar m and r_m^e is the number of sonar m in any combination e of sonar types.

Step 2: (Choose combination of e that gives the least $b(e)$).

Let

$$A_{u^*} = \left(\bigcup_{e=1}^{s} A_{e^*} \right) \subseteq R_m^e$$

such that $\exists \; r_m^{e^*} \in A_{e^*} : \; b(e^*) = \min_e b(e)$

Step 3:

$r_m^{e^*} \in A_{e^*}; \; m \in M = 1,2, \ldots . n; e^* = 1,2, \ldots s$

While $|A_{e^*}| > 0$

$\forall \; Place(i,k) \neq yes; \; \&\& \; numCover(i,k,t) < coverMax$

i. Compute overall risk reduction if sonar type m is placed in (i,k) at time t for combination e^*.

$$v_{i,k,t}^m = -h_{ikt} \ln(1 - p_m) - \sum_{(i\prime,k\prime,t\prime) \in N_l(i,k,t)} h_{ikt} \ln(1 - p_m^l)$$

ii. Rank eligible $Candidate(i,k,t)$ for sonar type m in descending order as an ordered list using criteria $\frac{v_{i,k,t}^m}{d_m}$.

iii. Update $Placement(i,k,t) = Candidate(i*, k*, t*)_m \cup Placement(i,k,t)$, where $Candidate(i*, k*, t*)_m$ is at the top of the ordered list for sonar type m using criteria $\frac{v_{i,k,t}^m}{d_m}$ .Set $Place(i*, k*) = yes.$

iv. Update $numCover(i,k,t) = numCover(i,k,t) + 1$ for $(i*, k*, t*)$ and $(i', k', t') \in N_l(i*, k*, t*)$

v. Remove $Candidate(i*, k*, t*)_m$ from the top of the ordered list

$$r_m^{e^*} = r_m^{e^*} - 1;$$

$$|A_{e^*}| = |A_{e^*}| - 1$$

End While

Step 4: For static sonars, placement remains un-changed irrespective of deployment period t.For mobile sonars, we use a simple MIP to determine relocation of the sonars.

Figure 6.1: Pseudocode for the algorithmic steps in g-SPP1

Step 0: Do Step 0 in g-SPP1
Step 1:
Set $bRem = B$;

a. Do (i) and (ii) in Step 3 of g-SPP1. However here, the overall risk reduction and ranking criteria are not only for any combination e^* but for all sonar type m.
b. While $bRem \geq d_m$
   $\forall\ Place(i,k) \neq yes;\ \&\&\ numCover(i,k,t) < coverMax$
      i. Do (iii-v) of Step 3 of g-SPP1 with the myopic greed routine using criteria $\frac{v_{i,k,t}^m}{d_m}$.
   $bRem = bRem - d_{m*}$
   End While

Step 2: Do Step 4 in g-SPP1

Figure 6.2: Pseudocode for the algorithmic steps in g-SPP2

Step 0: Do Step 0 in g-SPP1
Step 1:

a. Do step 1 (a) in g-SPP2
b. Find d_m^*,where d_m^* is the cost corresponding to the sonar type $m*$ at the top of the ordered list
c. Let $counter\ = \left\lfloor \frac{B}{d_m^*} \right\rfloor$
   While $counter > 0\ \&\&\ Place(i,k) \neq yes; \&\& numCover(i,k,t) < coverMax$
      i. Do (i-v) of Step 3 in g-SPP1 with the myopic greed routine using criteria $\frac{v_{i,k}^m}{d_m}$. (When $counter = \left\lfloor \frac{B}{d_m^*} \right\rfloor$, $Candidate(i*,k*,t*)_m$ corresponding to $m*$ is chosen. Else, $Candidate(i*,k*,t*)_m$ is chosen from the ordered list without recourse to the corresponding sonar type m.)
      $counter = counter - 1$
   End While
   Set $Placement(i,k,t)_m = Placement(i,k,t)$
d. If $\exists_{m' \in M'}: B - \left\lfloor \frac{B}{d_m^*} \right\rfloor \geq d_{m'}$ //If there exists any sonar type m'that can be procured with //the un-expended budget
   While $|M'| > 0$ && $Place(i,k) \neq yes; \&\& numCover(i,k,t) < coverMax$
      i. Repeat (b) and (c-i) using m'
   $|M'| = |M'| - 1$
   End While
   Set $Placement(i,k,t)_{m'} = Placement(i,k,t)$

Set $Placement(i,k,t) = Placement(i,k,t)_m \cup Placement(i,k,t)_{m'}$
Step 2: Do Step 4 in g-SPP1

Figure 6.3: Pseudocode for the algorithmic steps in g-SPP3

where,

$b(e)$	Un-expended budget for combination c of available sonar type (with different cost, detection coverage, etc.)
B	Available budget for the entire deployment
d_m	Cost of available sonar m
n_m^e	Number of sonar-type m in any combination c of sonars
A_{e^*}	Set that contains sonar combination e with minimum $b(e^*)$ i.e. $A_e : b(e^*) = \min_e b(e)$ (Each element of a combination c includes both sonar type m and number/quantity n to be deployed)
$Placement(i,k,t)$	Sonar placement location(i,k,t).
$Place(i,k)$	Holder for tracking (i,k) of $Placement(i,k,t)$
$numCover(i,k,t)$	Characterizes the number of times a candidate location (i,k,t) is covered by sonars
$coverMax$	A parameter (integer) that restricts the total number of times a location (i,k,t), is covered by sonars
$v_{i,k,t}^m$	Overall risk reduction if sonar type m is placed in placement location(i,k,t)
$N_l(i,k,t)$	Set containing (i',k',t') in the neighborhood of (i,k,t) that are also covered by sonar placed in(i,k,t).

The algorithmic steps 3-4 of g-SPP1 and all steps in g-SPP2 and g-SPP3 are quite self-explanatory and easy to follow. Hence, we provide an illustrative example to

explain procedures in steps 1-2 of g-SPP1. Suppose, we have three different sonar types with a total budget of $100 (in millions) for deployment as shown in Table 6.1.

Table 6.1: Illustrative example for steps 1-2 in g-SPP1

Budget =$100			
Sonar Types	Type 1	Type 2	Type 3
Cost	13	31	47

In this example, the number of sonar type n_i deployed is bounded by a mathematical inequality ($13n_1 + 31n_2 + 47n_3 \leq 100$). However, a deployment strategy may also involve non-deployment of a sonar type i, leading to an extra consideration in sonar-type combinations. Thus, the total number of possible combinations of sonar-type considered is $\left(1 + \left\lfloor\frac{100}{13}\right\rfloor\right) \times \left(1 + \left\lfloor\frac{100}{31}\right\rfloor\right) \times \left(1 + \left\lfloor\frac{100}{47}\right\rfloor\right) = 66$.Table 6.2 shows the optimal sonar type-combinations that gives the least un-expended budget in this example. The table indicates that four units of type 1, none of type 2 and one of type 3 gives the minimum un-expended budget of $1(in millions).

Table 6.2: Optimal sonar type combination for illustrative example of Table 6.1

Sonar Types	Type 1	Type 2	Type 3
Optimal n	4	0	1
		Un-expended Budget=$1	

6.3 Discussions and Analysis on the algorithms

Of the three algorithms, **g-SPP-**1 attempts to identify the combination(s) of sonar types from among several deployment strategies that gives the least unused

budget for any budget allocation i.e. before getting into the iterative placement procedure, it appraises the total budget for sonar placement, searches among all possible combinations of sonars that exhaust the budget and then chooses the combination that leaves the least unused budget. The premise behind this is that under the assumption of uniform detection probabilities of sonars, the optimal deployment of sonars involving candidate placement positions with uniform characteristics (criticalities) under strict budget limitation is synonymous with maximizing the number of the sonar types deployed (hence, minimizing left-over budget). Of course, the procedure cannot guarantee optimality; however, it gives a good starting solution.

We refer to both **g-SPP-**2 and **g-SPP-**3 as "myopic greedy' algorithms because neither of these two algorithms attempts to identify a dominant set that in any way tries to ensure optimality might be attained. Rather, they 'greedily' allocate sonar type-placement position pair with greatest metric that doesn't violate coverage conditions until allocated budget is expended. However, the algorithms are useful because they are quite fast and in some instances, numerical results (See Section 6.4) indicates little loss in optimality in comparison to results returned by **g-SPP-**1 and CPLEX.

The difference between **g-SPP-**2 and **g-SPP-**3 is that while the former (like **g-SPP-**1) iteratively identifies the sonar type-placement position pair with most favorable metric, the latter continues to use the same sonar type in the first iteration (until its availability is exhausted). Table 6.3 summarizes the algorithm(s). In Table 6.3, we identify the major procedures in the algorithms, highlighting major differences among the algorithms. Any similarity in procedure (algorithmic steps) is avoided in the summary provided.

Table 6.3: Descriptions of the greedy-based algorithms

Algorithms	Description
g-SPP-1	Minimize least un-expended budget and allocate sonar types based on this, taking into consideration benefit/sonar price index. Once a placement is made, the chosen subsection of the AOI (at a particular period) and others which it covers (if coverage limit is met) becomes ineligible for placement in the next iteration.
g-SPP-2	In each iteration, identify sonar type with highest benefit /sonar price index and place this identified sonar type in subsection of the AOI (at a particular period) corresponding to highest benefit /sonar price index. Like **g-SPP-**1, once a placement is made, the chosen subsection of the AOI and others which it covers (if coverage limit is met) becomes ineligible for placement in the next iteration.
g-SPP-3	Same as **g-SPP-**2 but once maximum benefit /sonar price is identified in the first iteration, the same sonar type is allotted till all budget is expended for this particular sonar type. Any un-spent budget (if adequate for more procurement) is allotted to the sonar type with the second highest cost/sonar price index.

It should be noted that Steps 1-2 of g-SPP1can be easily modeled as a simple optimization problem thus,

$$\min_{e}\left(b(e)\middle|\sum_{m} d_m n_m^e \le B \;\; \forall\, n_m^e \in N_m^e\right).$$

Hence, in practice, a simple MIP (using Branch and Bound techniques) or dynamic programming approach (with memory) would efficiently replace the enumerative search in the step. While the enumerative approach will not be scalable as problem size increases, the dynamic programming approach doesn't suffer from such limitations. However, due to the nature of the problem in this dissertation (where we study partial sonar coverage as a result of budget limitation), this issue does not arise. Although a dynamic programming approach (without memory) will suffice for this chapter, the approach with memory will be useful if any modification is required to identify any "next best" solution (See Chapter 7).

In addition, we could have more than one combination of sonar selections that gives least $b(e)$ and, in practice, $v_{i,k,t}^m$ can be computed during pre-processing operations. It should also be noted in step 2 of g-SPP1 that set A_{u*} contains combination e of sonars that leaves least budget unused. Whenever $\min_e b(e)$ exists for only a single combination of e, $\sum_{e^*=1}^{s} e^* = 1$; Else,$\sum_{e^*=1}^{s} e^* = s$.

6.3.1 Properties of Risk Measure $\left(\frac{v_{i,k,t}^m}{d_m}\right)$

The risk measure introduced in the algorithms essentially mirrors the objective function of the SPP model, with the added property that we have a measure for each candidate placement position corresponding to a sonar type. The risk measure is non-negative ($\frac{v_{i,k,t}^m}{d_m} \ge 0$) and we generally aim to maximize the measure. The risk measure is also non-decreasing. This means that for subsets $A \subseteq B \subseteq S$, it is always true that

$\frac{v_{i,k,t}^{m}}{d_m}(A) \leq \frac{v_{i,k,t}^{m}}{d_m}(B)$ i.e. as more sonars are placed, our overall risk measure improves or at worst remains unchanged. Hence, the optimization of underwater sonar placements for detecting underwater intrusion is considered a submodular optimization. As explained, the algorithms initialize with an empty placement and proceeds iteratively. At each iteration round, they select the sonar-candidate location that contributes most to reduction in the overall risk measure (picks the most profitable subset of elements in from the not-yet-selected elements) and adds it to the current set.

6.3.2 Computational Complexity

The analysis we present in this section is for mobile sonars and readily applies to the static sonars too (with slight modifications). However, the last step (Step 4 in g-SPP1, Step 2 in g-SPP2 and g-SPP3) is omitted in this analysis.

Suppose:

B	Available Budget
q	Available mobile sonar types to select from
n	Total number of mobile sonar types selected after placement methodology
m_i	Number of mobile sonar i selected in the placement methodology
N	Total number of candidate placement positions in the AOI across the whole periods
p	Average Procurement cost of mobile sonars

Assuming a sonar type i is selected at least once, then for steps 1-2 in **g-SPP-**1, the number of possible selections before entire budget is expended (or becomes insufficient for additional sonar) is approximately: $n = \sum_i^q m_i = \left\lfloor \frac{B}{p} \right\rfloor$. From Murty

(1981) and Ghafoori and Altiok (2012), the number of possible solutions to the problem of this approximate solution above is: C_{q-1}^{q+n-1} (A total number of C_{q-1}^{q+n-1} additional evaluations have to be carried out in Step 1). Hence for **g-SPP-**1 (in comparison to the other algorithms), there is an obvious increase in computational time.

For the placement mechanism (Steps 3 for **g-SPP-**1, Step 1 for **g-SPP-**2 and **g-SPP-**3), since N number of candidate placement positions and q number of sonars are available to choose from, we have $N \times q$ different combinations of placement positions and sonar types. In addition, the total number of iterations before the budget is expended is n ($n \leq q$). Thus we have a total of $N \times q \times n$ in the entire iterations. For each possible selection, there exists approximately $P_n^N \Big/ \prod_{i=1}^{q} \mathrm{m}_i!$ different placement schemes. Hence, giving the number of different possibilities in the feasible set as: $C_{q-1}^{q+n-1} \times P_n^N \Big/ \prod_{i=1}^{q} \mathrm{m}_i!$; and the time to find the solution is of order $O(N^q)$. With the exception of Steps 1-2 in **g-SPP-**1, the same analysis applies for **g-SPP-**2 and **g-SPP-**3 i.e. the number of different possibilities in the feasible set is: $P_n^N \Big/ \prod_{i=1}^{q} \mathrm{m}_i!$. Each algorithm is also of order $O(N^q)$ because the running time of each algorithm is proportional to the number of candidate placement locations N, and the number of sensors to be placed q.

From our analysis, it is evident that the region(s) considered in each of the three algorithms is much lesser than the feasible region of the optimization problem in the SPP, ensuring desirability of the algorithms for large scale problems within acceptable

levels of accuracies. Of course, the greedy-based algorithms do not guarantee that, upon termination, a maximum cover will be found for optimality (See experimental results in Section 6.4). However, results can be used to establish acceptable bounds for the placement problem. Based on some specified assumptions, we introduce below some theoretical insights that govern the performance of the greedy-based algorithms. Let:

K_{OPT}	Number of covered placement positions by the optimal solution to the SPP
p_i	Number of newly covered elements at the $i\ th$ iteration (using the algorithms)
q_i	Total number of covered elements up to the $i\ th$ iteration (using the algorithms), $q_i = \sum_{j=1}^{i} p_j$
r_i	Number of uncovered elements after the $i\ th$ iteration, (using the algorithms) $r_i = K_{OPT} - q_i$
k	Total number of iterations (using the algorithms)

Thus, at initialization, $p_0 = q_0 = 0$ and $r_0 = K_{OPT}$.

Proposition 6.1: *Assuming uniform sonar costs and detection probabilities, the number of uncovered placement positions at the $i\ th$ iteration is at most equal to k of the number of newly covered placement positions at the $(i+1)\ th$ iteration , i.e.,$r_i \leq k(p_{i+1})$*

Proof: Optimal solution covers K_{OPT} elements at k iterations. In essence, at each iteration, there should be some sets in a universal set U whose size is at least equal to the $\frac{1}{k}$ of the remaining uncovered elements, i.e., $\frac{r_i}{k}$. If this assertion is false, it will be impossible to cover K_{OPT} many placement positions at the end of the iterations in k steps.

On the contrary, a greedy-based algorithm (such as **g-SPP-**1 **g-SPP-**2 and **g-SPP-**3) at each step of the algorithm selects a set that covers the most number of eligible uncovered placement positions that are eligible for selection, choosing at least the $\frac{1}{k}$ of the remaining uncovered placement positions ($p_{i+1} \geq \frac{r_i}{k}$). This completes the proof.

Proposition 6.2: *Assuming uniform sonar costs and detection probabilities, the number of un-covered placement positions at the* $(i+1)$ th *iteration is at most* $\left(1-\frac{1}{k}\right)^{i+1}$ *of the number of covered placement positions by the optimal solution to the SPP i.e.*

$$r_{i+1} \leq \left(1-\frac{1}{k}\right)^{i+1} \times K_{OPT}.$$

Proof: We prove this proposition using induction.

For i = 0,

$$r_1 \leq \left(1-\frac{1}{k}\right) \times K_{OPT},$$

$$r_1 \leq K_{OPT} - \frac{1}{k} K_{OPT}.$$

From $r_1 = OPT - q_1$,

$$K_{OPT} - q_1 \leq K_{OPT} - \tfrac{1}{k} K_{OPT},$$

$$-q_1 \leq -\frac{1}{k} K_{OPT},$$

$$q_1 \geq \frac{1}{k} K_{OPT},$$

From $q_1 = p_1$,

$$p_1 \geq \frac{1}{k} K_{OPT}.$$

and rom $r_0 = K_{OPT}$,

$$p_1 \geq \frac{1}{k} r_0.$$

The above relationship is also true from proposition 6.1.

To prove by induction, we assume $r_i \leq \left(1 - \frac{1}{k}\right)^i \times K_{OPT}$ is true, and then show that $r_{i+1} \leq \left(1 - \frac{1}{k}\right)^{i+1} \times K_{OPT}$ is also true.

From $r_i = OPT - \sum_{J=1}^{I} p$,

$$r_{i+1} \leq r_i - p_{i+1}.$$

From Proposition 6.1,

$$r_{i+1} \leq r_i - \frac{r_i}{k},$$

$$r_{i+1} \leq r_i \left(1 - \frac{1}{k}\right).$$

From inductive hypothesis,

$$r_{i+1} \leq \left(1 - \frac{1}{k}\right)^i \times K_{OPT} \left(1 - \frac{1}{k}\right),$$

$$r_{i+1} \leq \left(1 - \frac{1}{k}\right)^{i+1} K_{OPT}.$$

This completes the proof.

Proposition 6.3: Assuming that a deployment involves the use of sonars with uniform costs, each of the greedy-based algorithms (**g-SPP-**1, **g-SPP-**2, and **g-SPP-**3) presented can achieve an approximation ratio of $(1 - 1/e)$ for the sonar placement problem.

Proof: We prove this proposition with the aid of Proposition 6.2 and '*Submodularity*', a widely discussed concept in combinatorial optimization and a key structure of our original placement model formulations. Submodularity conveys an intuitive diminishing returns property and guarantees why the greedy-based algorithm finds a nearly optimal solution.

For any sets A and B such that $A \subseteq B$, a set function F is said to be submodular (Nemhauser et al., 1978) if $F(A \cup \{k\}) - F(A) \geq F(B \cup \{k\}) - F(B)$. Also, a set function F is said to be non-decreasing if $A \subseteq B$ implies that $F(A) \leq F(B)$, for all sets A and B.

Consider the combinatorial optimization problem: $X^* = \arg\max_{|X| \leq K} F(X)$. From Nemhauser et al. (1978), given that $F(X)$ is a non-decreasing submodular function and that $F(\emptyset) = 0$. For any $K \geq 1$, then the following relationship: $F\big(OPT_h(K)\big) \geq \big(1 - {}^{1}/_{e}\big)F\big(OPT_*(K)\big)$ always hold,

where:

$OPT_*(K)$	Optimal Solution to combinatorial optimization problem
$OPT_h(K)$	Optimal Solution to combinatorial optimization problem

obtained by greedy-based algorithm

(Since results presented in Biobaku et al., 2015 clearly indicates the assumptions for non-decreasing objective function holds in our Sonar placement model, we omit their proofs).

Also, from Proposition 6.2, $r_i \leq \left(1 - \frac{1}{i}\right)^i \times K_{OPT}$.

Given that $r_i = K_{OPT} - q_i$, we have,

$$K_{OPT} - q_i \leq \left(1 - \frac{1}{i}\right)^i \times K_{OPT},$$

$$q_i \geq K_{OPT} - \left(1 - \frac{1}{i}\right)^i \times K_{OPT}.$$

From series convergence, $\left(1 - \frac{1}{i}\right)^i \approx \frac{1}{e}$, then,

$$q_i \geq K_{OPT} - \frac{K_{OPT}}{e},$$

$$q_i \geq K_{OPT}\left(1 - \frac{1}{e}\right).$$

Hence, our greedy-based algorithms can achieve at least an approximation ratio of $\left(1 - {}^1/_e\right)$ with uniform sonar costs. Based on this proposition, we claim that the greedy-based algorithms can achieve the *best performance guarantee that is possible* under the stated assumption. This completes the proof.

In comparison with other solution methods (MIP, or other meta algorithms search), the algorithms can be easily implemented in large-scale systems due to their low

computation complexities. Moreover, in a planning horizon when budget is expected to change, other solution approaches (especially those based on fixed multi-stage planning algorithms) are most likely to be subject to substantial performance loss when any of these model parameters change. On the contrary, the greedy-based algorithms we have presented will always achieve an approximation ratio of $(1 - 1/e)$ for any given budget if sonar costs are uniform.

It should be noted that when different sonar costs are involved, our algorithms do not guarantee the theoretical qualities enumerated above. However, slightly more complex algorithms that combine the greedy algorithm with partial enumeration, also achieves $1 - 1/e$ approximation guarantees by exploiting submodularity. See Sviridenko (2004), and Krause and Guestrin (2005).

6.4 Numerical Results

After analyzing the computational complexity of the algorithms, we present numerical results and runtimes of the algorithms in comparison to solutions obtained from a commercial solver (CPLEX) for some problem sizes. All proposed MIP models and algorithms are implemented in GAMS and solved using CPLEX (GAMS 2013). A relative tolerance of 3% duality gap is used as a stopping criterion for CPLEX, and all computational runs are made on a Linux server equipped with dual 3.00 GHz AMD processors (256 GB memory). Computational results presented in this section are based on data introduced in Chapter 4. However, only mobile sonars are used in the deployment.

We used different problem sizes in comparing solutions of our algorithms (representative problem sizes that are small enough to be solved exactly using CPLEX). In practice, increasing the AOI via adjusting the number of grid size (thus increasing the problem size) is open to interpretation. Firstly, increasing the AOI could be considered as further dividing subsections of the AOI into smaller sections in order to address non-homogeneity of these subsections. In the alternate, increasing the AOI could simply imply a physical increase in the AOI as a result of covering a larger region for surveillance operations. We adopt the latter interpretation in our discussions in this section.

Numerical experiments indicate that with a sparse distribution of sonars in any AOI, the results of the algorithms are very close to those obtained from the solver. Due to the high cost of sonar deployment, budget limitations in real world applications are expected to result into sparse distributions of the sonars within the AOI. This observation lays credence to the applicability of our algorithms in solving real world/practical problems. For applications requiring non-sparse distribution of the sonars, the algorithms will be of great help in establishing good bounds (upper/lower bounds, depending on the optimization goal). With increased budget allocations, the execution time of the CPLEX solver increases exponentially, making it impracticable to obtain solutions within acceptable time limits. It should be noted that for the 25X25 grid case, CPLEX search for optimality exceeds 3600 seconds for most budget considerations (Similarly for the 50x50 case, search for optimality exceeds 7200 seconds for most budget considerations). In addition to showing the solution times for each algorithm, figures 6.5, 6.7, and 6.9 also shows the overall time if all the algorithms are combined.

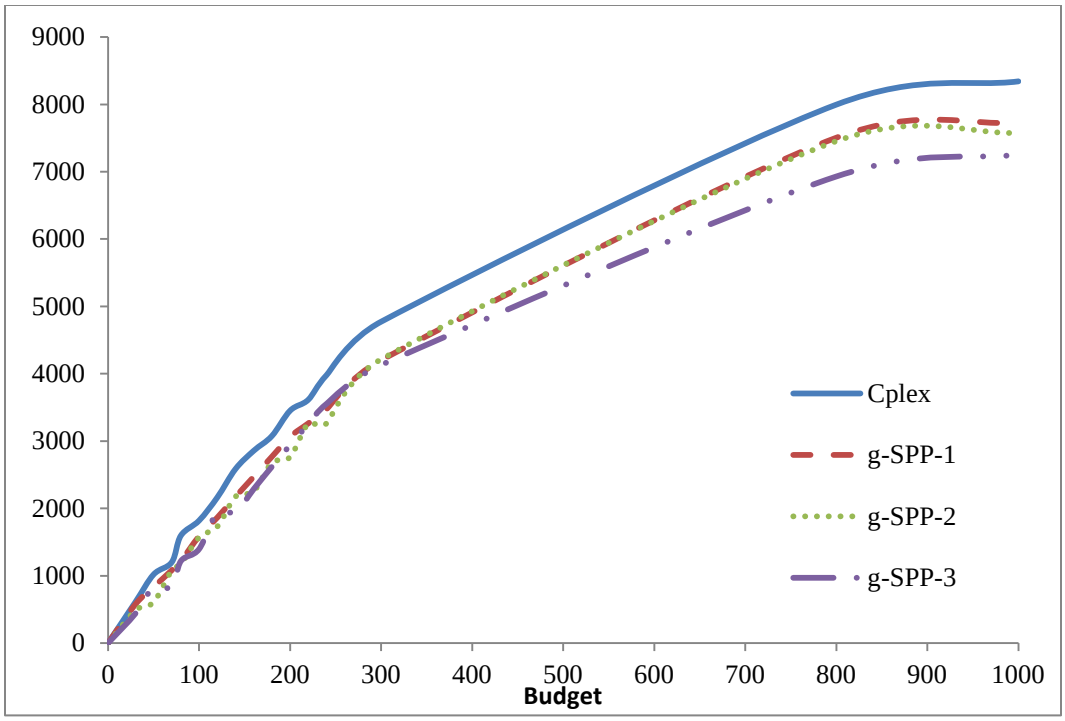

Figure 6.4: (Equivalent) objective functions vs. available budget-5x5 grid size

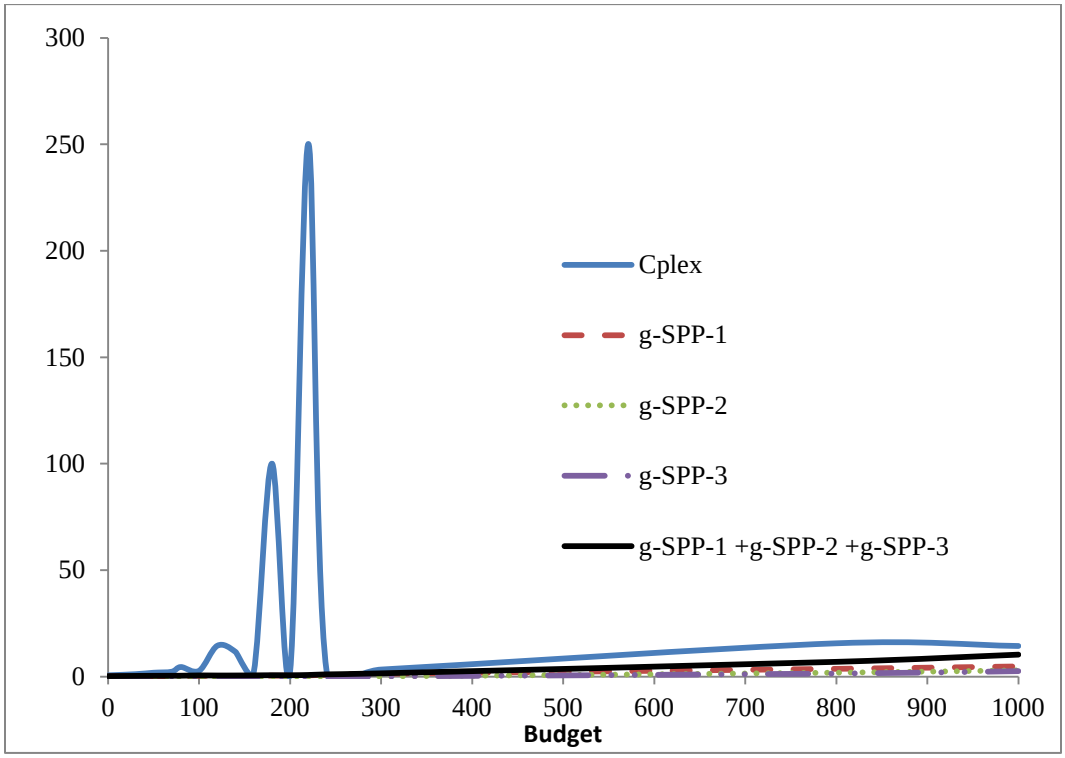

Figure 6.5: Solution time (seconds) vs. available budget-5x5 grid size

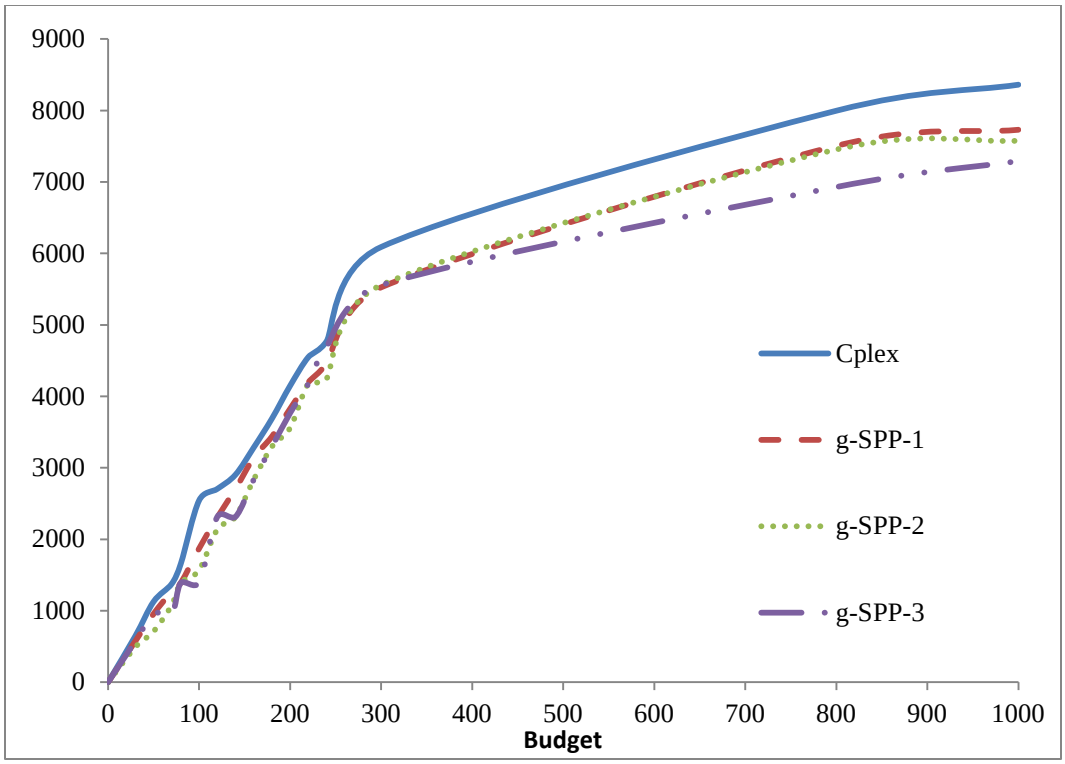

Figure 6.6: (Equivalent) objective functions vs. available budget-25x25 grid size

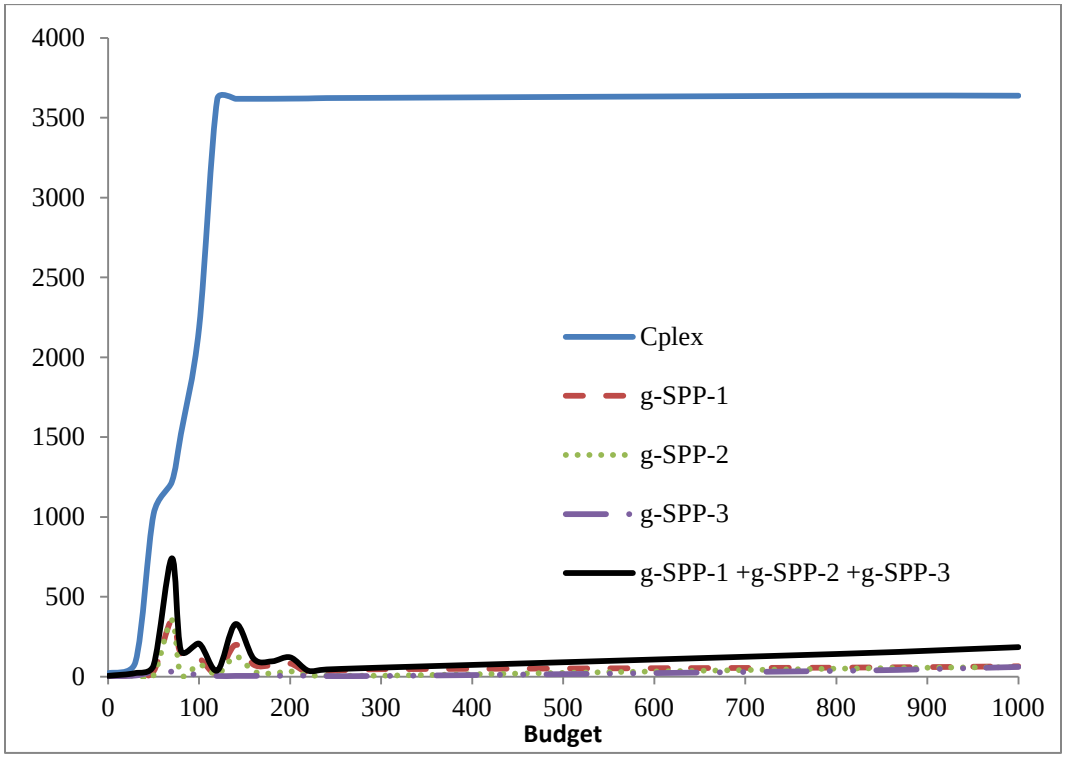

Figure 6.7: Solution time vs. available budget-25x25 grid size

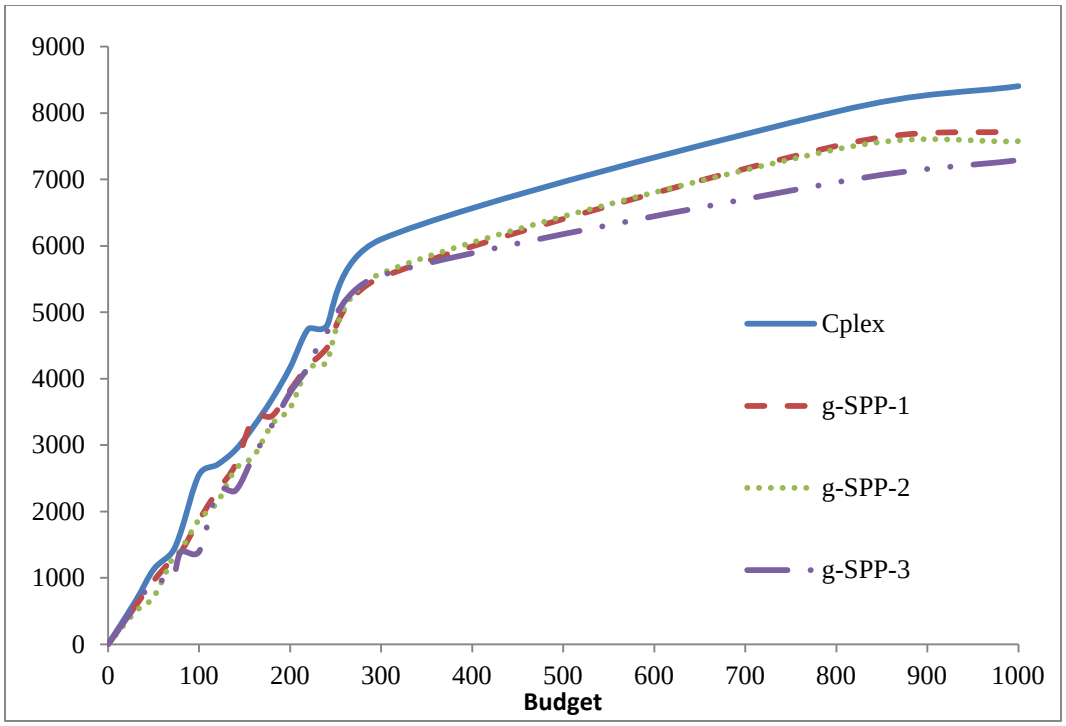

Figure 6.8: (Equivalent) objective functions vs. available budget-50x50 grid size

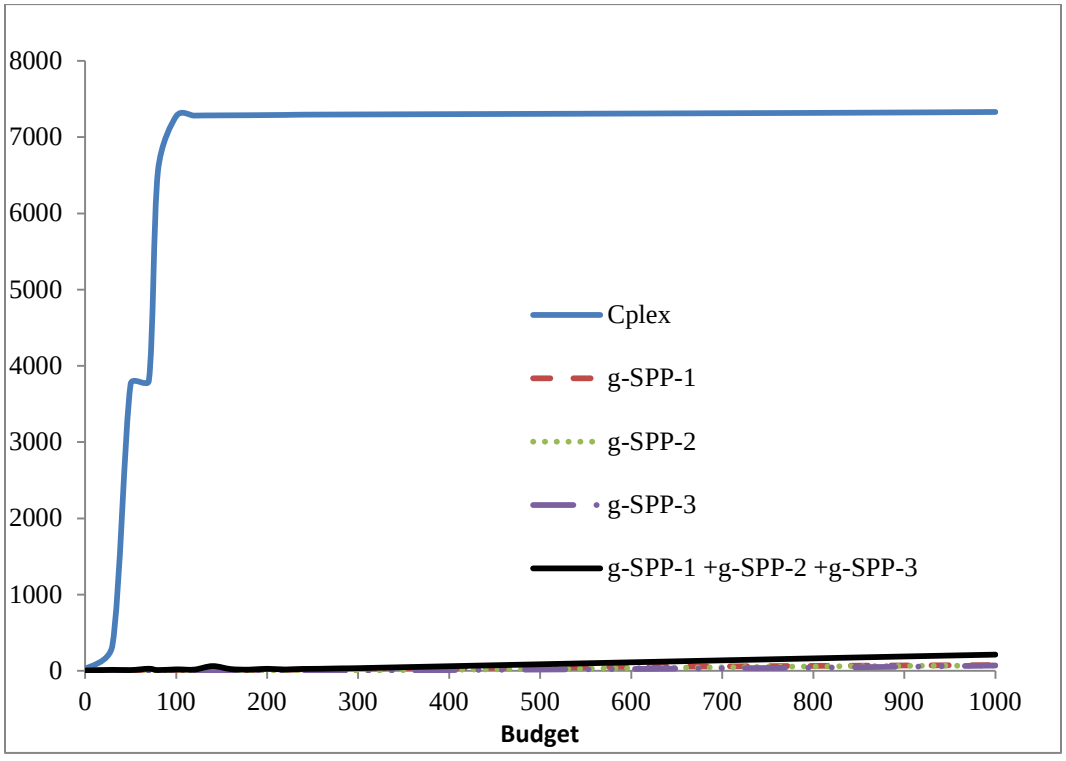

Figure 6.9: Solution time vs. available budget-50x50 grid size

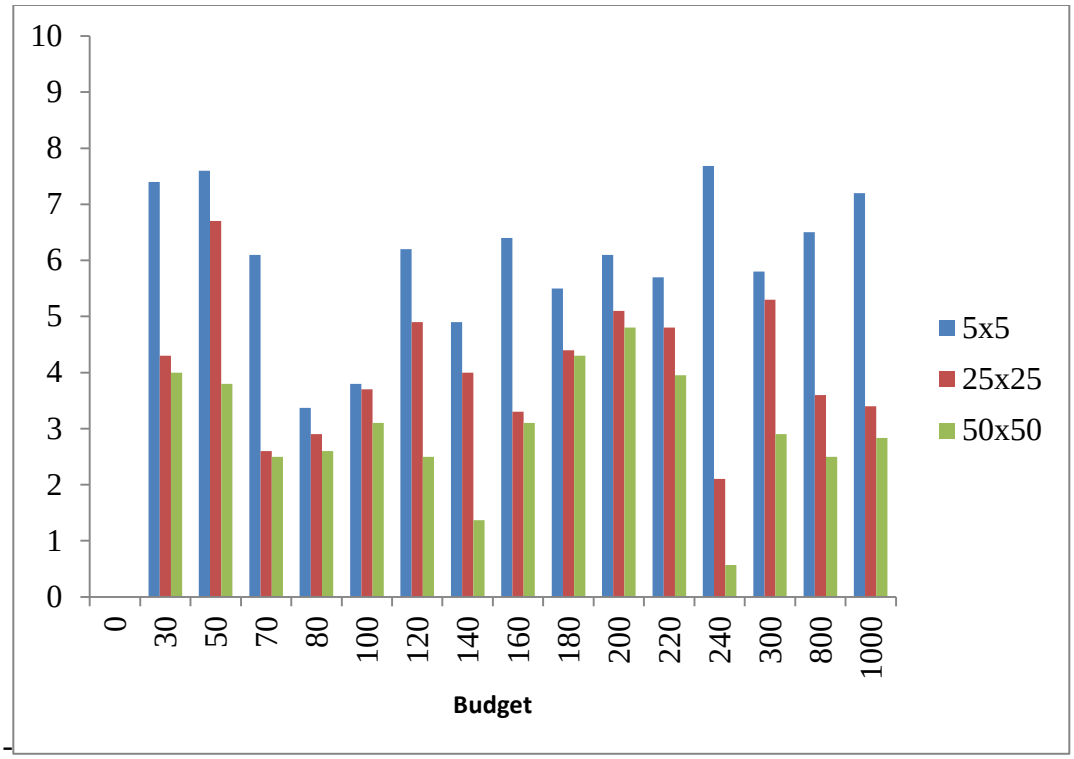

Figure 6.10: Changes (%) in optimality for selected budget availabilities

Figure 6.10 compares results of our algorithms with optimal solutions returned by CPLEX (from Figures 6.4, 6.6 and 6.8, we consider the 'best' solutions returned by our algorithms) for some selected budgetary allocations. Also, Table 6.4 summarizes results of this figure, showing maximum, average and minimum (for only non-zero budget allocations) changes in optimality. Both figure and table suggests that our algorithm returns 'better' solutions as problem size increases.

Table 6.4: (Maximum, Average and Minimum) Changes in optimality for grid sizes

Grid Size (Placement node size)	5x5	25x25	50x50
Maximum Change in optimality (%)	8.4	7.2	6.7
Average Change in optimality (%)	4.8	4.4	3.9
Minimum Change in optimality (%)	2.5	2.4	2.1

Overall, our results show that with increased AOIs, our algorithms give solutions closer to the CPLEX solution. This is because, the increase in the size of the AOI results into a sparse distribution of sonars in the AOI, irrespective of budget allocations. This in turn, leads to less effects of multiple sonar coverage on the objective function. In practice, this observation lends credence to the effectiveness of our algorithms because surveillance using underwater sonars involves sparse distribution of sensors due to the inhibiting costs of sonar coverage systems and the vast expanse of marine waterways that needs to be protected.

6.5 Conclusion

In this chapter, we developed evaluation procedures that exploit submodularity to significantly reduce the number of sonar-placement location pair locations that need to be checked in attaining an optimal solution to the SPP introduced in Chapter 4, thus speeding up computation time. Under certain assumptions, we provided approximation algorithms that are within $(1 - 1/e)$ of the optimal global solution.

Our empirical experiments indicate that each of the simple greedy-based algorithms we proposed for optimizing partial coverage provides coverage performance that is very close to the optimal solution in problems that are small enough to be solved exactly (tractable problems) and far outperforms CPLEX solutions in terms of solution time. By extension, comparable performance (even if sub-optimal) is expected in larger problems. For the case study solved, each of the algorithms outperforms the CPLEX solution in terms of scalability. When grid size is increased beyond 50x50, CPLEX solutions are non-tractable, failing to generate a global optimal solution. In contrast, our algorithms (**g- SPP**-1, **SPP**-2 and **g-SPP**-3) have been successfully tested up to 100x100

grid sizes but these results are not shown in Section 6.4 because non-tractability of solutions returned by CPLEX does not permit comparisons of solution quality and solution times.

In comparing all the algorithms, it is evident that **g-SPP-**1 consistently yields better solution than the other two algorithms (**g-SPP-**2 and **g-SPP-**3). However, **g-SPP-**2 and **g-SPP-**3 outperforms the former in terms of execution times. Depending on the problem parameters, solution quality and solution time varies for **g-SPP-**2 and **g-SPP-**3.

Chapter 7

Sonar Placement problem under Uncertainty considerations

7.1 Introduction

In prior chapters of this dissertation, we assume, like most optimization problems that associated data related to the Sonar placement problem (SPP) are exact. However, this assumption could be misleading and may lead decision makers to make inappropriate decisions. Errors as a result of not incorporating uncertainties could have significant effects on validity of optimal solutions. Hence, uncertainty considerations in model formulations could help to guarantee that a decision made as a result of any solution (from modelling approach) will be reasonably appropriate and relevant in reality. In our case, uncertainty can arise as a result of human errors, measuring errors, changes in sensing environments, etc.

Despite the benefits of uncertainty considerations in any optimization problem, some practical considerations have limited their use. Generally, we expect an increase in problem complexities related not only to the mathematical formulations but also to the algorithms that may be proposed to solve such problems. Also, identifying suitable probability distributions to address uncertainties have proved to be difficult in any practical application.

Several methods and approaches have been adopted to address uncertainties in optimization problems. An obvious approach is to replace parameter values subject to variability with their average values. While this approach could be valid for the specific

data instance, its results are subject to sub-optimality. Another approach is the use of Sensitivity Analysis for a ‘what-if’ analysis on problem optimality and feasibility when input data are subject to changes. Though useful, the approach doesn’t help to control variability in the modelling approach.

Perhaps, the three most promising methodologies in addressing uncertainties in modelling and formulation are Chance-Constraint programming (C-CP), Stochastic Programming (SP), and Robust Optimization (RO). The last two framework methodologies have been identified as the two principal methods used to address data uncertainty in literature (Bertsimas and Sim, 2003; Poss, 2013; and Pessoa et al., 2015).

In C-CP (often considered a technique under SP), constraints with at least one random coefficient are modeled as probabilistic functions. The probability distributions of uncertain coefficients are assumed to be known and the constraints are required to be met with a minimum probability. Although particular cases of C-CP models are often easy to solve but their reformulations often results into non-linear formulations (Birge and Louveaux, 2011) and thus approximate solution techniques are often sought.

Stochastic Programming (SP) assumes that parameter variability has an accurate probabilistic description for computing statistical features (Bertsimas et al. 2011). It uses probability distributions to replace model parameters subject to variability and thereafter attempts to optimize an expectation with each scenario balanced by an occurrence probability (Birge and Louveaux, 2011). In a nutshell, stochastic optimization tries to find the optimal nominal design parameters such that under the impact of parameter variations around some nominal values, the objective function is optimized in an average sense, ensuring that constraints are satisfied with a specified probabilistic guarantee.

Literature often credit Dantzig (1965) as the pioneer of SP. Amongst other drawbacks, a major pitfall of SP is the determination of an inherent distribution function that characterizes an uncertain parameter.

Compared to SP, the RO is a more recent attempt at addressing uncertainties. In general, the approach attempts to compute feasible solutions for a whole range of scenarios of the uncertain parameters i.e., rather than finding the solution robust to stochastic uncertainty in a probabilistic sense, it constructs a solution that is feasible for any realization of parameter variation. RO is very useful in practice, since it is tailored to the information at hand, and it leads to computationally tractable formulations (Gorissen et al., 2015).Several RO methodologies have been proposed in literature. In this dissertation, we focus on the methodology proposed by Bertsimas and Sim (2004), where data is assumed to belong to some set without a specific probability distribution. Although other approaches such as El Ghaoui et al. (1998) and Ben-Tal and Nemirovski (2000) exist, the output models from such approaches are computationally more complex. Among several interesting features, the robust framework of Bertsimas and Sim (2004) has the advantage of preserving the original problem's linearity property.

The RO methodology is well equipped to address variability (uncertainty) in optimization problems. The methodology ensures feasibility of all possible scenarios of the data within a given uncertainty set. Computing uncertainty sets for robust linear constraints requires less information on the parameters and, as long as these sets are defined by a conic system of constraints, the resulting optimization problems are essentially of the same computational complexity as their deterministic counterparts (Ben-Tal et al., 2009, Poss et al., 2013, and Pessoa et al., 2015). As such, the RO

methodology becomes most relevant when we only have limited information with less detailed structure, such as bounds on the magnitude of the uncertain quantities.

In this Chapter, we propose and present a robust optimization methodology for the uncertain Sonar placement problem (SPP) and develop solution methods to solve the resulting model. Although, several data in the SPP could be subject to uncertainty, we address uncertainties related to sonar costs and detection probabilities. The RO approach used in this Chapter produces model formulations of the same type as the original model by maintaining linearity of the original model.

7.2 Robust Optimization- Bertsimas and Sim's (2004) formulation

In this chapter, we say that solution to a problem instance is ‘‘robust" if it is insensitive to data variations but within a certain data range. By acceptable standards, the robust solution of an optimization problem is feasible for different scenarios of the data; hence its solution is not necessarily optimal for any one of them. We base our model development on the RO approach proposed by Bertsimas and Sim (2004) where the concept of ‘budget of uncertainty' was first introduced. Their model establishes a probabilistic guarantee for robust design that can be computed a priori, that is, as a function of the structure and size of uncertainty set. In general, RO presumes that the values attained by the uncertain parameters are merely described by a set (often finite or convex), without assuming the knowledge of specific probability weights (Pessoa et al., 2015).

In relation to our work, ‘the budget of uncertainty ‘can be described as the number of sonar placement parameters that are allowed to have variations. If we can

establish a valid relationship between placement optimality and uncertainty set, we may achieve robust designs that are close to the results by stochastic modeling while avoiding complicated stochastic computations. In practice, for an uncertain mixed integer programming (MIP) problem with interval data, solving robust counterparts for budgeted uncertainty sets is much easier than finding the minmax regret solution (Feizollahi and Feyzollahi, 2015) of Stochastic optimization.

The underlying idea of uncertainty budgeting is to provide a guaranteed model performance by manipulating the size of the uncertainty set associated with the particular model parameter. The idea essentially addresses the issue of the lack of information (valid or adequate) on probabilistic descriptions of parameters subject to uncertainty by seeking a probabilistic guarantee for the robust solution, providing a level of flexibility in trade-off between robustness and model performance. An important premise behind this flexibility is that it is unlikely all uncertain data can attain their worst case values. Depending on how conservative a decision maker or modeler is, the level of conservativeness (ranging from the most optimistic nominal equivalent with data certainties to the most pessimistic robust solution where worst case scenarios are expected of uncertain modeling elements) can be controlled.

Consider a standard nominal linear programming problem:

$$\begin{aligned} &\text{Maximize} && c'x\,, \\ &\text{Subject to} && Ax \le b\,, \\ & && l \le x \le u\,. \end{aligned}$$

Bertsimas and Sim (2004) assume that data uncertainty only affects elements of matrix A and introduced the following parameters and sets:

J_i Set of coefficients in row *i* (of the matrix *A*) that are subject to uncertainty.

$\tilde{a}_{ij}$ Symmetric and bounded random variable of $a_{ij}, j \in J_i$ with values in range $[a_{ij} - \hat{a}_{ij}, a_{ij} + \hat{a}_{ij}]$,

Γ_i Parameter (not necessarily integer) that takes values in the interval $[0, |J_i|]$

Our interests lie in studying situations whereby exact values of a_{ij} are unknown but are characterized by a symmetric and random variable $\tilde{a}_{ij}$ that belongs to a known interval $[a_{ij} - \hat{a}_{ij}, a_{ij} + \hat{a}_{ij}]$ where a_{ij} represents the variable's nominal value. For each uncertain parameter $\tilde{a}_{ij}$, another random variable $\eta_{ij} = (\tilde{a}_{ij} - a_{ij})/\hat{a}_{ij}$ which obeys an unknown but symmetric distribution and takes values in $[-1\ 1]$ is also defined. Also, at most Γ_i coefficients can change from their nominal value $(\hat{a}_{ij})$ to any arbitrary value within the interval and this parameter denotes the level of guarantee with respect to data uncertainty we desire in our robust model.

In practice, it is unlikely that all $a_{ij}, j \in J_i$ will change, thus the aim of the robust framework is to protect against all cases such that up to $\lfloor \Gamma_i \rfloor$ of these coefficients are permitted to change. The methodology has the property that if this assumption holds, then the robust solution will be feasible deterministically, and moreover, even if more than $\lfloor \Gamma_i \rfloor$ change, then the robust solution will still be feasible *with very high probability* (Bertsimas and Sim, 2004).

With the above assumptions and using strong duality, a robust optimization equivalent linear formulation of the nominal model is given thus:

maximize $c'x,$

Subject to

$$\sum_j a_{ij}x_j + z_i\Gamma_i + \sum_{i\in J_i} p_{ij} \le b_i \qquad \forall\, i\,,$$

$$z_i + p_{ij} \ge \hat{a}_{ij}y_j \qquad \forall\, i,j \in J_i,$$

$$-y_j \le x_j \le y_j \qquad \forall\, j\,,$$

$$l_j \le x_j \le u_j \qquad \forall\, j\,,$$

$$p_{ij} \ge 0 \qquad \forall\, i,j \in J_i,$$

$$y_j \ge 0 \qquad \forall\, j\,,$$

$$z_i \ge 0 \qquad \forall\, i\,,$$

where p_{ij}, y_j and z_i are variables (including dual variables) introduced during the transformation process. We refer readers interested in the specifics of the transformation to Bertsimas and Sim (2004), where probability bounds are also derived on constraint violations. Although uncertainty is not considered in the objective function, it can easily be re-modelled as a constraint by introducing an auxiliary variable (See Ben-Tal et al., 2009).

7.3 Robust formulation of the Sonar Placement Problem (r-SPP).

To enable us carry out some analysis on robust formulation of the sonar placement problem, we introduce optimization models with optimal values z_{NF}, z_{RF} , and z_{RFBS}. The function z_{NF} is the optimal objective function of the nominal SPP in Chapter 4 and z_{RF} is its corresponding optimal objective function under uncertainties due to cost and detection probabilities of sonars. Also, z_{RFBS} is the problem's objective

function using the robust formulation of Bertsimas and Sim (2004) introduced in Section 7.2. Readers should note that SPP in Chapter 4 can be easily re-formulated as a maximization problem as done in Chapter 5. For ease of analysis (in the model corresponding to z_{NF}) , we only introduce a decision variable x, an objective function and the model constraint subject to uncertainty. Variables and parameters in the models are as in standard optimization formulations. The model corresponding to z_{RF} is considered a worst case scenario and is described in Soyster (1973). This is because it strictly mandates all constraints related to uncertainty to be feasible without any violation. In the model corresponding to z_{RFBS}, if Γ is large (the number of uncertain parameters in a constraint involving an uncertain parameter), the entire variation in all parameters might be achieved, and this is equivalent to the worst case scenario described by Soyster (1973). If it is small, simultaneous large variations in many parameters are excluded.

(z_{NF}) $$\max\left(c'\boldsymbol{x}\middle| a_j x_j \le b\ \forall\, j, x_j \ge 0\ \forall\, j.\right).$$

(z_{RF}) $$\max\left(c'\boldsymbol{x}\middle|\begin{array}{c}\sum_j a_{sj}x_j + \sum_{j\in J_s}\hat{a}_{sj}y_j \le b_s\ \forall\, s; -y_j \le x_j \le y_j\ \forall\, j;\\ x_j \ge 0\ \forall\, j;\ y_j \ge 0\ \forall\, j.\end{array}\right).$$

(z_{RFBS}) $$\max\left(c'\boldsymbol{x}\middle|\begin{array}{c}\sum_j a_{sj}x_j + z_s\Gamma_s + \sum_{j\in J_s} p_{sj} \le b_s\ \forall\, s;\\ z_s + p_{sj} \ge \hat{a}_{sj}y_j\ \forall\, s, j \in J_s;\\ -y_j \le x_j \le y_j\ \forall\, j\ ; x_j \ge 0\ \forall\, j; p_{sj} \ge 0\ \forall\, s, j \in J_s;\\ y_j \ge 0\ \forall\, j; z_s \ge 0\ \forall\, s.\end{array}\right).$$

As highlighted in Section 7. 2, the justification for Bertsimas and Sim's (2004) approach is that worst case scenarios are very unlikely and even if more than $\lfloor\Gamma\rfloor$change,

then the robust solution will be feasible *with very high probability*. Since the robust transformation only introduces linear constraints, the approach is applicable to MIP. This is because the integrality constraints are still preserved after transformation.

Proposition 7.1 *Consider the sonar placement problem SPP with uncertain budget and detection probabilities, the robust counterpart of the problem deploying only mobile sonars is formulated by introducing new variables v, q, r; replacing constraints (4.3) and (4.13) in Model 4.1 with constraints (7.1) and (7.4) respectively; and introducing new constraints (7.2-7.3) and (7.5-7.7)***:**

$$\sum_{b} c_b . \sum_{i} \sum_{k} Y_{ik}^{bt} + v_{1_t} \times \Gamma_{1_t} + \sum_{s \in J_t} q_{1_{st}} \leq B_t \quad \forall\, t\,, \tag{7.1}$$

$$v_{1_t} + q_{1_{st}} \geq \hat{c}_{bst} \times r_{1_{bikt}} \forall\, s \in\, J_t, t\,, \tag{7.2}$$

$$-r_{1_{bikt}} \leq Y_{ik}^{bt} \leq r_{1_{bikt}}\ \forall\, b, i, k, t\,, \tag{7.3}$$

$$-Qb_{ikt} - \sum_{b^z} W_{ik}^{b,b^z,t} \ln(1 - p_{b^z}) + v_{2\ i,k,b,t} \times \Gamma_{2_{i,k,b,t}} + \sum_{s \in J_t} q_{2\ i,k,b,s,t} \geq 0 \quad \forall\, i, k, b, t\,, \tag{7.4}$$

$$v_{2\ i,k,b,t} + q_{2\ i,k,b,s,t} \geq r_{2_{bb^zikt}} \ln(1 - \hat{p}_{b^z}) \qquad \forall\, b^z, s \in\, J_t, i, k, b, t\,, \tag{7.5}$$

$$-r_{2_{bb^zikt}} \leq W_{ik}^{b,b^z,t} \leq r_{2_{bb^zikt}}\ \forall\, b, i, k, t\,, \tag{7.6}$$

$$q_{1_{st}}, r_{1_{bikt}}, v_{1_t} \geq 0; q_{2\ i,k,b,s,t}, r_{2_{bb^zikt}}, v_{2\ i,k,b,t}\ free\ \forall\, s \in\, J_t, i, k, b, b^z, t\,. \tag{7.7}$$

where,

Γ_1 Robust parameter for sonar cost

Γ_2 Robust parameter for sonar detection probability

$\hat{c}_b$ Nominal sonar cost parameter

$\hat{p}_{b^z}$ Nominal detection probability parameter

Proof: (See Bertsimas and Sim, 2004)

It should be noted that for the cost parameter $\tilde{c}_b$ subject to uncertainty, we use the interval range $[c_b - \hat{c}_b, c_b + \hat{c}_b]$ as presented in Section 7.2. However, for the detection probability parameter, $\tilde{p}_{b^z}$ subject to uncertainty, the interval range $[p_{b^z} - \hat{p}_{b^z}, p_{b^z}]$ is used to avoid infeasibilities (possibility of having $\tilde{p}_{b^z} > 1$). In practical applications, this means we assume detection probabilities in manufacturers' specifications to be upper sensing limits. Moreover, as indicated in Chapter 4, we expect detection probabilities to be less than 100%. In addition, the equality sign in the nominal formulation (See constraints 4.13 in Chapter 4) is changed to an inequality to avoid infeasibilities. It should also be noted that similar introduction of new variables and replacement of constraints are applicable when static sonars are considered in the deployment.

Proposition 7.2 *For every realization of* Γ_1 *and* Γ_2,

$$z_{RF} \leq z_{RFBS}(\Gamma_1, \Gamma_2) \leq z_{NF}$$

Proof: The robust formulation of the nominal formulation becomes redundant whenever these two conditions occur simultaneously:

1. Γ_1 coincides with the cardinality of the random set representing cost of sonars
2. Γ_2 coincides with the cardinality of the random set representing detection probability coefficients.

From above, it is evident that $z_{RF} \leq z_{RFBS}(\Gamma_1, \Gamma_2)$. It should be noted that if $\Gamma_1 = \Gamma_2 = 0$ (for all constraints affected by uncertainty), $z_{NF} = z_{RFBS}(\Gamma_1, \Gamma_2)$. Likewise,

uncertainty considerations in the theory of robust formulation indicates that $z_{RF} \leq z_{NF}$. Hence, it follows that $z_{RF} \leq z_{RFBS}(\Gamma_1, \Gamma_2) \leq z_{NF}$. This completes the proof.

Proposition 7.3 *As Γ_1 and/or Γ_2 increase, the optimal value of function $z_{RFBS}(\Gamma_1, \Gamma_2)$ is monotonically non-increasing.*

Proof: Select ${\Gamma_1}'_t, {\Gamma_2}'_{i,k,b,t}, {\Gamma_1}''_t, {\Gamma_2}''_{i,k,b,t}$ such that ${\Gamma_1}'_t \leq {\Gamma_1}''_t$ and ${\Gamma_2}'_{i,k,b,t} \leq {\Gamma_2}''_{i,k,b,t}$

For any sonar deployment, the feasible region of the robust formulation using ${\Gamma_1}'_t$ and ${\Gamma_2}'_{i,k,b,t}$is no smaller than using ${\Gamma_2}'_{i,k,b,t}$ and ${\Gamma_2}''_{i,k,b,t}$. Thus, as Γ_1 and/or Γ_2 increases in component values, the function $\mathrm{z_{RFBS}}(\Gamma_1, \Gamma_2)$ is non-increasing. This completes the proof.

Proposition 7.4 *In any deployment scheme involving both static and mobile sonars, the minimum number of sonars deployed under any period t is $\left\lfloor \frac{B}{min_b(c_b + \hat{c}_b)} \right\rfloor$, and its maximum number is $\left\lfloor \frac{B}{min_a(c_a - \hat{c}_a)} \right\rfloor$ (See Chapter 4 for description of model variables and parameters).*

Proof: For any sonar placement (optimal or otherwise) in grid (i, k) during deployment period t involving both static and mobile sonars,

$$c_a . X_r^a \leq c_b . Y_s^{bt} \quad \forall\, r \in (i,k), s \in (i,k) \backslash r, t, a, b$$

For any budget allocation under uncertainty, the minimum number of sonars is deployed in the worst case scenario (i.e. with optimization model corresponding to z_{RF}, or with optimization model corresponding to z_{RFBS} when Γ is considerably large) and due to different sonar sensing specifications, minimum cost of the different sonar types

(Static and Mobile) are $\min_a \tilde{c}_a$ and $\min_b \tilde{c}_b$ respectively, where $\tilde{c}$ indicates random parameter c subject to uncertainty and we assume that $(\tilde{c}_b = c_b + \hat{c}_b) > (\tilde{c}_a = c_a + \hat{c}_a)$ and $(\tilde{c}_b = c_b - \hat{c}_b) > (\tilde{c}_a = c_a - \hat{c}_a)$ under all possible scenarios. It should be noted that $B \times \left(\frac{B}{\min_b(c_b+\hat{c}_b)} - \left\lfloor\frac{B}{\min_b(c_b+\hat{c}_b)}\right\rfloor\right) < (c_b + \hat{c}_b)\ \forall\ b$ and $B \times \left(\frac{B}{\min_a(c_a-\hat{c}_a)} - \left\lfloor\frac{B}{\min_a(c_a-\hat{c}_a)}\right\rfloor\right) < (c_a - \hat{c}_a)\ \forall\ a$, where $B \times \left(\frac{B}{\min_b(c_b+\hat{c}_b)} - \left\lfloor\frac{B}{\min_b(c_b+\hat{c}_b)}\right\rfloor\right)$ and $B \times \left(\frac{B}{\min_a(c_a-\hat{c}_a)} - \left\lfloor\frac{B}{\min_a(c_a-\hat{c}_a)}\right\rfloor\right)$ are portions of the budget left un-utilized because these dollar equivalents are not enough to procure additional sonars. This completes the proof.

Proposition 7.5 *Consider fixed robust parameters Γ_1 and Γ_2 for any solution $OPT(Y)$ that deploys only mobile sonars and let η_1 and η_2 represent the symmetric random variable introduced in Section 7.2 for sonar cost and detection probabilities respectively. Then, for integer-valued Γ_1 and Γ_2, a worst-case scenario for Y can be found when $\eta_1 = 1$ for the largest values of $2\hat{c}_b Y_{ik}^{bt}$ and $\eta_2 = -1$ for the largest value of $\hat{p}_{b^z} \times W_{ik}^{b,b^z,t}$. For other values of $\tilde{c}_b$ and $\tilde{p}_{b^z}$ in this scenario,$\eta_1 = \eta_2 = 0$.*

Proof: We note that while interval length of uncertainty range in $\tilde{c}_b$ is$2\hat{c}_b$, its equivalent in $\tilde{\mathrm{p}}_{\mathrm{b}^z}$ is$\hat{p}_{b^z}$. Since $W_{ik}^{b,b^z,t} \geq Y_{ik}^{bt} \geq 0$ (Remember Y_{ik}^{bt} is binary and $W_{ik}^{b,b^z,t}$ is an integer) for all realizations (scenarios) of the robust solution. Then $OPT(Y)$ is a non-decreasing function of the uncertainty sets $\tilde{c}_b$ and $\tilde{p}_{b^z}$ for given protection levels Γ_1 and Γ_2 i.e. $OPT_{\tilde{c}_b,\tilde{p}_{b^z}}(Y) \leq OPT_{\hat{c}_b,\hat{p}_{b^z}}(Y)$. Hence, there exists an extreme point of η_1^Y and η_2^Y such that $\sum_J \eta_1^Y = \Gamma_1$, $\sum_J \eta_2^Y = \Gamma_2$, and η_1^Y and η_2^Y make up the worst case scenario for Y that optimizes value of $OPT(Y)$ over protection levels Γ_1 and Γ_2. For integer values of

protection levels, $\lfloor \Gamma \rfloor = \Gamma$; Hence, for other η_1^Y and η_2^Y, we have values attaining 0. This completes the proof.

7.4 Modification of g-SPP (Chapter 6) for uncertainty considerations

Our goal in this section is to propose an approach to address data uncertainty in the algorithms introduced in Chapter 6. We aim to adapt the greedy –based algorithms in a very natural way to take robustness into account. Experimental results from Chapter 6 indicate that solutions for g-SPP3 are often dominated by **g-SPP1 and g-SPP2.** Hence, we exclude developing an equivalent robust version of the former algorithm and present robust adaptations of the latter algorithms in Sections 7.4.1-7.4.2.

7.4.1 Robust adaptation of g-SPP1

Recall from Section 6.2 of Chapter 6 that d_m is the dollar cost of available sonar m and r_m^c is the number of sonar m in any combination e of sonar types. Since we now deal with uncertain $\widetilde{d}_m$, with values in the range $[d_m - \hat{d}_m, d_m + \hat{d}_m]$, we have a situation whereby any combination e of sonar types that gives the minimum un-expended budget might become infeasible. To address this issue, we note that $\left\lfloor \frac{B}{(d_m - \hat{d}_m)} \right\rfloor > \left\lfloor \frac{B}{(d_m + \hat{d}_m)} \right\rfloor, \forall\ \hat{d}_m > 0$. Since value of r_m^e for any sonar type is bounded by $r_m^e \leq \left\lfloor \frac{B}{(d_m - \hat{d}_m)} \right\rfloor$ and $r_m^e \leq \left\lfloor \frac{B}{(d_m + \hat{d}_m)} \right\rfloor$ for the most optimistic and pessimistic scenario respectively. Thus, $0 \leq r_m^e \leq \left\lfloor \frac{B}{(d_m + \hat{d}_m)} \right\rfloor \leq \left\lfloor \frac{B}{(d_m - \hat{d}_m)} \right\rfloor$ i.e. the number of sonars to be deployed in any combination ranges from 0 (none) to $\left\lfloor \frac{B}{(d_m - \hat{d}_m)} \right\rfloor$.

In the robust counterpart of the algorithm, we need to check feasibility of these combinations. Thus, we slightly modify Step 1 of the algorithm (See Chapter 6). After computing un-expended budget for each combination and sorting in decreasing order according to this metric, we then iteratively select the combination at the top of this list that doesn't violate any of the constraints in the robust model. We represent the set of these combinations as G and the combination at the top of the list as g' and assign $r1 := \sum_{Placement(i,k,t) \in g'} v_{i,k,t}^{m}$ as the solution of this procedure. Figure 7.1 shows the pseudocode used to accomplish this procedure.

While $|G| > 0$ and $boolean = false$
g' := first combination in ordered list G;
Set $A_{e^*} := A_{e^*} \cup g'$ and do Step 3 in **g-SPP1**
    If g' is not feasible in robust model then
        $G := G \backslash g'$; $A_{e^*} = \emptyset$; $boolean = false$
    Else:
        $boolean = true$ ……..Combination g' is chosen
End While

Figure 7.1: Pseudocode for robust adaptation of Step 3 in **g-SPP1**

In addition, it is possible that for some combinations e that are infeasible with the robust model, a subset of the sonars in the combination can still be feasible. Thus, we establish a procedure that also ranks the sonars making up the combination and then replace (if possible) the last few sonar(s) in the list with alternate sonars such that feasibility is ensured. Thus we carry out the following steps if g' is infeasible:

i. Check metric $\frac{v_{i,k,t}^{m}}{d_m}$ and rank sonar type(s) that constitutes elements in g'(including the number) based on metric $\frac{v_{i,k,t}^{m}}{d_m}$.

ii. Deploy eligible sonar-Placement pair using metric, ensuring only sonars in ordered list of $g'$are eligible for selection.

iii. After deployment of each sonars in this list, check for robust feasibility. Stop and exclude currently eligible sonar whenever feasibility is violated. Let set A represent sonar type-Placement position pair obtainable from this procedure

iv. Now consider the original ordered list of metric $\frac{v_{i,k,t}^{m}}{d_m}$ and attempt to allocate sonar-Placement pair (Check for robust feasibility in each attempt. If feasibility fails, discard sonar-Placement position pair under consideration and move to next pair on the list. Continue until nominal budget is expended or none of the pair is robust feasible. Return set A' as the sonar type-Placement position pair obtainable from this procedure

v. Set allocation $A = A \cup A'$. This placement is robust feasible. Return $r2 = \sum_{Placement(i,k,t)\in A} v_{i,k,t}^{m}$

vi. Afterwards, we chose the best solution from $r1 := \sum_{Placement(i,k,t)\in g'} v_{i,k,t}^{m}$ and $r2 = \sum_{Placement(i,k)\in A} v_{i,k}^{m}$

Figure 7.2 shows the pseudocode used in a robust adaptation of all steps in g-SPP, including the above procedure.

7.4.2 Robust adaptation of g-SPP2

In **g-SPP2,** we simply include a feasibility check for the robust problem when each additional sonar type-Placement position pair is chosen. Figure 7.3 shows the pseudocode used to accomplish this procedure.

r1=r2=0; $A_{e^*} = \emptyset$; $boolean = false$;---- c_s-Cost of sonar s
While $|G| > 0$ AND $boolean = false$;
g' ≔ first combination e in ordered list G;
Do Step 3 in **g-SPP1**
If g' is not feasible in robust model, then
$g'(i)$: =ordered sonar types in g'; $1 \leq i \leq |g'|$;$g'(1)$: =First element (sonar) at the top of ordered list g'; $i = 1$, $A = \emptyset$
While $i \leq |g'|$
Do Step 3 in **g-SPP1** using sonar$g'(i)$. Identify the $g'(i)$-Placement position pair chosen, $A(i)$ and check for robust feasibility.
If feasible then
$A = A \cup A(i)$
End If
$i = i + 1$;
End While
Compute expended budget for A, $b(A)$ and set $q = B - b(A)$
Loop (sonar type s,
While $q \geq c_s$,
Repeat Step 3 in **g-SPP1** without recourse tog'. Identify the sonar type-Placement position pair chosen, $A'$and check for robust feasibility.
If feasible then
$A = A \cup A'$; $q = q - c_s$
End If
End While
End Loop.
Return $r2(g') := max(r2, \sum_{Place(i,k) \in A} v_{i,k}^m)$ and track its corresponding sonar-Placement Position pairs.
Set $r2 := \max_{g'} r2(g')$ and track its corresponding sonar-Placement Position pairs.

$G := G \backslash g'$;
Else:
$boolean = true$ $(Combination\ g'\ is\ feasible)$
**********(i.e. Combination g' is chosen)*********
Return metric $r1 := \sum_{Place(i,k) \in g'} v_{i,k}^m$

End If
End While
Return $Obj_1 = max(r1, r2)$ and track its corresponding sonar-Placement Position pairs.

Figure 7.2: Pseudocode for robust adaptation of all steps in **g-SPP1**

$B = \emptyset$
Do Step 4 (**g-SPP2**). Identify the sonar type-Placement position pair chosen (in each iteration), $B'$and check for robust feasibility.
    If feasible then
        $B = B \cup B'$
    Else:
        $B = B \cup \emptyset$
Return $Obj_2 = \sum_{Place(i,k) \in B} v_{i,k}^m$ and track its corresponding sonar-Placement Position pairs.

Figure 7.3: Pseudocode for robust adaptation of all steps in **g-SPP2**

7.5 Numerical Results and Analysis

In this section, we present numerical results and runtimes of the robust adaptations of the algorithms presented in Chapter 6. Like prior chapters, models and algorithms are implemented in GAMS and solved using CPLEX (GAMS 2013). All MIPs are solved within a relative tolerance of 3% duality gap, and all computational runs are made on a Linux server equipped with dual 3.00 GHz AMD processors (256 GB memory). Computational results presented in this section are based on data introduced in Chapter 4. Like Chapter 6, only mobile sonars are used in the deployment.

In our numerical experiments, we used the same value of parameter Γ in all the affected robust constraints. Uncertainty was modeled assuming that both budget and detection probability parameters could vary within a maximum of 5%, 10%, and 15% of their nominal values. We also considered parameter Γ to take values between 0 (nominal case) and 200 (worst case) in the specific instance we consider for both sources of uncertainties. Under these assumptions, we determined the value of Γ using the theoretical bounds introduced in Bertsimas and Sim (2004). With a visual basic script embedded in a spreadsheet, we determined Γ to be 90. Choosing $\Gamma_i = 80$ satisfies the theoretical bound when model parameters subject to uncertainty (budget and detection

probability parameters) are within a maximum of 5% and 10%. Likewise, $\Gamma_i = 90$ suffices to satisfy the theoretical bound when the parameters are within 15% of their nominal values. Similar trend is observed for other budget considerations. However, for convenience, we set $\Gamma_i = 90$ in all of our experiments in the chapter. The theoretical bound used to determine our choice of Γ is presented in Appendix II. In comparison to the nominal problem, this model is larger. However, it is still a linear program.

Of course, robust solutions are only guaranteed to be feasible when Γ attains its maximum value of 200, giving a possibility that for some scenarios the solution might be infeasible for other values of Γ between 0 and 200. However, the theoretical bound used to compute Γguarantees that the probability of a constraint violation is less than 1% (Bertsimas and Sim, 2004). Hence, for a large scale problem such as the one considered in this Chapter, feasibility analysis of robust solutions is unnecessary. Figures 7.4-7.9 show numerical results and runtimes of the robust adaptations of the algorithms as we varied available budget for different problem sizes. Since the procedure adopted in the robust adaptation continually checks for feasibility, results are not necessarily monotonic non-decreasing.

Our approach was tested to as much as 100x100 grid size and we show results only for 5x5, 25x25, and 50x50 grid problem sizes. The problem size has a large impact on solution run times and generally increases as problem size increases. Also, as problem size increases, objective function increases only slightly for all budget limitations. This is because same resources (sonars) are available for any problem size.

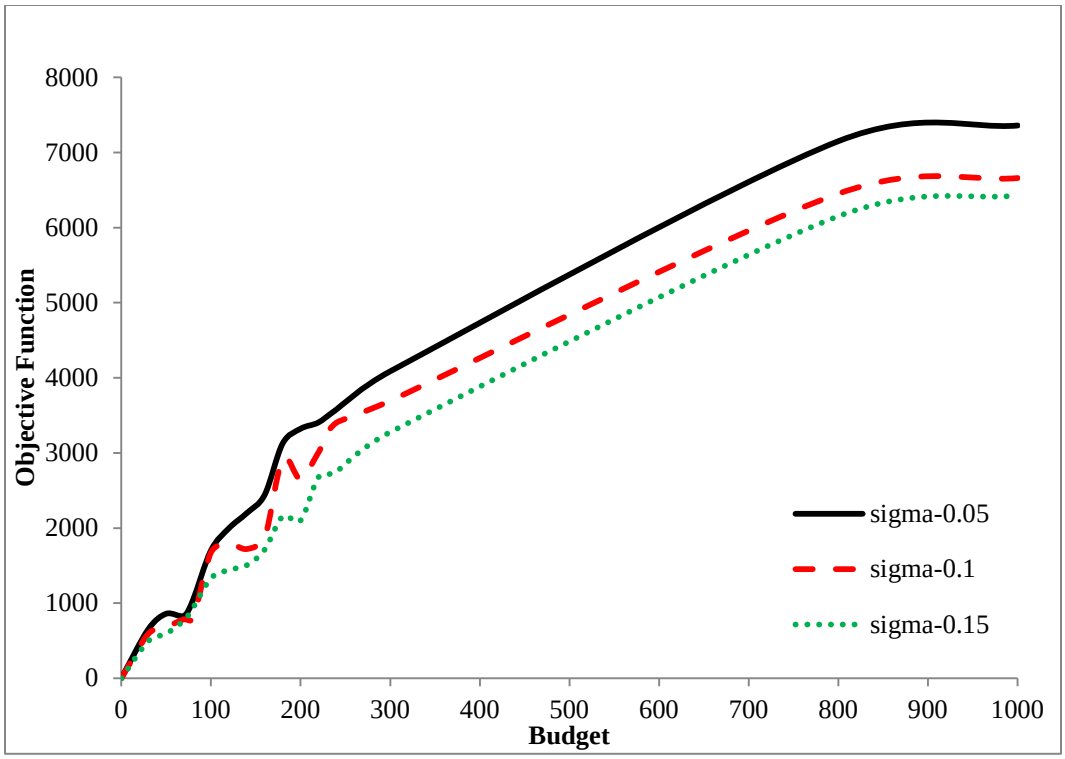

Figure 7.4: (Equivalent) objective functions vs. available budget-5x5 grid size

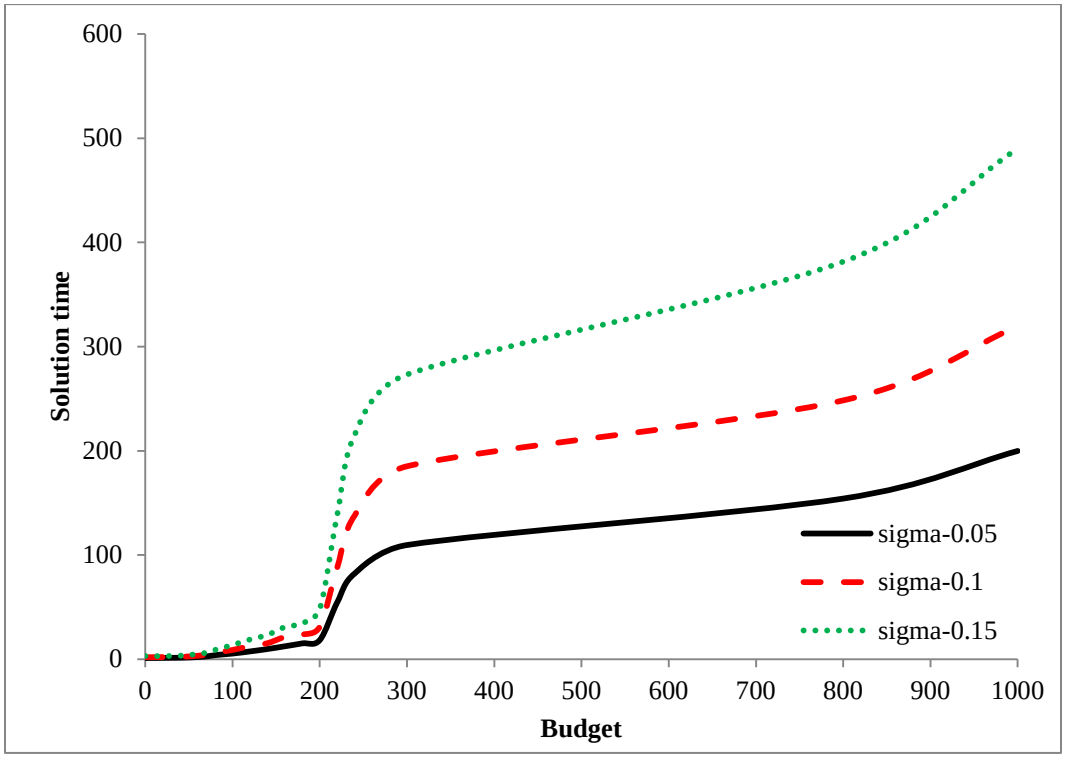

Figure 7.5: Solution time vs. available budget-5x5 grid size

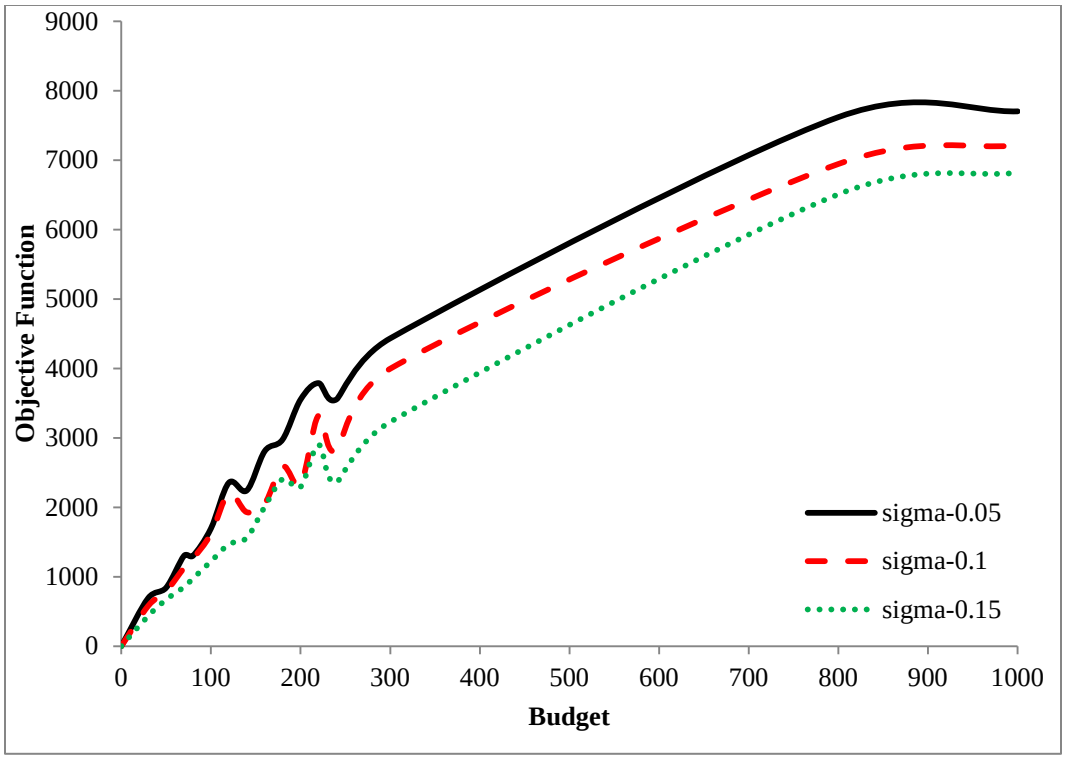

Figure 7.6: (Equivalent) objective functions vs. available budget-25x25 grid size

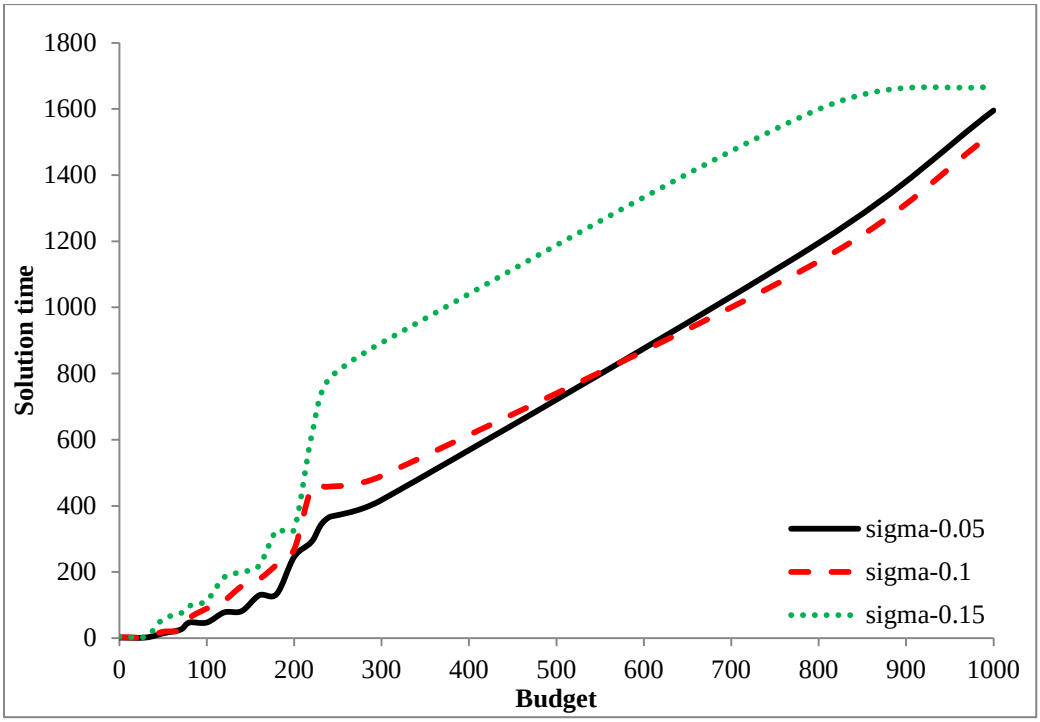

Figure 7.7: Solution time vs. available budget-25x25 grid size

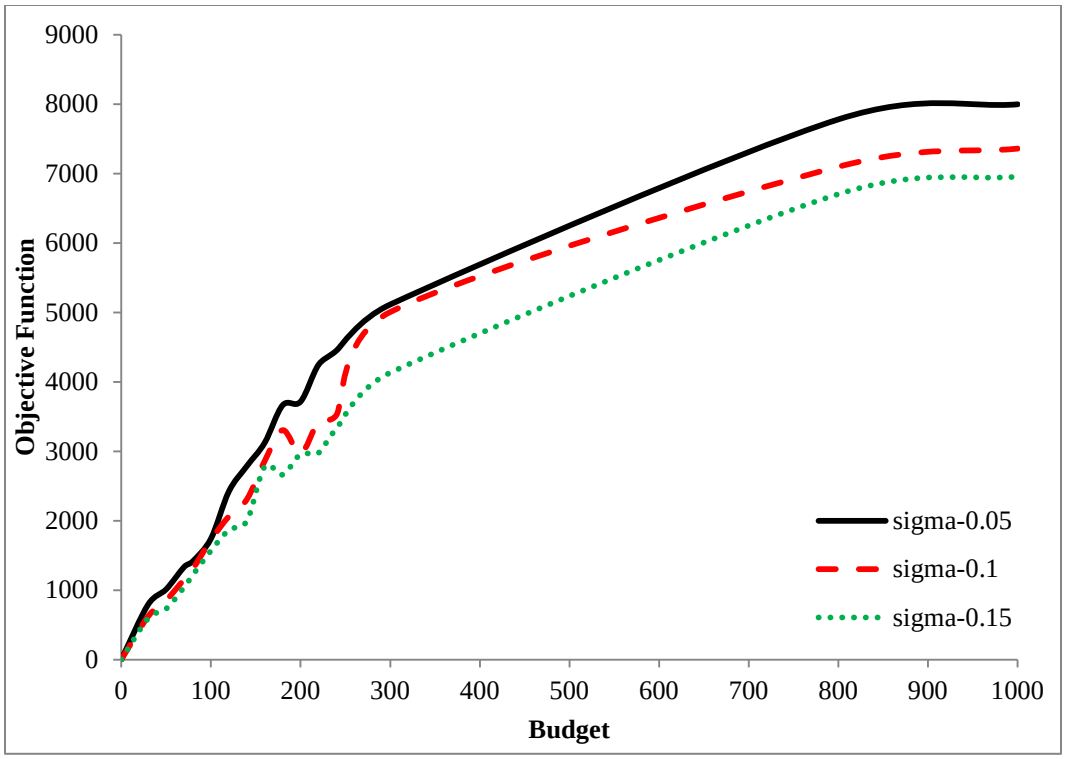

Figure 7.8: (Equivalent) objective functions vs. available budget-50x50 grid size

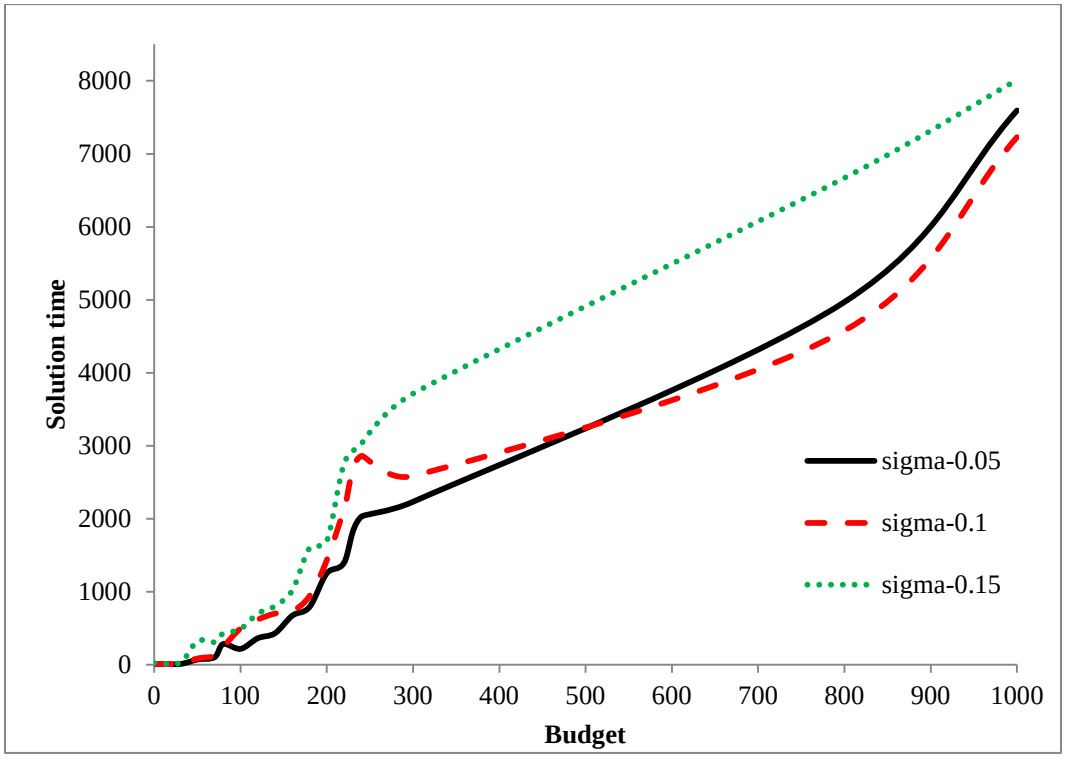

Figure 7.9: Solution time vs. available budget-50x50 grid size

Figures 7.10-7.12 compare results of our robust adaptation with deterministic optimal solutions returned by CPLEX for some selected budgetary allocations. Also, Table 7.1 summarizes these percentage deviations for all the variabilities, showing maximum, average and minimum (for only non-zero budget allocations) changes in optimality. As expected, changes from optimal values increase as uncertain parameters deviate from their nominal values. However, no specific claim can be made on behavior of deviations from CPLEX optimal values as problem size changes. A plausible reason for this is that since the robust adaptation regularly checks for feasibility before accepting a solution, inconsistent changes associated with optimal values should be expected. Results from the nominal case using our algorithms follow similar trend, albeit with better results.

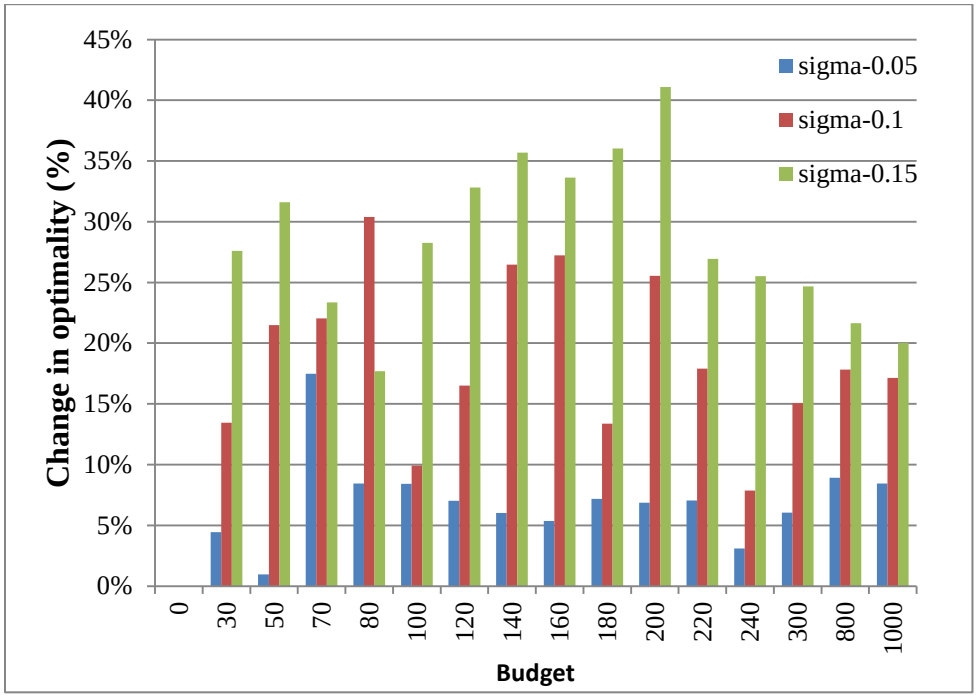

Figure 7.10: Robust adaptation solutions vs. CPLEX deterministic optimal solutions
Changes (%) in optimality for selected budget availabilities (5x5 grids)

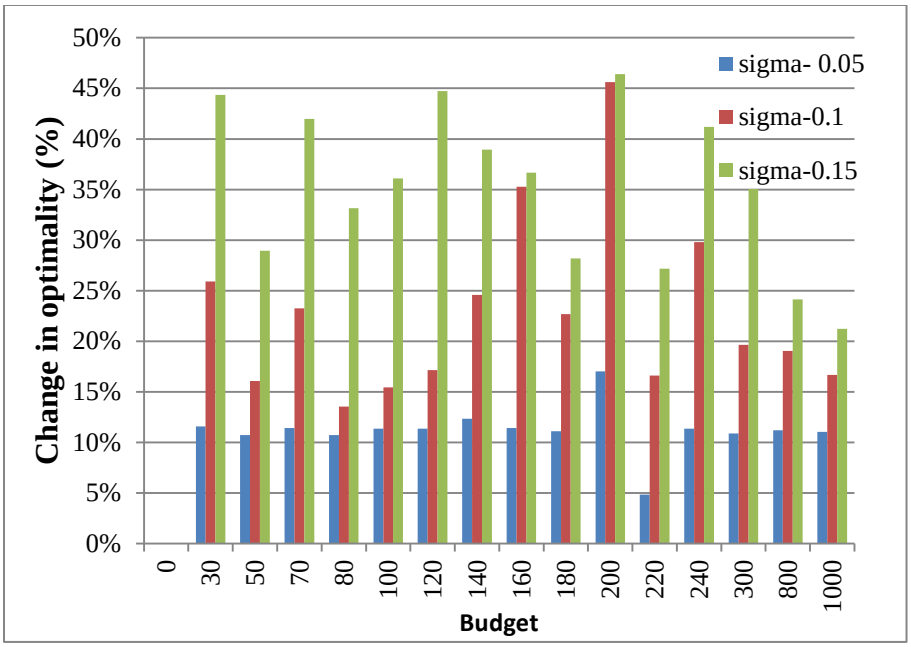

Figure 7.11: Robust-adaptation solutions vs. CPLEX deterministic optimal solutions
Changes (%) in optimality for selected budget availabilities (25x25 grids)

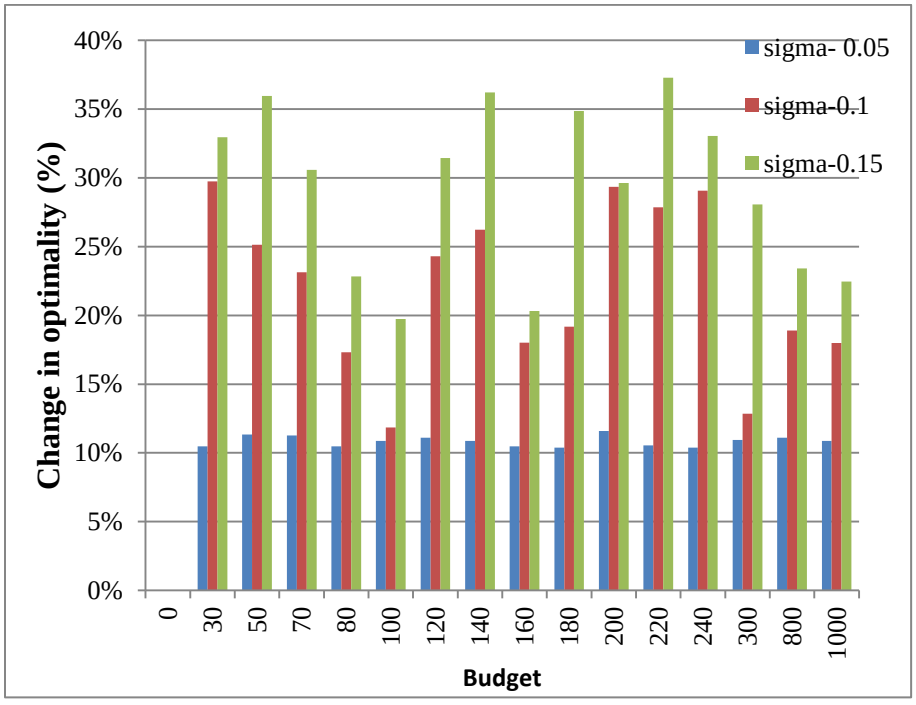

Figure 7.12: Robust-adaptation solutions vs. CPLEX deterministic optimal solutions
Changes (%) in optimality for selected budget availabilities (50x50 grids)

Table 7.1: Summary of Changes in optimality for problem sizes

Grid Size (Placement node size)	5x5	25x25	50x50
Maximum Change in optimality (%)	43.9	46.4	37.2
Average Change in optimality (%)	22.2	23.1	20.4
Minimum Change in optimality (%)	5.7	4.9	10.4

7.6 Conclusion

In this Chapter, we applied Γ -robustness to the sonar placement problem SPP with uncertain budget and detection probabilities. We proposed a MILP re-formulation of the SPP subject to parameterized levels of uncertainty using robust optimization. This robust approach limits the number of uncertain coefficients by a robustness parameter Γ. The framework combines linear programming approach of Soyster (1973) and also provides the possibility to control the level of conservatism in the nature of the data subject to uncertainty. Robust optimization addresses a need to hedge against uncertainty, and these uncertainties are bound to be of importance in any practical application. Moreover, most of our model's parameters are based on expert judgement (mostly manufacturer specifications) or incomplete source data and these data are subject to fluctuations during the years after deployment.

Although the basic motivation of using the robust optimization approach we presented in this Chapter is the lack of statistical knowledge about uncertain parameters in the SPP model, the methodology is also applicable when the probability distributions of these parameters are also known because solving robust counterparts of the model is

almost always easier than solving its non-convex stochastic or chance-constrained equivalent. A sacrifice in over-conservatism of the optimal solutions can help to arrive at acceptable solutions without a precise knowledge of probability distributions. To suit decision makers' preferences, this level of conservatism can also be adjusted as desired.

Chapter 8

Summary and Future Work

This dissertation focusses on ensuring the integrity of maritime assets and infrastructures. In this chapter, we present a summary of the dissertation and suggest future studies to extend and improve the current methodologies, models, and results of the studies.

To address protection of maritime assets, Chapter 3 of the dissertation concentrated on the development of a framework for risk-based shipping of LNG vessels. We found that unlike the maritime transportation of other hazard materials such as crude oil, the existing safety records of LNG vessels have been taken for granted and risk consideration in the transportation of LNG vessels are non-existent in literature. To the best of our knowledge, our methodology is the first in literature that focused on developing quantitative risk-based approach in the optimal scheduling of LNG vessels. Taking into consideration the disposition of a decision maker towards cost and risk measures, the methodology determines optimal cargo delivery schedules between liquefaction and re-gasification terminals. Results and discussions on a sample case study were also provided.

Using surveillance measures, Chapters 4-7 addressed the protection of maritime infrastructures such as waterways, harbors, jetties, etc. In Chapter 4, we introduced the sonar placement problem (SPP), introduced an alternate grid system for sonar deployment, and formulated an MIP bi-objective optimization model to solve the

problem within a periodic deployment. Amongst others, we observed that our sonar placement methodology not only improves the objective functions but also permits other regions in the area of interest which may never have been covered by sonars (due to budgetary constraints) to be eligible for coverage at other periods.

To address the influence of an opposing decision maker with counter-objectives to the desire of a decision maker (System Planners), we introduce in Chapter 5, a fortification methodology whereby interactions between these two agents affects the modeling of the SPP problem addressed in Chapter 4. Using a multi-level optimization approach, we presented a tri-level optimization model and an algorithm to solve the SPP where optimal partial coverage is desired. Typically, a game-theoretic approach is often adopted in a problem of this nature where competing rational agents with conflicting interests are the decision makers. In comparison to a game-theoretic based approach where only two levels of interface relationships (whether collaborative or non-collaborative) are considered in a strategic planning framework, our fortification model produces a superior protection plan because it considers an additional third level of non-collaborative relationship between the *defender* and the *attacker*, and thereafter selects the optimal strategy to thwart the attacker's efforts based on the optimal strategic plan adopted by the latter. Using practical data, we implemented the algorithm to solve the tri-level problem. In contrast to other approaches such as the traditional Benders-dual algorithm, which requires the sub-problem to be an LP problem, our algorithm is indifferent to such limitations. Although non-traditional methods using heuristics have been proposed to address this issue with the Benders approach, there are no guarantees the sub problem can be solved to integer optimality. We emphasize that though protection

is desirable, its desirability in terms of reducing vulnerability of the AOI should be dependent on the maximum resource capability of the *'Attacker'*. With small attack budgets, benefits of providing protection are often minimal and investment in providing protection may be regarded as un-necessary. However, with increased resource availabilities to the attacker(s) and a consequent ability to intrude in the AOI, the significance of investing in protection resources becomes apparent. As such, decision-makers (System planners) can adopt a protection plan after reviewing cost and inherent benefits associated with the protection plan. Proposal of an alternate algorithm that will overcome the slow computation time we have observed and a consequent comparison of this proposal with results presented in this chapter will be an insightful extension of this study.

Our work in Chapter 6 is in response to observed slow computation times in the previous chapters when problem sizes increase. Exploiting submodularity of the SPP model, we developed greedy-based algorithms that help to speed up computation time without significant impacts on solution quality. Although the greedy-based algorithms we presented in this chapter only obtain initial 'good' solutions before a local technique can be used to improve the solution, the modelling approach we have adopted best suits the prevailing situation in practical deployment due to limitations posed by available budget. As a future work, it will be interesting (using variants of meta heuristics such as Simulated annealing) to come up with a procedure whereby an exchange of sonar placement positions is attempted in each iteration round and this exchange is 'approved' if a positive change in the overall metric of measure is attained. Likewise, a parallel evolution approach (Genetic algorithm GA) that use binary codified hypothetical sonar

sets and a corresponding fitness function (similar to our metric measure in Chapter 7) to determine optimal placement using evolution techniques such as crossover mutations, natural selections, etc. can replace the placement procedures we introduced in the greedy algorithms of Chapter 6. An ideal fitness function will attempt to strike a balance between the sub-sections of the AOI that are covered and the number of deployed sonars. At each iterative stage of the evolution approach, a simultaneous adjustment of sonar placement locations and their orientations can be made to determine maximum partial coverage within budget and coverage limitations. The increased number of sonars and placement positions under a GA implies a higher computational cost, and hence a higher computing time. This inhibition will make it difficult to deal with large problem sizes. This is the premise behind our suggestion of a parallelization approach of the GA algorithm. For this purpose, OpenMP, a known API for shared-memory parallel programming will prove adequate.

Chapters 4-6 of this dissertation assume that associated data related to the Sonar placement problem (SPP) are exact. This idealistic assumption fails to consider the inherent uncertainties associated with some modelling parameters. Chapter 7 of this dissertation addresses this issue and helps to guarantee that uncertainty considerations do not nullify optimization solutions. Using a robust formulation that maintains the linearity of the SPP model, we adopt a framework, where we introduce parameters and new decision variables that addresses uncertainties in two modelling parameters (sonar cost and detection probabilities). A major advantage of the modelling approach is that lack of statistical knowledge about these uncertain parameters does not affect the procedure. In addition, we incorporated the greedy algorithms developed in Chapter 6 to take this

robust approach into consideration in any sonar deployment. In our work in Chapter 6, we relied on a theoretical bound to compute the value(s) for a robust parameter. Our numerical experiments indicate that there are slight variations in the actual value of the parameter in comparison to the value computed using the theoretical bound. It will be worthwhile to investigate this observation and consequently modify the bounds using mathematical theoretical techniques. Perhaps, the most attractive feature of the robust methodology of Chapter 7 is that it maintains linearity in any LP/MIP model. However, a shortcoming of the approach is that the feasibility of the problem might be affected under some conditions. Further studies can also be done to evaluate the theoretical bounds of solutions along with theoretical bounds on infeasibilities imposed by the robust approach. Another possible extension to this work is to identify alternate robust approaches applicable to the SPP and consequently compare solutions to the robust approach we have presented in this dissertation.

References

1. Adams, W. P., Forrester, R. J., & Glover, F. W. (2004). Comparisons And Enhancement Strategies for Linearizing Mixed 0-1 Quadratic Programs. *Discrete Optimization, 1*(2), 99-120.

2. Alguacil, N., Delgadillo, A., & Arroyo, J. M. (2014). A Trilevel Programming Approach for Electric Grid Defense Planning. *Computers & Operations Research*, *41*, 282-290.

3. Altınel, İ. K., Aras, N., Güney, E., & Ersoy, C. (2008). Binary Integer Programming Formulation and Heuristics for Differentiated Coverage in Heterogeneous Sensor Networks. *Computer Networks*, *52*(12), 2419-2431.

4. Alves Pessoa, A., Di Puglia Pugliese, L., Guerriero, F., & Poss, M. (2015). Robust Constrained Shortest Path Problems under Budgeted Uncertainty. *Networks*, *66*(2), 98-111.

5. Andersson, H., Christiansen, M., & Fagerholt, K. (2010). Transportation Planning and Inventory Management in the LNG Supply Chain. In *Energy, natural resources and environmental economics* (pp. 427-439). Springer Berlin Heidelberg.

6. Armaous, A., & Demetriou, M. A. (2006, June). Using Spatial H2 Norm for Sensor Placement in Parabolic Partial Differential Equations. In *2006 American Control Conference* (pp. 1467-1472). IEEE.

7. Bard, J. F. (1998). *Practical bilevel optimization: Algorithms and applications*.

Dordrecht: Kluwer Academic Publishers.

8. Ben-Tal, A., & Nemirovski, A. (2000). Robust Solutions of Linear Programming Problems Contaminated with Uncertain Data. *Mathematical programming*, *88*(3), 411-424.

9. Ben-Tal, A., El Ghaoui, L., & Nemirovski, A. (2009). *Robust Optimization.* Princeton University Press.

10. Berry, J. W., Fleischer, L., Hart, W. E., Phillips, C. A., & Watson, J. P. (2005). Sensor Placement in Municipal Water Networks. *Journal of Water Resources Planning and Management*, *131*(3), 237-243.

11. Bertsimas, D., & Sim, M. (2003). Robust Discrete Optimization and Network Flows. *Mathematical programming*, *98*(1-3), 49-71.

12. Bertsimas, D., & Sim, M. (2004). The Price of Robustness. *Operations research*, *52*(1), 35-53.

13. Bertsimas, D., Brown, D. B., & Caramanis, C. (2011). Theory and Applications of Robust Optimization. *SIAM review*, *53*(3), 464-501.

14. Bier, V. M., Gratz, E. R., Haphuriwat, N. J., Magua, W. & Wierzbicki, K. R. (2007). Methodology for Identifying Near-Optimal Interdiction Strategies for a Power Transmission System. *Reliability Engineering & System Safety*, 92(9), 1155–1161.

15. Biobaku, T., Lim, G., Cho, J., Bora, S., & Parsaei, H. (2014). Under-Water Sonar Placement. In *Proceedings of the Annual Industrial and Systems*

Engineering Research Conference, Montreal, Canada.

16. Biobaku, T. & J Lim, G. (2015). Literature Survey on Underwater Threat Detection. *Transactions on Maritime Science* 4(01), 14–22.

17. Biobaku, T., Lim, G. J., Bora, S., Cho, J., & Parsaei, H. (2016). An Optimal Sonar Placement Approach for Detecting Underwater Threats under Budget Limitations. *Journal of Transportation Security*, *9*(1-2), 17-34.

18. Birge, J. R., & Louveaux, F. (2011). *Introduction to Stochastic Programming*. Springer Science & Business Media.

19. Bopp, A. E., Kannan, V. R., Palocsay, S. W., & Stevens, S. P. (1996). An Optimization Model for Planning Natural Gas Purchases, Transportation, Storage and Deliverability. *Omega*, *24*(5), 511-522.

20. Borowski, B., Sutin, A., Roh, H. S., & Bunin, B. (2008). Passive Acoustic Threat Detection in Estuarine Environments. In *SPIE Defense and Security Symposium* (pp. 694513-694513). International Society for Optics and Photonics.

21. Brown, G., Carlyle, M., Salmeron, J., & Wood, K. (2005). Analyzing the Vulnerability of Critical Infrastructure to Attack and Planning Defenses. *Tutorials in Operations Research: Emerging Theory, Methods, and Applications*, 102-123.

22. Brown, G., Carlyle, M., Salmerón, J., & Wood, K. (2006). Defending Critical Infrastructure. *Interfaces*, *36*(6), 530-544.

23. Castello, C. C., Fan, J., Davari, A., & Chen, R. X. (2010). Optimal Sensor

Placement Strategy for Environmental Monitoring using Wireless Sensor Networks. In *2010 42nd Southeastern Symposium on System Theory (SSST)* (pp. 275-279). IEEE.

24. Chakrabarty, K., Iyengar, S. S., Qi, H., & Cho, E. (2002). Grid Coverage for Surveillance and Target Location in Distributed Sensor Networks. *IEEE transactions on computers*, *51*(12), 1448-1453.

25. Chatterjee, N., & Geist, J. M. (1972). Effects of Stratification on Boil-Off Rates in LNG Tanks. *Pipeline and Gas Journal*, *199*(11).

26. Cho, J., J Lim, G., Biobaku, T., Bora, S., & Parsaei, H. (2014). Liquefied Natural Gas Ship Route Planning Model Considering Market Trend Change. *Transactions on Maritime Science*, *3*(02), 119-130.

27. Clouqueur, T., Phipatanasuphorn, V., Ramanathan, P., & Saluja, K. K. (2002). Sensor Deployment Strategy for Target Detection. In *Proceedings of the 1st ACM international workshop on Wireless sensor networks and applications* (pp. 42-48). ACM.

28. Cormen, T. H. (2009). *Introduction to Algorithms*. MIT press.

29. Dantzig, G., Eisenberg, E., & Cottle, R. (1965). Symmetric Dual Nonlinear Programs. *Pacific Journal of Mathematics*, *15*(3), 809-812.

30. Delgadillo, A., Arroyo, J. M. and Alguacil, N. (2010). Analysis of Electric Grid Interdiction with Line Switching. *Power Systems, IEEE Transactions on* 25(2), 633–641.

31. Dhillon, S. S., Chakrabarty, K., & Iyengar, S. S. (2002). Sensor Placement for Grid Coverage under Imprecise Detections. In *Information Fusion, 2002. Proceedings of the Fifth International Conference on* (Vol. 2, pp. 1581-1587). IEEE.

32. Dhillon, S. S., & Chakrabarty, K. (2003). Sensor Placement for Effective Coverage and Surveillance in Distributed Sensor Networks. In *Wireless Communications and Networking, 2003. WCNC 2003. 2003 IEEE* (Vol. 3, pp. 1609-1614). IEEE.

33. Dobrota, Đ., Lalić, B., & Komar, I. (2013). Problem of Boil-Off in LNG Supply Chain. *Transactions on Maritime Science*, *2*(02), 91-100.

34. El Ghaoui, L., Oustry, F., & Lebret, H. (1998). Robust Solutions to Uncertain Semidefinite Programs. *SIAM Journal on Optimization*, *9*(1), 33-52.

35. Esseghir, M., Bouabdallah, N., & Pujolle, G. (2005). Sensor Placement for Maximizing Wireless Sensor Network Lifetime. In *VTC-2005-Fall. 2005 IEEE 62nd Vehicular Technology Conference, 2005.* (Vol. 4, pp. 2347-2351). IEEE.

36. Etkin, D. S. (1999). Estimating Cleanup Costs for Oil Spills. In *International oil spill conference* (Vol. 1999, No. 1, pp. 35-39). American Petroleum Institute.

37. Ezell, B. C., Bennett, S. P., Von Winterfeldt, D., Sokolowski, J., & Collins, A. J. (2010). Probabilistic Risk Analysis and Terrorism Risk. *Risk Analysis, 30*(4), 575-589.

38. Feizollahi, M. J., & Feyzollahi, H. (2015). Robust Quadratic Assignment

Problem with Budgeted Uncertain Flows. *Operations Research Perspectives*, *2*, 114-123.

39. Garey, M. R., & Johnson, D. S. (1979). *Computers and intractability: A guide to the theory of NP-completeness* (19th ed.). New York, NY: W.H.Freeman & Co.

40. Ghafoori, A., & Altiok, T. (2012). A Mixed Integer Programming Framework for Sonar Placement to Mitigate Maritime Security Risk. *Journal of Transportation Security*, *5*(4), 253-276.

41. Glover, F. (1975). Improved Linear Integer Programming Formulations of Nonlinear Integer Problems. *Management Science*, *22*(4), 455-460.

42. Golen, E. F., Mishra, S., & Shenoy, N. (2010). An Underwater Sensor Allocation Scheme for a Range Dependent Environment. *Computer Networks*, *54*(3), 404-415.

43. Golen, E. F., Shenoy, N., & Incze, B. I. (2007). Underwater Sensor Field Design Using Game Theory. In *MILCOM 2007-IEEE Military Communications Conference* (pp. 1-7). IEEE.

44. Gorissen, B. L., Yanıkoğlu, İ., & den Hertog, D. (2015). A Practical Guide to Robust Optimization. *Omega*, *53*, 124-137.

45. Grønhaug, R., & Christiansen, M. (2009). Supply Chain Optimization for the Liquefied Natural Gas Business. In *Innovations in distribution logistics* (pp. 195-218). Springer Berlin Heidelberg.

46. Grønhaug, R., Christiansen, M., Desaulniers, G., & Desrosiers, J. (2010). A

Branch-And-Price Method for a Liquefied Natural Gas Inventory Routing Problem. *Transportation Science, 44*(3), 400-415.

47. Guzelsoy, M., & Ralphs, T. K. (2007). Duality for Mixed-Integer Linear Programs. *International Journal of Operations Research, 4*(3), 118-137.
48. Halvorsen-Weare, E. E., & Fagerholt, K. (2013). Routing and Scheduling in a Liquefied Natural Gas Shipping Problem with Inventory and Berth Constraints. *Annals of Operations Research* 203(1), 167–186.
49. Halvorsen-Weare, E. E., Fagerholt, K., & Rönnqvist, M. (2013).Vessel Routing and Scheduling under Uncertainty in the Liquefied Natural Gas Business. *Computers & Industrial Engineering* 64(1), 290–301.
50. Heidemann, J., Stojanovic, M., & Zorzi, M. (2012). Underwater Sensor Networks: Applications, Advances and Challenges. *Phil. Trans. R. Soc. A, 370*(1958), 158-175.
51. Heidemann, J., Ye, W., Wills, J., Syed, A., & Li, Y. (2006). Research Challenges and Applications for Underwater Sensor Networking. In *IEEE Wireless Communications and Networking Conference, 2006. WCNC 2006.* (Vol. 1, pp. 228-235). IEEE.
52. Hightower M., Petti, J., & Lopez, C. (2013). Risk Mitigation of LNG Ship Damage from Large Spills. In *17th International Conference & Exhibition on Liquefied Natural Gas. LNG* 17 (pp.1-17).
53. Holland, J. (1975). Genetic Algorithms, Computer Programs that evolve in ways that even their Creators do not fully understand. *Scientific American* pp. 66–72.

54. Hsieh, Y. C. (2003). A Linear Approximation for Redundant Reliability Problems with Multiple Component Choices. *Computers & industrial engineering*, *44*(1), 91-103.

55. Iakovou, E. T. (2001). An Interactive Multiobjective Model for the Strategic Maritime Transportation of Petroleum Products: Risk Analysis and Routing. *Safety Science*, *39*(1), 19-29.

56. Iakovou, E., Douligeris, C., Li, H., Ip, C., & Yudhbir, L. (1999). A Maritime Global Route Planning Model for Hazardous Materials Transportation. *Transportation science*, *33*(1), 34-48.

57. Ibrahim, S., Cui, J. H., & Ammar, R. (2007). Surface-Level Gateway Deployment for Underwater Sensor Networks. In *MILCOM 2007-IEEE Military Communications Conference* (pp. 1-7). IEEE.

58. International Tanker Owners Pollution Federation Limited, ITOPF (2014.). Oil Tanker Spill Statistics. Retrieved November 24, 2014, from http://www.itopf.com/information-services/data-and-statistics/statistics/

59. Jae-Hyun, S. E. O., Yong-Hyuk, K. I. M., Hwang-Bin, R. Y. O. U., Si-Ho, C. H. A., & Minho, J. O. (2008). Optimal Sensor Deployment for Wireless Surveillance Sensor Networks by a Hybrid Steady-State Genetic Algorithm. *IEICE transactions on communications*, *91*(11), 3534-3543.

60. Karaboga, D. (2005). *An idea based on honey bee swarm for numerical optimization* (Vol. 200). Technical report-tr06, Erciyes University, Engineering faculty, Computer engineering department.

61. Koopman, B. O. (1980). *Search and Screening: General Principles with Historical Applications*. Pergamon Press.

62. Krause, A., & Guestrin, C. (2005). *A Note on the Budgeted Maximization of Submodular Functions*. Technical report, CMU-CALD-05-103, 2005.

63. Krause, A., Guestrin, C., Gupta, A., & Kleinberg, J. (2006). Near-Optimal Sensor Placements: Maximizing Information while Minimizing Communication Cost. In *Proceedings of the 5th international conference on Information processing in sensor networks* (pp. 2-10). ACM.

64. Kumar, S., Kwon, H. T., Choi, K. H., Cho, J. H., Lim, W., & Moon, I. (2011). Current Status and Future Projections of LNG Demand and Supplies: A Global Prospective. *Energy Policy*, *39*(7), 4097-4104.

65. Lee, R. W., & Kulesz, J. J. (2008). A Risk-Based Sensor Placement Methodology. *Journal of hazardous materials*, *158*(2), 417-429.

66. Leung, M., Lambert, J. H., & Mosenthal, A. (2004). A Risk-Based Approach to Setting Priorities in Protecting Bridges against Terrorist Attacks. *Risk Analysis*, *24*(4), 963-984.

67. Li, D., Li, Z., Ma, W., & Chen, H. (2010). Constrained Surface-Level Gateway Placement For Underwater Acoustic Wireless Sensor Networks. In *International Conference on Combinatorial Optimization and Applications* (pp. 46-57). Springer Berlin Heidelberg.

68. Li, H., Iakovou, E., & Douligeris, C. (1996). Strategic Planning Model for Marine Oil Transportation in the Gulf of Mexico. *Transportation Research Record: Journal of the Transportation Research Board*, (1522), 108-115.

69. Li, K. X., Yin, J., Bang, H. S., Yang, Z., & Wang, J. (2014). Bayesian Network with Quantitative Input for Maritime Risk Analysis. *Transportmetrica A: Transport Science*, *10*(2), 89-118.

70. Lin, F. Y., & Chiu, P. L. (2005). A Near-Optimal Sensor Placement Algorithm to Achieve Complete Coverage-Discrimination in Sensor Networks. *IEEE Communications Letters*, *9*(1), 43-45.

71. McGill, W. L., Ayyub, B. M., & Kaminskiy, M. (2007). Risk Analysis for Critical Asset Protection. *Risk Analysis*, *27*(5), 1265-1281.

72. Murty, V. N. (1981). Counting the Integer Solutions of a Linear Equation with Unit Coefficients. *Mathematics Magazine*, *54*(2), 79-81.

73. Meguerdichian, S., Koushanfar, F., Potkonjak, M. and Srivastava, M. (2001). Coverage Problems in Wireless Ad-Hoc Sensor Networks. In INFOCOM 2001. Twentieth Annual Joint Conference of the IEEE Computer and Communications Societies. Proceedings. (Vol. 3, pp. 1380– 1387). IEEE.

74. Mhatre, V. P., Rosenberg, C., Kofman, D., Mazumdar, R., & Shroff, N. (2005). A Minimum Cost Heterogeneous Sensor Network with a Lifetime Constraint. *IEEE Transactions on Mobile Computing*, *4*(1), 4-15.

75. Mosleh, A., Bier, V. M., & Apostolakis, G. (1988). A Critique of Current Practice for the Use of Expert Opinions in Probabilistic Risk Assessment. *Reliability Engineering & System Safety*, *20*(1), 63-85.

76. Motto, A. L., Arroyo, J. M., & Galiana, F. D. (2005). A Mixed-Integer LP Procedure for the Analysis of Electric Grid Security under Disruptive Threat.

IEEE Transactions on Power Systems, *20*(3), 1357-1365.

77. Nagy, B. N. (2003). Shortest Paths in Triangular Grids with Neighbourhood Sequences. *CIT. Journal of computing and information technology*, *11*(2), 111-122.

78. Nagy, B. (2003). A Family of Triangular Grids in Digital Geometry. In *Image and Signal Processing and Analysis, 2003. ISPA 2003. Proceedings of the 3rd International Symposium on* (Vol. 1, pp. 101-106). IEEE.

79. Nagy, B. (2004). Generalized Triangular Grids in Digital Geometry. *Acta Mathematica Academiae Paedagogicae Nyíregyháziensis*, *20*(1), 63-78.

80. Nagy, B., & Strand, R. (2008). A Connection between $\mathbb{Z}^n$ and Generalized Triangular Grids. In *International Symposium on Visual Computing* (pp. 1157-1166). Springer Berlin Heidelberg.

81. National Consortium for the Study of Terrorism and Responses to Terrorism (START). (2014). Global Terrorism Database [Data file]. Retrieved November 20, 2014, from https://www.start.umd.edu/gtd

82. Nemhauser, G. L., Wolsey, L. A., & Fisher, M. L. (1978). An Analysis of Approximations for Maximizing Submodular Set Functions—I. *Mathematical Programming*, *14*(1), 265-294.

83. Ngatchou, P. N., Fox, W. L., & El-Sharkawi, M. A. (2006). Multiobjective Multistatic Sonar Sensor Placement. In *2006 IEEE International Conference on Evolutionary Computation* (pp. 2713-2719). IEEE.

84. Organisation for Economic Co-operation and Development (OEDC). (2014). Security in maritime transport: Risk factors and economic impact. Retrieved August 01, 2014, from http://www.oecd.org/sti/transport/maritimetransport/18521672.pdf/

85. Papanikolaou, A., Eliopoulou, E., & Mikelis, N. (2006). Impact of Hull Design on Tanker Pollution. In *Proc. 9th International Marine Design Conference (IMDC06).*

86. Pashko, S., Molyboha, A., Zabarankin, M., & Gorovyy, S. (2008). Optimal Sensor Placement for Underwater Threat Detection. *Naval Research Logistics (NRL), 55*(7), 684-699.

87. Poss, M. (2013). Robust Combinatorial Optimization with Variable Budgeted Uncertainty. *4OR-Q J Oper Res*, *11*(1), 75-92.

88. Psarros, G., Skjong, R., & Vanem, E. (2011). Risk Acceptance Criterion for Tanker Oil Spill Risk Reduction Measures. *Marine pollution bulletin*, *62*(1), 116-127.

89. Rakke, J. G., Stålhane, M., Moe, C. R., Christiansen, M., Andersson, H., Fagerholt, K., & Norstad, I. (2011). A Rolling Horizon Heuristic for Creating a Liquefied Natural Gas Annual Delivery Program. *Transportation Research Part C: Emerging Technologies*, *19*(5), 896-911.

90. Ren, Z. G., Feng, Z. R., Ke, L. J., & Zhang, Z. J. (2010). New Ideas for Applying Ant Colony Optimization to the Set Covering Problem. *Computers & Industrial Engineering*, *58*(4), 774-784.

91. Saharidis, G. K., & Ierapetritou, M. G. (2013). Speed-Up Benders Decomposition using Maximum Density Cut (MDC) Generation. *Annals of Operations Research*, *210*(1), 101-123.

92. Salmeron, J., Wood, K., & Baldick, R. (2004). Analysis of Electric Grid Security under Terrorist Threat. *IEEE Transactions on Power Systems*, *19*(2), 905–912.

93. Seo, J. H., Im, C. H., Kwak, S. Y., Lee, C. G., & Jung, H. K. (2008). An Improved Particle Swarm Optimization Algorithm Mimicking Territorial Dispute between Groups for Multimodal Function Optimization Problems. *IEEE Transactions on Magnetics*, *44*(6), 1046-1049.

94. Schoellhammer, T., Wong, J., Hansen, M., Potkonjak, M., & Estrin, D. (2006). *Sensor Deployment Using Interleaved Experimentation, Modeling, and Optimization*. Technical report, Center for Embedded Network Sensing, 2006.

95. Sen, J., Chandra, M. G., Balamuralidhar, P., Harihara, S. G., & Reddy, H. (2007). A Distributed Protocol for Detection of Packet Dropping Attack in Mobile Ad Hoc Networks. In *Telecommunications and Malaysia International Conference on Communications, 2007. ICT-MICC 2007. IEEE International Conference on* (pp. 75-80). IEEE.

96. Shakkottai, S., Srikant, R., & Shroff, N. B. (2005). Unreliable Sensor Grids: Coverage, Connectivity and Diameter. *Ad Hoc Networks*, *3*(6), 702-716.

97. Shukri, T. (2004). LNG Technology Selection. *Hydrocarbon engineering*, *9*(2), 71-76.

98. Siddiqui, A., & Verma, M. (2013). An Expected Consequence Approach to

Route Choice in the Maritime Transportation of Crude Oil. *Risk Analysis*, *33*(11), 2041-2055.

99. Simonoff, J. S., Restrepo, C. E., & Zimmerman, R. (2007). Risk-Management and Risk-Analysis-Based Decision Tools for Attacks on Electric Power. *Risk Analysis*, *27*(3), 547-570.

100. Soyster, A. L. (1973). Convex Programming with Set-Inclusive Constraints and Applications to Inexact Linear Programming. *Operations research*, *21*(5), 1154-1157.

101. Stålhane, M., Rakke, J. G., Moe, C. R., Andersson, H., Christiansen, M., & Fagerholt, K. (2012). A Construction and Improvement Heuristic for a Liquefied Natural Gas Inventory Routing Problem. *Computers & Industrial Engineering*, *62*(1), 245-255.

102. Sundar, S., & Singh, A. (2012). A Swarm Intelligence Approach to the Early/Tardy Scheduling Problem. *Swarm and Evolutionary Computation*, *4*, 25-32.

103. Sviridenko, M. (2004). A Note on Maximizing a Submodular Set Function Subject to a Knapsack Constraint. *Operations Research Letters*, *32*(1), 41-43.

104. U.S. Department of Homeland Security (2013). *NIPP 2013: Partnering for Critical Infrastructure Security and Resilience*. Retrieved July 22, 2015, from http://www.dhs.gov/sites/default/files/publications/National-Infrastructure-Protection-Plan-2013-508.pdf

105. van Dorp, J. R., & Merrick, J. R. (2011). On A Risk Management Analysis Of Oil Spill Risk Using Maritime Transportation System Simulation. *Annals of Operations Research*, *187*(1), 249-277.

106. Vanem, E., Antao, P., Østvik, I., & de Comas, F. D. C. (2008). Analysing the Risk of LNG Carrier Operations. *Reliability Engineering & System Safety*, *93*(9), 1328-1344.

107. Waite, A. D. (2002). *Sonar for Practising Engineers*. John Wiley & Sons Incorporated.

108. Wang, B. (2010). *Coverage Control in Sensor Networks*. Springer Science & Business Media.

109. Wang, J., & Zhong, N. (2008). Minimum-Cost Sensor Arrangement for Achieving Wanted Coverage Lifetime. *International Journal of Sensor Networks*, *3*(3), 165-174.

110. Wang, W., Srinivasan, V., & Chua, K. C. (2008). Coverage in Hybrid Mobile Sensor Networks. *IEEE Transactions on Mobile Computing*, *7*(11), 1374-1387.

111. Wilhelm, W. E., & Gokce, E. I. (2010). Branch-And-Price Decomposition to Design a Surveillance System for Port and Waterway Security. *IEEE Transactions on Automation Science and Engineering*, *7*(2), 316-325.

112. Willis, H. H. (2007). Guiding Resource Allocations Based On Terrorism Risk. *Risk analysis*, *27*(3), 597-606.

113. Wu, C. H., Lee, K. C., & Chung, Y. C. (2007). A Delaunay Triangulation

Based Method for Wireless Sensor Network Deployment. *Computer Communications*, *30*(14), 2744-2752.

114. Yao, Y., Edmunds, T., Papageorgiou, D., & Alvarez, R. (2007). Trilevel Optimization in Power Network Defense. *IEEE Transactions on Systems, Man, and Cybernetics, Part C (Applications and Reviews)*, *37*(4), 712-718.

115. Yates, J., Batta, R., & Karwan, M. (2011). Optimal Placement of Sensors and Interception Resource Assessment for the Protection of Regional Infrastructure from Covert Attack. *Journal of Transportation Security*, *4*(2), 145-169.

116. Yelbay, B., Birbil, Ş. İ., & Bülbül, K. (2012). The Set Covering Problem Revisited: An Empirical Study Of The Value Of Dual Information. *European Journal of Operational Research*.

117. Yuan, W., Zhao, L., & Zeng, B. (2014). Optimal Power Grid Protection through a Defender–Attacker–Defender Model. *Reliability Engineering & System Safety*, *121*, 83-89.

118. Zeng, B., & Zhao, L. (2013). Solving Two-Stage Robust Optimization Problems Using a Column-And-Constraint Generation Method. *Operations Research Letters*, *41*(5), 457-461.

119. Zhang, G., Lu, J., Montero, J., & Zeng, Y. (2010). Model, Solution Concept, and Kth-Best Algorithm for Linear Trilevel Programming. *Information Sciences*, *180*(4), 481-492.

120. Zhao, C., Yu, Z., & Chen, P. (2007). Optimal Deployment of Nodes Based on Genetic Algorithm in Heterogeneous Sensor Networks. In *2007 International*

Conference on Wireless Communications, Networking and Mobile Computing.

121. Zou, Y., & Chakrabarty, K. (2004). Sensor Deployment and Target Localization in Distributed Sensor Networks. *ACM Transactions on Embedded Computing Systems (TECS)*, *3*(1), 61-91.

Appendix I:

Liquefied Natural Gas (LNG) Ship Route Planning Model (Cho et al., 2014)

This appendix presents a highlight of the LNG transportation model we developed in Cho et al. (2014). Although the study also included a stochastic extension, we only include the deterministic model developed in this appendix.

The model generates shipping schedules to maximize revenue, meet customer demands, and maintain optimal LNG production and inventory level at the liquefaction terminal in each time period. All operating vessels must initiate a tour from a liquefaction terminal at the depot and complete the tour after unloading cargoes at their final destinations.

All LNG carriers have their specific tank capacities, loading conditions and average vessel speeds. The tank capacity ranges from 140,000 billion cubic meter (bcm) to 216,000 bcm. The fleet of heterogeneous vessels can be divided into two groups depending on loading conditions: Type I (no partial tank filling allowed) and Type II (partial tank filling is allowed). Type I vessels are prohibited from partial loading, which means that the amount of LNG in a tank must be over a specific level (or empty tank) to avoid sloshing impact (Sloshing is situation whereby considerable liquid movement takes place in the containment system of the LNG vessel, creating high impact pressure on the tank surface). These types of vessels can only serve individual customers unless the additional short-term or spot demand is very small. Type II vessels have no restriction on partial tank filling so that multiple customers can be served by an assigned LNG vessel

within the given tank capacity. We formulate the problem as a multi-vehicle routing model and also consider the Boil-off gas (BOG) rate (The BOG is gas generated by evaporation of the LNG cargo during maritime transport). In addition, we give a small buffer on the time window by allowing few deviations from the target delivery date to ensure flexibility of transportation.

Mathematical formulations

Indices and Sets:

S	Set of LNG terminals;
T	Set of time periods;
K	Set of LNG tankers;
$s \in S$	Index of LNG terminal;
$t \in T$	Index of time period;
$k \in K$	Index of LNG tanker;
$G(V, A)$	Directed graph nodes $V = \{1,2, \dots, \lvert S \rvert = s + max(s)(t-1)\}$ as the set of terminals and $A = \{(i,j): i,j \in V, i \neq j\}$ as the set of arcs in the planning time horizon;
$h \in H$	Index of the origin (depot), where $h = 1 + \lvert S \rvert (t-1) = max(s) \cdot (t-1)$ in the planning time horizon, $H \subseteq V$;
$r \in R$	Index of Type I LNG tanker, $R \subseteq K$.

Data:

$DAY_{i,j}$	Estimated travel time from *i* to *j*
DSC_k	Daily shipping cost of vessel type *k*;
$D_{j,t}$	Demand at *j* in time period *t*;
REV	Unit revenue of LNG per billion cubic meters (bcm) ;
CYC_j	Expected target delivery date at *j*;
VC_k	Cargo capacity of vessel *k*;
VN_k	Total number of vessel *k*;
$STCOST_t$	Unit storage cost in time period *t*;
$PDCOST_t$	Unit production cost in time period *t*;
TM	Maximum number of terminals can be visited in a route;
M	Big-M;
α	Cargo filling limit ratio (%) of Type I LNG tankers;
β	Time window - number of acceptable days from target delivery date;
ε	Boil-off rate (BOR) (%) $[\underline{\varepsilon}, \overline{\varepsilon}]$;
δ	Storage level at liquefaction terminal $[\underline{\delta}, \overline{\delta}]$.

Decision variables:

$y_{i,j}$	Amount of LNG delivering from *i* to *j*;
$x^1_{i,j,k}$	$\begin{cases} 1 & \text{if vessel } k \text{ operates from terminal } i \text{ to terminal } j \\ 0 & \text{otherwise} \end{cases}$
x^2_t	Production level in time period *t*;
x^3_t	Inventory level in time period *t*;

x_i^4 Vessel arrival time (date) at i, and $x_1^4 = 0$;

x_j^5 Accumulated travel time (days) from initial supply terminal to j, and set departure time at the depot as $x_1^5 = 0$;

u_i Flow in the vessel after it visits *i*.

Objective function:

$$\underset{x \in X, y \in Y}{maximize}$$

$$\sum_{(i,j)\in A} REV \cdot (1 - \varepsilon DAY_{i,j}) y_{i,j} \quad - \sum_{t \in T} (PC_t\, x_t^2) \; - \sum_{t \in T} SC_t x_t^3 \; - \sum_{(i,j)\in A} \sum_{k \in K} (DAY_{i,j}\, DSC_k x_{i,j,k}^1). \tag{1}$$

The objective function maximizes the overall revenue considering all potential cost factors in the supply chain. The first term of the objective maximizes profit by considering the cost of evaporated gas as a result of BOG, duration of shipping, and the amount of LNG in a cargo tank. The second and third term minimize production and storage costs respectively. These values are dependent not only on the production level and storage level, but also on the amount of BOG. The last term of the objective serves to minimize overall vessel operating cost based on daily shipping cost of each vessels and ship duration from a previous terminal to the next destination.

Constraints:

The model considers multiple time periods in a model. However, it is formulated as a single time period model by re-indexing the terminal index with time period index. Hence, index of terminals implies which specific terminal may be served at which time

period. Thus, we use constraints (2) and (3) to nullify the repeating indices of liquefaction terminals in the model.

$$\sum_{k \in K} x^1_{s,s+|S|(t-1),k} = 0, \qquad \forall s \in S, t \in T \backslash \{1\} \text{ and} \qquad (2)$$

$$\sum_{k \in K} x^1_{s+|S|(t-1),s,k} = 0, \qquad \forall s \in S, t \in T \backslash \{1\}. \qquad (3)$$

When a route decision is made, a vessel assignment also has to be determined simultaneously. Once a vessel is assigned, the vessel must complete the tour without being replaced by other vessels returning to the liquefaction terminal. Constraints (4) serve to enforce this requirement.

$$x^1_{i,j,k} \leq \sum_{l \in V} x^1_{j,l,k} \leq N - (N-1) x^1_{i,j,k}, \qquad \forall (i,j) \in A, k \in K. \qquad (4)$$

When a ship is assigned to a route, the amount of laden LNG cargo must be less than the tank capacity of the vessel (Constraints 5) and the number of operating vessels must also be less than the number of vessels in a fleet (Constraints 6).

$$y_{i,j} \leq \sum_{k \in K} VC_k \, x^1_{i,j,k}, \qquad \forall (i,j) \in A, \text{ and} \qquad (5)$$

$$\sum_{j \in V} \sum_{h \subseteq V} x^1_{h,j,k} \leq VN_k \,, \qquad \forall k \in K. \qquad (6)$$

Constraints (7) ensure that all departed vessels must return to the original liquefaction terminal after completing a voyage. Constraints (8) and (9) establish the condition that a customer can receive a shipment by one designated vessel in each time period.

$$\sum_{j\in V}\sum_{k\in K} x^1_{h,j,k} = \sum_{i\in V}\sum_{k\in K} x^1_{i,h,k}, \qquad \forall h \subseteq V, \tag{7}$$

$$\sum_{j\in V}\sum_{k\in K} x^1_{i,j,k} = 1, \qquad \forall i \in V\backslash\{1\}, \text{ and} \tag{8}$$

$$\sum_{i\in V}\sum_{k\in K} x^1_{i,j,k} = 1, \qquad \forall j \in V\backslash\{1\}. \tag{9}$$

As stated above, all departed vessels from the depot must return to the origin, and should not terminate the tour while making any sub-tours. For each routing decision, we use sub-tour elimination constraints to filter any possible sub-tours in Constraints (10),

$$u_i \ - u_j \ + TM \sum_{k\in K} x^1_{i,j,k} \leq TM - 1, \qquad \forall (i,j) \in A. \tag{10}$$

Constraints (11) denote the relationship between the amount of LNG loading to a cargo tank and the demands in each time period. Particularly, as evaporated gas losses are expected during transportation, an additional amount of LNG is considered in the constraints.

$$\sum_{i\in V}(1 - \varepsilon DAY_{i,j})y_{i,j} - \sum_{t\in T} D_{j,t} = \sum_{l\in V} y_{j,l}, \qquad \forall j \in V\backslash\{1\}. \tag{11}$$

In practice, once a laden LNG vessel unloads all cargoes at regasification terminals, the returning vessel must be empty (excluding the minimum amount of LNG cargo for cooling purposes). Hence, Constraints (12) set the cargo level of laden LNG vessel returning to a liquefaction terminal as ‘0’,

$$\sum_{i\in V} y_{i,h} = 0, \qquad \forall h \in H. \tag{12}$$

Based on LNG contract terms, specific amount of LNG cargoes have to be delivered to customers at the expected time. However, these contracts often include a grace period. Constraints (13) and (14) accumulate the sailing time of an operating vessel and constraints (15) set the time window from an expected delivery date on a target customer:

$$x_j^5 \geq x_i^5 + DAY_{i,j} - M(1 - x_{i,j,k}^1)\,, \qquad \forall (i,j) \in A, k \in K, \tag{13}$$

$$x_i^4 \geq x_i^5 + DAY_{i,j} - M\left(1 - x_{i,1,k}^1\right), \qquad \forall i \in \backslash\{1\}, k \in K, \text{ and} \tag{14}$$

$$\left|x_j^5 - CYC_j\right| \leq 0.5\beta, \qquad \forall j \in A. \tag{15}$$

As type I LNG vessels have strict filling limits on cargo tanks during voyages, constraints (16) set this condition based on the allowed filling limit ratio (α),

$$y_{i,j} \geq \alpha VC_r x_{i,j,r}^1, \qquad \forall (i,j) \in A, r \subseteq K, \tag{16}$$

Planning inventories and production levels are determined by the demand level in each time period in constraint (17). Finally, safety stocks and maximum storage levels at the depot are set up in constraints (18),

$$x_t^2 - x_t^3 + x_{t-1}^3 = \sum_{j \in V} D_{j,t}, \qquad \forall t \in T, \tag{17}$$

$$\underline{\delta} \leq x_t^3 \leq \overline{\delta}, \qquad \forall t \in T. \tag{18}$$

Appendix II:

Theoretical Bound to determine robust parameter Γ (Bertsimas and Sim, 2004)

To determine robust parameter Γ used in Chapter 7, we use the theoretical bound proposed by Bertsimas and Sim (2004),

$$B(n,\Gamma_i) \leq (1-\mu)C(n,\lfloor v \rfloor) + \sum_{l=\lfloor v \rfloor+1}^{n} C(n,l).$$

where,

$$C(n,l) = \begin{cases} \frac{1}{2^n}, if\ l = 0\ or\ l = n, \\ \frac{1}{\sqrt{2\pi}}\sqrt{\frac{n}{(n-l)l}}.\exp\left(n\log\left(\frac{n}{2(n-l)}\right) + l\log\left(\frac{(n-l)}{l}\right)\right), otherwise. \end{cases}$$

$$B(n,\Gamma_i) = \frac{1}{2^n}\left((1-\mu)\sum_{l=\lfloor v \rfloor}^{n}\binom{n}{l} + \mu\sum_{l=\lfloor v \rfloor+1}^{n}\binom{n}{l}\right),$$

$$= \frac{1}{2^n}\left((1-\mu)\binom{n}{\lfloor v \rfloor} + \sum_{l=\lfloor v \rfloor+1}^{n}\binom{n}{l}\right),$$

$$n = |J_i|,$$

$$v = (\Gamma_i + n)/2,$$

$$\mu = v - \lfloor v \rfloor.$$